SLAC-397
UC-414
(A)

ANALYSIS OF THE OPTICS OF THE FINAL FOCUS TEST BEAM USING LIE ALGEBRA BASED TECHNIQUES*

Ghislain J. Roy

Stanford Linear Accelerator Center
Stanford University
Stanford, California 94309

September 1992

Prepared for the Department of Energy
under contract number DE-AC03-76SF00515

Printed in the United States of America. Available from the National Technical Information Service, U.S. Department of Commerce, 5285 Port Royal Road, Springfield, Virginia 22161.

*Ph. D. thesis

Table of Contents

Acknowledgments

I first want to thank Professor Jean Buon. He initiated my steps on the way to accelerator physics. His teaching and friendship are very precious.

My thoughts also go to John Irwin. He also taught me a great deal. For the numerous discussions, your great patience and disponibility, thank you John.

To Michel Davier who accepted to chair the jury and to Jean-Eudes Augustin for being part of it, my sincere thanks. Olivier Napoly also accepted the position of "rapporteur" for this thesis and I thank him for this; his comments are always important to me.

I want to express my very sincere thanks to J.M. Paterson and Ron Ruth for hosting me in their Accelerator Theory and Special Projects group at SLAC for these three years. It has been a great privilege to learn among some of the greatest. Special thanks go to Matt Sands.

I am indebted to the FFTB Optics group. Thanks to K. Oide, K. Brown, R. Helm, N. Yamamoto, F. Bulos. Special thanks to Peter Tenenbaum and Rick Iverson for your questions and the discussions they triggered. Of course I want to express my gratitude to the entire FFTB collaboration. A special mention goes to Bernie Denton, Gerry Fischer, Finn Halbo and Dieter Walz; Their great experience and very high professionalism were remarkable. They have been true models for me. Thank you also Dave Burke for leading the FFTB with such enthusiasm.

For their help with the codes and machines, let me acknowledge the help and advice of M. Berz, A. Dragt, R. Servranckx and T. Knight.

A special thought goes to those at SLAC who have always encouraged me and have become true friends. Nick Walker, Paul Emma, Tanya Boysen, Bill Gabella and the happy group. Let them be thanked here. A special word must go to Lia Merminga; For these discussions and advices late at night, thank you so much.

And to all who have shown their support; the friends from Stanford but also the members of the St Ann's choir, their families and friends.

To all of you, I dedicate this work.

Introduction

High energy e^+e^- colliders are currently limited on the way to energies higher than 100 GeV by synchrotron radiation. When their trajectories are bent by a magnetic field, charged particles emit electromagnetic radiation. The power radiated is proportional to the fourth power of the energy of the particles and inversely proportional to the square of the bending radius of the trajectory. In order to keep the radiated power down to a manageable level, the highest energy e^+e^- collider ring to date, LEP at CERN, has a circumference of about 27 kilometers for a maximum energy of 100 GeV per beam.

One requirement for colliders in the next twenty years is to increase the energy by an order of magnitude and reach the 1 TeV center-of-mass energy for e^+e^- collisions. The scaling of LEP to such energies, keeping a constant radiated power per unit length, would lead to a ring twenty five times larger or about 700 kilometers in circumference. Clearly not an economically feasible machine. The other way to build high-energy machines, which would not require such a gigantic size, is the linear collider. Here two linear accelerators facing each other accelerate the two beams. They are brought in collisions at the Interaction Point and discarded. The concept of such a machine has been tested at SLAC with the Stanford Linear Collider (SLC[1]) which has been a success as such; a number of specific problems have been studied, some even discovered (muon shielding, collimation) and for others the true complexity of these machines has been unveiled. This is particularly true for the problems linked with production and conservation of small emittances as well as for final focus systems. However the SLC is not a true linear collider. The beams are accelerated concurrently in a single linac then two arcs and final focus lines bring the beams in collision at the IP. The SLC has nonetheless demonstrated the feasibility of such linear machines. The lessons learned form the SLC could not have been obtained by any other way.

The other challenge of high-energy e^+e^- colliders is the luminosity required to investigate very rare events. The next generation of machines will require a luminosity between 10^{33} and 10^{34} $cm^{-2}s^{-1}$. There are three main parameters to the luminosity: The frequency of the collisions, the population of each bunch and the cross-sectional area of the beams at the IP. The first two parameters are the strong point of circular machines. The circulating current,

proportional to the bunch populations times the repetition frequency of the collisions, is fairly high albeit subject to limitations. For LEP the revolution frequency is of the order of 10^4 Hz and a typical bunch population in colliding mode is 10^{12} particles corresponding to a current of the order of a milliampere per bunch. On the other hand it is not possible to achieve very small beam sizes in circular machines since the beam-beam instabilities (disruption) could lead to the loss of the beams.

This last parameter is the strong point of linear colliders: Since the beams are discarded after the collision, it is possible to have very small spot sizes at the IP and run in a disrupted mode where the beam-beam effects are very strong. On the other hand, the wakefields excited by the beams in the linacs, as well as the total "wall-plug" power used by the machine restrict the repetition frequency, of the order of 100 Hz, and bunch population, 10^{11} particles per train of ten microbunches. Studies are actively carried out to solve these problems but the most promising way of achieving a high luminosity at a future linear collider is to focus the beams very strongly at the IP.

This is the task of the Final Focus System, together with keeping the beams in collision. At the SLC the final focus delivers a round beam at the IP with transverse dimensions of the order of two microns. Typically a next generation linear collider requires flat beams a third of a micron wide and only a few nanometers high. The experience gained at the SLC in building and operating such a line is extremely valuable. However the new scale for spot sizes in linear collider projects prompts for more careful studies of such systems. The design of the optics calls for more stringent cancellation of stronger aberrations. The tight requirements on tolerances and stability, both mechanical and electrical, the precision required for the beam instrumentation and more powerful techniques for diagnostics and correction of the beamline have to be investigated and tested.

The Final Focus Test Beam is being built at SLAC by an international collaboration of physicists and engineers from different laboratories worldwide; SLAC, KEK, INP-Novosibirsk, LAL-Orsay, DESY and MPI-Munich participate in this enterprise. Using the 50 GeV electron beam from the SLAC linac, the goal is to form and measure a spot size 1 μm wide and 60 nm high at the focal point of the system. Designed with possible parameters of a future linear collider in mind, the FFTB is a scaled prototype of most of the hardware, software and procedures required for the building and operation of a final focus system for a future linear collider. The demagnifications and the values of the betatron functions at the

IP are identical to those for the Next Linear Collider (NLC). The emittances and the energy of the beam establish the scale of the FFTB compared to the NLC.

The optics of the FFTB is first presented in chapter 1. The principle of the correction of the chromatic aberrations of the final quadrupoles is described. The introduction of sextupoles and bending magnets for this cancellation gives rise to new non-linear chromatic aberrations. The FFTB layout, section by section, is then detailed and finally the most important remaining aberrations are discussed. The intent of this chapter is simply to introduce the reader to the FFTB, the layout, main features and the notations used in the rest of this thesis. More information can be found in the FFTB design report[3] and the design handbook in preparation.

The motivation for the work presented in this thesis is the following. Since we are trying to achieve a very small spot size by careful cancellation of some strong aberrations, it is important not only to check that the aberration content of the lattice is low enough - this can be done with tracking codes - but most importantly to understand the mechanisms by which cancellations happen or new aberrations arise. Most mathematical tools for the study of theoretical optics go only to second order. They are based on the matrix formulation[6] of Courant and Snyder that was made popular by the program[8] *Transport*. A few good references can be found in the bibliography.

The optics of the FFTB is corrected at second order. The investigation of third and higher order effects, which currently limit the performance of our designs, is crucial for the optimization of the design of the final focus systems for a next generation linear collider. The extension of the *Transport* formalism to third order has been started[11] but this is not an easy task. Also it is not easy to find one's way in this wealth of coefficients. Although some higher order effects have been identified at the FFTB using an analytical approach based on kicks, there is no general way to systematically study these aberrations at third and higher order.

There exists a theory based on Differential Algebra which has been in use for some time, mostly applied to circular accelerators. Pioneered in this field by, among others, E. Forest and M. Berz, DA methods provide so called maps of a given system. A map is the representation of the transformation of a function and can be given at very high orders from the Hamiltonian of the system. DA techniques are currently being used mostly, instead of tracking, for stability studies for large hadron colliders such as the SSC in the United States

and the LHC at CERN. It is indeed possible to concatenate the maps of individual elements and form a high order map of one turn of a very large machine. Successive applications of this map has then been shown to give results equivalent to tracking results. However the concatenation of those high order maps does not provide very much insight on the problem and especially on the mechanism by which aberrations cancel or a new aberration arises from the interaction of lower order effects. And this is our primary concern in the design of final focus systems.

Another theory has been known for some time. Alex Dragt has proposed in the seventies to apply the theory of Lie transformations to some dynamical problems.[19,18] Assuming one knows the Hamiltonian of a system the solution is simply and elegantly given by the associated Lie transformation applied to the functions associated with the canonical variables. Although this work was known it has not been much applied outside of the computer code *Marylie*[13] developed by Dragt and his team. One reason for this is, I believe, the decomposition chosen in order to separate the effects of different orders in a product of independent Lie transformations. This stems directly from the Factorization Theorem[19] of Dragt and Finn. Even for simple elements it is sometimes non-trivial to find this decomposition at order higher than three; fifth order contributions for most elements are now being incorporated to *Marylie*.

A simpler formulation was then proposed[20] by John Irwin and used for the first time at the FFTB for the analysis of the optics. The expansion used is simpler since it consists only in the separation of linear and nonlinear terms. The design linear terms are then treated using the matrix formalism while the non-linear terms are treated separately. The concatenation is performed using the CBH theorem. The simplification arises mostly from the fact that the arguments of the Lie transformations are mostly the potentials of the elements to be considered, which are easily accessible.

Chapter 2 exposes the mathematical basis needed to establish the physics in chapter 3. The theory of Lie groups and Lie algebra is generally non trivial. However the subset needed for the application to optics is simple. The notions of Lie algebra and operators on these algebras are reviewed. Then the central definition of the Lie transformation is presented. The simple examples of the uniform motion and the harmonic oscillator are detailed, using both the resolution of the equations of motion derived from Hamilton's equations, and the application of the Lie transformation. These two examples are very similar to the case of

the motion of a charged particle in a drift space and a quadrupole respectively. Finally the theorem of the similarity transformation and the Campbell-Baker-Hausdorff theorem are presented. They are the two essential tools on which the methods presented in this thesis stand.

The application of these mathematical concepts to the physics of magnetic optics is the subject of chapter 3. I start here from the general electromagnetic Hamiltonian of a charged particle in a magnetic potential typical of accelerator magnets. Some assumptions are made at this point that enable us to simplify the analytical calculations. It should be emphasized that these restrictions are not essential to the method and should the need arise to remove one or more of these assumptions, the same type of analysis would still be possible, albeit with a heavier formalism. The potentials used are expressed for dipoles and multipoles. The Lie transformation associated to the Hamiltonians with these potentials, when applied to the angular position functions of the particle, gives the kick, or change in direction, applied to the particle. This is essentially the expression in the thin lens approximation. The long element expression is then built using the CBH theorem and linear changes of coordinates. The same method lets us build a beamline composed of different long elements. The method is described in detail and involves the separation of the design linear optics from the non-linear and error-induced effects.

Finally the last part of this third chapter shows how more elaborate manipulations can be done using the methods presented. The example of the Chromatic Correction Section is taken. The well known cancellation of the geometric aberrations of two sextupoles separated by a $-I$ module is first shown. Then the more complex example of a fourth order aberration, *i.e.* a fifth order Hamiltonian, is discussed. The basis for these elaborate manipulations is the similarity transformation. A discussion on the errors and induced effects ends the chapter.

The second part of the thesis consists in an application of the methods to the case of the Final Focus Test Beam. The aberration content of the FFTB at order up to five in the Hamiltonian, or fourth order optical effects, is analyzed in chapter 4. The approach is here analytical and since the number of potential aberrations is rather high, some arguments are derived in order to reduce the number of terms that actually need to be estimated. Several arguments are invoked here, including one that uses the characteristic phase advance pattern of final focus systems. The aberrations are then studied order by order. I actually make a distinction between two types of aberrations. Those that are present by design, in the perfect

line, are called inherent aberrations while those that arise because of some error (position, strength, *etc.*) are called induced aberrations. The orders quoted in the next paragraphs are the orders in the Hamiltonians which is one more than the actual optical order.

Since we have already removed the design linear optics as explained in chapter 3, the only aberrations present at first and second order are induced. At higher order inherent and induced aberrations are mixed. The FFTB is corrected at third order except for one identified term for which a correction is proposed. The significant fourth and fifth order aberrations are then reviewed. Finally I show how the aberration pattern at the FFTB is closed at fifth order. That is there cannot be a significant aberration at order higher than five.

Finally the last chapter reviews some stability tolerances for the FFTB. Although Lie algebra is not needed for this mostly first order study, it shows that it is possible to treat linear problems in a very simple way using these methods also. The individual tolerances are derived for the position stability of the magnets. The effects of steering at the IP as well as the dispersion, normal and skew quadrupole effects induced by the subsequent orbit displacement are reviewed. The tolerances on strength stability and rotation are also derived. Finally the tolerances on the sextupolar harmonic content of quadrupoles is also given.

Throughout this thesis I will freely use without further definition some basic concepts of accelerator physics such as the betatron functions, the phase advance, *etc.*. The notations are those in use in the United States. The orientation of the axes follows also the american convention of the y direction being in the transverse plane and pointing upwards. Directions z and s are the longitudinal axes in respectively the cartesian and curvilinear coordinate systems.

2. Lie Algebra

2.1. Introduction

I give in this chapter an overview of the mathematical basis on which we will build the methods we have applied to accelerator physics. Starting form the definition of a Lie algebra, I show how this applies to Hamiltonians with the Poisson bracket as the Lie product. Lie operators and Lie transformations are then introduced with their basic properties. I then show, using two simple examples, how to actually find the equations of motion for Hamiltonian systems using Lie transformations. Finally I introduce without demonstration two theorems, the Campbell-Baker-Hausdorff theorem and the similarity transformation, which are at the center of the methods we use in the next chapter.

I have tried to keep these mathematical considerations simple and clear. There are a number of references on the mathematical theories of Lie groups and Lie algebras where all proofs and further development can be found by the interested reader. There is no need however to go beyond the concepts presented in this chapter to understand and use the methods I present in this thesis.

2.2. Definition

I give in this section a formal definition of an algebra and the additional properties needed to constitute a Lie Algebra. These definitions are purely mathematical and quite simple. I have not attempted here to provide a comprehensive set of definitions. I assume that the reader is familiar with such mathematical notions as fields and vector spaces.

2.2.1. Algebra

A formal definition of an algebra can be given as follows:

An algebra over a field F is a vector space U over F together with a product operation $U \times U \rightarrow U$ written $(x, y) \rightarrow x.y$, which satisfies the bilinearity properties of multiplication

by an element of the field and the distribution (left and right) of the product with respect to the addition:

$$\alpha(x.y) = (\alpha x).y = x.(\alpha y) \qquad \alpha \epsilon F \tag{2.1}$$

$$\begin{aligned} &(x_1 + x_2).y = x_1.y + x_2.y \\ \text{and} \qquad &x.(y_1 + y_2) = x.y_1 + x.y_2 \end{aligned} \tag{2.2}$$

In addition, but this is not a required property, the algebra is associative if the product satisfies

$$x.(y.z) = (x.y).z = x.y.z \tag{2.3}$$

We will see later that this property is important for the definition of a Lie algebra.

2.2.2. Lie Algebra

Furthermore if the two following properties of antisymmetry and Jacobi Identity are verified for the product, the product is called a Lie product and the algebra is a Lie Algebra:

$$x.y = -y.x \tag{2.4}$$

$$x.(y.z) + y.(z.x) + z.(x.y) = 0 \tag{2.5}$$

We can note here that the property of associativity of the product, not required to form an algebra, is sufficient to show that the product is not a Lie product. In other words the associativity property on the one hand and the antisymmetry and Jacobi identity on the other hand are mutually exclusive and an associative algebra cannot be a Lie algebra.

2.2.3. Examples

As simple examples of algebras and Lie algebras we can consider the well known set of the $n \times n$ square matrices.

We can first show very easily that this set, with the common matrix product, defines an algebra over the field of real numbers. I will not carry the demonstration out here since it is trivial.

However we can remark that the matrix product is not antisymmetric, namely $A.B \neq -B.A$ which is one of the two properties required for a product to be a Lie product. The common matrix product is not a Lie product and the associated algebra is not a Lie algebra.

It would have been equivalent to state that because the normal matrix product is indeed associative, the algebra of the square $n \times n$ square matrices with the normal matrix product cannot be a Lie algebra

Let us now consider the commutator of two square matrices as the "product" on the same vector field, $[A, B] = A.B - B.A$ where the dot still represents the normal matrix product. It can easily be shown that this is indeed an algebra and the commutator product is not associative. The commutator product is easily shown to be antisymmetric and the Jacobi identity can be verified for all A, B and C in the vector field by a trivial expansion of $[A,[B,C]+[B,[C,A]]+[C,[A,B]]=0$. The commutator product is a Lie product and the set of the square $n \times n$ matrices with this product is a Lie algebra.

In accelerator physics this set of the square $n \times n$ matrices is well known since its introduction by E. Courant and H. Snyder as the mathematical frame for their work on strong focusing. It is the basis of the formalism used in the computer code Transport[8]and is the most widely used nowadays. Each element of an accelerator can be represented by a matrix mapping the coordinates of a particle (or ray) at the entrance of the element into coordinates at the exit. However the product used in this formalism is the common matrix product. An example of the Lie algebra based on the commutator in accelerator physics is the set of the symplectic matrices (SP_{2n}). For a detailed discussion on this subject, see reference 18.

2.3. Hamiltonians and Poisson Brackets

The notion of Hamiltonian in a dynamical system arises from the more general formulation of Lagrangian mechanics. If the equations of motion in Lagrangian formulation consist of s, the number of degrees of freedom, equations of second order, there are $2s$ equations of order one to solve in the case of the Hamiltonian formulation. These equations are called canonical equations because of their simple formulation and their symmetry[29]. In general the Hamiltonian of a system is a function that does not depend on time if the potential itself does not depend on time.

The equations of motion for the canonical variables q_i, p_i $(i = 1, 2 \ldots, s)$ are expressed by the equations of Hamilton:

$$\frac{dq}{dt} = \dot{q}_i = \frac{\partial H}{\partial p_i}; \qquad \frac{dp}{dt} = \dot{p}_i = -\frac{\partial H}{\partial q_i} \tag{2.6}$$

Let f be a function of the q, p and t variables; the total derivative of f with respect to the time variable is written using the chain rule for derivation:

$$\frac{df}{dt} = \frac{\partial f}{\partial t} + \sum_i \frac{\partial f}{\partial q_i}\dot{q}_i + \frac{\partial f}{\partial p_i}\dot{p}_i \tag{2.7}$$

The Poisson Bracket $[f, g]$ of two functions f and g of the variables p_i, q_i is defined as

$$[f, g] = \sum_i \frac{\partial f}{\partial q_i}\frac{\partial g}{\partial p_i} - \frac{\partial f}{\partial p_i}\frac{\partial g}{\partial q_i} \tag{2.8}$$

Using the equations of Hamilton (2.6) the total derivative of f with respect to time (2.7) is then rewritten

$$\frac{df}{dt} = \frac{\partial f}{\partial t} + [f, H] \tag{2.9}$$

Particularly by taking $f = H$ one gets $\frac{dH}{dt} = \frac{\partial H}{\partial t}$ and if H does not explicitly depend on time $\frac{dH}{dt} = 0$ which expresses the conservation of some quantity H, usually the energy of the system.

I do not wish to elaborate more on this at this point. I will come back to this subject in the next chapter when it comes to building the Hamiltonian of optical magnetic elements for an accelerator.

2.4. The Lie Algebras on Hamiltonians

Consider the vector space of the differentiable functions of the generalized real variables $\{q, p\} = \{q_i, p_i, i = 1, 2, \ldots, s\}$ and the time t. The product defined as the Poisson bracket $f.g = [f, g]$, is effectively a Lie product and the algebra hereby defined is a Lie algebra.

The proof is readily obtained: From the linearity and distributivity of the derivative one infers the bilinearity and the distributivity of the Poisson bracket.

$$[\alpha f, g] = [f, \alpha g] = \alpha [f, g] \tag{2.10}$$

$$\begin{aligned} & [f + g, h] = [f, h] + [g, h] \\ \text{and} \qquad & [f, g + h] = [f, g] + [f, h] \end{aligned} \tag{2.11}$$

The antisymmetry property results from the minus sign in the definition of the Poisson bracket:

$$[f, g] = -[g, f] \tag{2.12}$$

The Jacobi identity is the least obvious from the definition of the Poisson bracket but is easily developed. In terms of Poisson brackets it is written

$$[f, [g, h]] + [g, [h, f]] + [h, [f, g]] = 0 \tag{2.13}$$

This Lie algebra is the one on which we will base the rest of the work presented here.

2.5. Lie Operators

To every function $f(q, p, t)$ we associate a "Lie operator", $:f:$, operating on any function $g(q, p, t)$ and defined as

$$:f:g = [f, g] \tag{2.14}$$

In the words of Alex Dragt, "the Lie operator is a Poisson bracket waiting to happen". The powers of Lie operators are defined as

$$\begin{aligned} :f:^0 g &= g \\ :f:\, g &= [f, g] \\ :f:^2 g &= :f:(:f:g) = [f, [f, g]] \end{aligned} \tag{2.15}$$

The set of the Lie operators forms a vector space:

$$a:f: + b:g: = :af + bg: \qquad \text{with a and b scalars} \tag{2.16}$$

They act as a differentiation operator with respect to the common product and the Poisson

bracket:

$$:f:\,(gh) = (:f:\,g)\;h + g\;(:f:\,h) \tag{2.17}$$

$$:f:\,[g,h] = [:f:\,g\;,\;h] + [g\;,\;:f:\,h] \tag{2.18}$$

Note here that we can rewrite equation (2.9) using the antisymmetry property of the Poisson bracket and the definition of the Lie operator

$$\frac{df}{dt} = \frac{\partial f}{\partial t} - :H:f \tag{2.19}$$

And when the function f does not explicitly depend on the time variable ($\frac{\partial f}{\partial t} = 0$), which is the case for the functions we will study later in this thesis, the equation can even be restricted to the following notation

$$\frac{d}{dt} = -:H: \tag{2.20}$$

showing that the Hamiltonian Lie operator simply consists in a time derivation.

I can now rewrite equation (2.18) for this particular case as

$$-:H:\,[g,h] = \frac{d}{dt}[g,h] = [\frac{dg}{dt},h] + [g,\frac{dh}{dt}] \tag{2.21}$$

which forms the differentiation rule for a Poisson bracket.

Finally one can also define a product on Lie operators as the commutation between the two individual operators:

$$\{:f:,:g:\} = :f::g: - :g::f: \tag{2.22}$$

Applying this new operator to any function $h(q,p,t)$ we get

$$\begin{aligned}\{:f:,:g:\}\;h = :f::g:\;h - :g::f:\;h \;&=\; [f,[g,h]] - [g,[f,h]] \\ = [[f,g],h] \;&=\; :[f,g]:h\end{aligned} \tag{2.23}$$

so that we can write $\{:f:,:g:\} = :[f,g]:$

The commutator has already been shown to be a Lie product. The algebra of Lie operators with the commutator as a Lie product is a Lie algebra. Notice that this Lie algebra of Lie operators is constructed upon the Lie algebra of functions of generalized variables with the Poisson bracket as the Lie product and is therefore homomorphic to the later.

2.6. Lie Transformations and properties

2.6.1. Definition

Powers of Lie operators belong to the space of Lie operators. It is possible to introduce the functions that can be expanded in integral series of Lie operators and these functions also belong to the space of Lie operators. In particular the exponential function

$$\exp(:f:) = \sum_{n=0}^{\infty} \frac{1}{n!} (:f:)^n \tag{2.24}$$

is defined as the Lie transformation and its action on a function $g(q,p,t)$ is the series

$$\exp(:f:)g = g + [f,g] + \frac{1}{2!}[f,[f,g]] + \dots \tag{2.25}$$

2.6.2. Properties

The following properties can be verified using the series expansion of equation (2.25) and equations (2.17) and (2.18).

$$\begin{aligned} e^{:f:}(gh) &= (e^{:f:}g)(e^{:f:}h) \\ e^{:f:}[g,h] &= [e^{:f:}g, e^{:f:}h] \\ e^{:f:}g(z) &= g(e^{:f:}z) \end{aligned} \tag{2.26}$$

The first two properties are easily shown. The last one above should be emphasized for it will be central in the treatment of optics. It can be expressed as the following rule: *"to transform a function through a Lie transformation, one needs only transform the coordinates of this function"*.

If we now apply the Lie transformation $e^{-\tau:H:}$ where H is the Hamiltonian, to the functions of canonical variables q_i, p_i when these functions do not explicitly depend on time but are taken at time t_0, we have

$$e^{-\tau:H:} f_{t_0} = \sum_{n=0}^{\infty} \frac{\tau^n}{n!} \frac{d^n f}{dt^n}|_{t_0} = f_{t_0+\tau} \tag{2.27}$$

which is the usual definition of the translation of a system by a time τ using the Taylor series expansion of the function at a time t_0.

2.6.3. Examples

2.6.3.1. Uniform motion

Let us assume the Hamiltonian $H = \frac{p^2}{2m}$ for the movement in one dimension of an object of mass m with generalized coordinates q and p. This Hamiltonian corresponds to a motion with speed $\dot{q} = \frac{\partial H}{\partial p} = \frac{p}{m}$ and the motion is uniform since $\dot{p} = \frac{\partial H}{\partial q} = 0$. The solution comes then from integrating these two equations and we have, with q_0 and p_0 the initial conditions:

$$p = p_0; \qquad q = q_0 + p_0 t \tag{2.28}$$

If we now try to solve the same problem using Lie algebraic methods, we have to evaluate the transformation of the coordinate function $f(q) \equiv q$ evolving according to the Hamiltonian H. We see here that the approach is quite different in the two methods. The classical method derives an equation of motion and therefore "maps" the input to the output coordinates, while the second method attempts to find the transformation of the function representing those coordinates. Notice here that physicists are often lax when it comes to making fine distinctions of this sort and often overlook these differences. I have found that it is however an important point here since the "mapping" approach of the problem, corresponding to the first method presented here and relying on coordinates is so obvious and natural and the manipulation of functions bearing the same name as the coordinates is often overlooked.

Following equations (2.27)and (2.25), the solution is simply the Lie transformation:

$$e^{-t:H:}q = q - t[H,q] + \frac{t^2}{2}[H,[H,q]] + \ldots \tag{2.29}$$

As one can see the operations involved here are Poisson brackets which involve only derivations. There is no integration to perform and we already can see that if a computer can be made to analytically perform a differentiation, which is one of the great results of the Differential Algebra techniques, it will be very easy to make it calculate analytically the evolution of the function q. Note that it results from the assumptions that the Hamiltonian of a classical dynamical system can be differentiated as many times as necessary.

The individual Poisson brackets to be calculated are:

$$\begin{aligned} [H,q] &= [\frac{p^2}{2m},q] = -\frac{p}{m} \\ [H,[H,q]] &= -[\frac{p^2}{2m},p] = 0 \end{aligned} \tag{2.30}$$

It is seen here that this system is actually closed and replacing the results in equation (2.29), we get, assuming that the functions at $t = 0$ evaluate to $p(t = 0) = p_0$ and $q(t = 0) = q_0$:

$$q(t) = q_0 + \frac{p_0}{m}t \tag{2.31}$$

In the same way we get the evolution of the momentum function p:

$$\begin{aligned} & e^{-t:H:}p = p - t[H,p] + \ldots \\ \text{with} \quad & [H,p] = [\frac{p^2}{2m},p] = 0 \\ \text{giving} \quad & p(t) = p_0 \end{aligned} \tag{2.32}$$

We have seen here how to get the same result using two different methods. In the usual method one needs to integrate the equations of Hamilton to get the result. The second one makes use of the Lie algebraic properties of the space of physical functions with the Poisson bracket as a Lie product. The evolution of any function of position and momentum is given by the Lie transformation that only requires the calculation of Poisson brackets of the Hamiltonian describing the system with these functions. Moreover according to the last property in (2.26), one needs only calculate the Poisson brackets with the functions position q and momentum p.

I have chosen this elementary example to develop the method in detail. It may appear that the first method is simpler but the reader is reminded that in many practical cases, Hamilton's equations are not easily integrable.

2.6.3.2. The harmonic oscillator.

I can now present a more elaborate example. The harmonic oscillator is similar to the problem of the motion in a quadrupole in accelerator physics and it involves an open system. A reduced Hamiltonian for the harmonic oscillator can be written $H = \frac{1}{2}(p^2 + q^2)$.

Ones needs to calculate the different powers of the Lie operator associated with the Hamiltonian and their action on the functions position q and momentum p:

$$\begin{aligned} [H,q] = :H:q = -p \quad ; \quad :H:^2 q = -:H:p = -q \quad ; \quad :H:^3 q = p \quad ; \quad :H:^4 q = q \quad \ldots \\ :H:p = q \quad ; \quad :H:^2 p = :H:q = -p \quad ; \quad :H:^3 p = -q \quad ; \quad :H:^4 p = p \quad \ldots \end{aligned} \tag{2.33}$$

which allows us to write for the solution

$$\begin{aligned} e^{-t:H:}q &= q - t:H:q + \frac{t^2}{2}:H:^2 q - \frac{t^3}{3!}:H:^3 q + \ldots \\ &= q + pt - q\frac{t^2}{2} - p\frac{t^3}{3!} + \ldots \\ &= q\,(1 - \frac{t^2}{2} + \ldots) + p\,(t - \frac{t^3}{3!} + \ldots) \\ &= q\cos(t) + p\sin(t) \end{aligned} \tag{2.34}$$

$$\begin{aligned} e^{-t:H:}p &= p - t:H:p + \frac{t^2}{2}:H:^2 p - \frac{t^3}{3!}:H:^3 p + \ldots \\ &= p - qt - p\frac{t^2}{2} + q\frac{t^3}{3!} + \ldots \\ &= p\,(1 - \frac{t^2}{2} + \ldots) + q\,(t - \frac{t^3}{3!} + \ldots) \\ &= p\cos(t) - q\sin(t) \end{aligned} \tag{2.35}$$

The last step in (2.34) and (2.35) involves the recognition of the familiar series of the sine and cosine functions.

From this second example it should now be clear how one can treat those problems in a very general way given the Hamiltonian of the system. An extension of these examples to more than one dimension (two degrees of freedom) is also straightforward.

I present here the last two theorems needed for the rest of this work. Any Lie transformation is associated to one Hamiltonian. In the case of systems with piecewise Hamiltonians, the whole system is represented as a product of the different Lie transformations. It is often desirable to combine these into one global transformation or in other words to find the one Hamiltonian representing the whole system.

The general problem of finding the combination of two Lie transformations is solved by the Campbell-Baker-Hausdorff theorem:

$$\begin{aligned} & e^{:f:}\, e^{:g:} \;=\; e^{:h:} \\ \text{with} \qquad & h \;=\; f+g \;+\; \frac{1}{2}[f,g] \;+\; \frac{1}{12}\Big[f-g,[f,g]\Big] \;+\ldots \end{aligned} \tag{2.36}$$

There is no general expression for this series but one important aspect for computational purposes is the fact that the right hand side of equation (2.36) contains only Poisson brackets of increasing order, or derivatives of f and g of increasing order but no terms of order higher than one in f or g. The demonstration of this theorem is not easy and one can refer for example to the one given by A. Dragt and J. Finn in reference 19.

The algebra of Lie transformation is non-commutative and the reordering of a product of such transformations can be performed using the similarity transformation; it is readily seen with the CBH theorem that the inverse of a Lie transformation $e^{:f:}$ is the Lie transformation $e^{-:f:}$ and inserting the identity $e^{:f:}e^{-:f:}$, one gets

$$\begin{aligned} e^{:g:}\, e^{:f:} &= e^{:f:}\,(e^{-:f:}\, e^{:g:}\, e^{:f:}) \\ &= e^{:f:}\, e^{:e^{-:f:}g:} \\ &= e^{:f:} e^{:g':}. \end{aligned} \tag{2.37}$$

Then following the last property in (2.26) we get that $g'(z)$, with $z = \{q_i, p_i\}$, is the same function g expressed now in terms of the coordinate functions transformed by f: $g'(z) = g(e^{:f:}z)$.

The similarity transformation can be interpreted as a simple coordinate transformation.

$$\begin{aligned} q_i &\rightarrow q_i + [f, q_i] + \frac{1}{2!}\Big[f,[f,q_i]\Big] + \dots \\ p_i &\rightarrow p_i + [f, p_i] + \frac{1}{2!}\Big[f,[f,p_i]\Big] + \dots \end{aligned} \tag{2.38}$$

If f is a quadratic polynomial the change of coordinates is linear and can be represented in a matrix form. This is the Lie algebra equivalent of the familiar change of coordinates in the algebra of matrices $M' = RMR^{-1}$ where R^{-1} is the inverse of R.

Assuming a series of transformations, it is now possible to reorder this series by successive applications of the similarity transformation. For example considering a series of mixed linear (f_i) and non-linear (g_i) transformations, it is possible to move all the non-linear terms together by successively moving them through the linear terms as in the following example:

$$\begin{aligned} e^{:g_1:}\, e^{:f_1:}\, e^{:g_2:}\, e^{:f_2:} &= e^{:g_1:}\, e^{:f_1:}\, e^{:f_2:}\, e^{:g_2(e^{:f_2:}z):} \\ &= e^{:f_1:} e^{:f_2:} \quad e^{:g_1(e^{:f_2:}e^{:f_1:}z):} e^{:g_2(e^{:f_2:}z):} \end{aligned} \tag{2.39}$$

The non-linear transformations keep the same form although the coordinates on which they act are now different. Note that since the f_i are linear transformations the familiar tools of matrix algebra can be applied here to concatenate the linear terms. The CBH theorem can be used to find a single non-linear term so that the whole series is reduced to one linear transformation times one non-linear term.

2.8. Conclusion

We now have at hand all the mathematical tools necessary to approach the Hamiltonian formulation of accelerator optics using Lie algebras. Let me summarize here the essential mathematical tools we will use: At the center of the theory is the notion of the Lie algebra on Hamiltonians with the Poisson bracket. The evolution of the system is given by the Lie transformation associated with the Hamiltonian of the system. Finally the CBH theorem lets us concatenate Lie transformations while the reordering of the transformations is achieved using the similarity transformation, which can also be seen as a change of variables. The separation of linear and non-linear terms is also easily achieved as shown in the last section. The similarity transformation and the CBH theorem are the main tools for the rest of this

study. The mathematical basis for Lie algebra is far richer than the very quick presentation I have made here. I can only encourage the reader to further investigate this very elegant area of mathematics.

3. Application to Optics

3.1. Introduction

I describe in this chapter the techniques used to apply the mathematical tools previously developed to the problem of magnetic optics in accelerators. After transforming the general Hamiltonian into a more specific and more manageable form I show how to separate the optics into the linear and higher-order parts using coordinate changes and the similarity transformation. The treatment of long elements and its extension to the case of beam-lines is then shown.

Two different approaches to finding higher-order effects are presented. One is a straightforward algorithm giving a good global picture of the aberrations in the beamline. The other approach is better used for the analysis of specific effects and analytical calculations. I present some examples of such analysis based on the case of the CCS at the FFTB. Finally I describe how to take some errors into account.

3.2. Hamiltonians

3.2.1. The Electro-Magnetic Hamiltonian

The general Hamiltonian of a particle of rest mass m_0, charge e and canonical position and momentum $\vec{q}$ and $\vec{p}$, placed in an electromagnetic field deriving from the scalar and vector potentials Ψ and $\vec{A}$ is written, with the time t as the independent variable:

$$H = (m_0^2c^4 + c^2(\vec{p} - e\vec{A})^2)^{1/2} + e\Psi \tag{3.1}$$

If the vector and scalar potentials $\vec{A}$ and Ψ do not explicitly depend on time so that $\frac{\partial H}{\partial t} = 0$ the Hamiltonian is a constant of motion ($\frac{dH}{dt} = 0$) as well as an integral of motion ($[H, H] = 0$). The Hamiltonian in equation (3.1) is a constant and represents the total energy of the system ($H = E$).

It is convenient in accelerator physics to change the coordinate system and analyze the dynamics of the particles with respect to a design trajectory. The x and y axes lie in the plane perpendicular to the trajectory of the reference particle and the s axis is along this reference trajectory. This curvilinear coordinate system has been described in many places and is very familiar to accelerator physicists.

The change of coordinates[6,30] generates a new Hamiltonian, still written H however. The new constant of motion, $H = -p_s$, is the longitudinal momentum. Denoting by $\rho(s)$ the curvature of the design trajectory along the machine we get the following Hamiltonian:

$$H = -eA_s - (1 + \frac{x}{\rho})\left[\frac{(E - e\Psi)^2}{c^2} - m_0^2c^2 - (p_x - eA_x)^2 - (p_y - eA_y)^2\right]^{\frac{1}{2}} \qquad (3.2)$$

I shall now restrict the scope of the problem to the magnetostatic case of typical accelerator magnets, where $\Psi = 0$ and the vector potential $\vec{A}$ does not vary with time. It is also convenient and, because of time independence, legitimate to scale the Hamiltonian by the total momentum of the particle p. This requires that we scale the coordinate p_x and p_y giving $x' = p_x/p$, the angle that the trajectory of the particle makes with the design trajectory in the horizontal direction (x plane) taken in the approximation of small angles. Similarly in the vertical plane $y' = p_y/p$. The new Hamiltonian is

$$H = -\frac{e}{p}A_s - (1 + \frac{x}{\rho})\left[1 - (x' - \frac{e}{p}A_x)^2 - (y' - \frac{e}{p}A_y)^2\right]^{\frac{1}{2}} \qquad (3.3)$$

3.2.2. Approximations

I assume for the rest of this study that the only non-zero component of the vector potential is the longitudinal component A_s. Since $\vec{B} = \nabla \times \vec{A}$, this assumes that the longitudinal component of the magnetic field is zero everywhere. Although I neglect as a consequence the fringe fields of magnetic elements, which is a good approximation in our case, the formalism is quite general. Including elements with axial magnetic fields and fringe fields would not present any additional problem.

I can now expand the square root in a series since the angles x' and y' are typically very small: of the order of a few tenth of a microradian in most elements at the FFTB, and up to a maximum of 300 to 500 microradians at the focal point.

$$H = -\frac{e}{p}A_s - (1+\frac{x}{\rho})\left[1 - \frac{1}{2}(x'^2+y'^2) - \frac{1}{8}(x'^2+y'^2)^2 + \ldots\right] \tag{3.4}$$

Also using the same argument of small angles, we get that the effects of the fourth and higher-order terms in x' and y' in the above expansion are negligible. Note that some very general aberrations, well known to spectrometer designers, do disappear from the calculations due to this approximation; for example there are higher-order geometric aberrations appearing in quadrupoles if one keeps more terms in the development. They are due to large enough x' and y' that change the path length inside the magnet. Their effects can be calculated as perturbations and shown to be negligible for the FFTB.

All the terms we have dropped may be included in situation where they are important.

Note that the first term of the series in (3.4), a constant, does not have any effect on the dynamics of the system and can be dropped. Finally I can express the total momentum p of the particle in terms of the design momentum p_0 and $\overline{\delta} = \frac{p-p_0}{p}$ a momentum deviation* so that the final expression for the Hamiltonian is, given as a function of the vector potential A_s:

$$H = -\frac{e}{p_0}\,(1-\overline{\delta})\,A_s \;-\; \frac{x}{\rho} \;+\; \frac{1}{2}(1+\frac{x}{\rho})(x'^2+y'^2) \tag{3.5}$$

The equations of motion can then be obtained from Hamilton's equations (2.6) and the motion, solution of these equations, can be found by integration or alternatively by applying the Lie transformation to a given coordinate function, as shown in chapter 2.

3.2.3. Potentials

The expression for the vector potential A_s can be obtained from Maxwell's equations expressed in curvilinear coordinates.

$\star$ The deviation usually quoted in accelerator physics, $\delta = \frac{p-p_0}{p_0}$, would lead to an infinite series of chromatic terms at all orders $1/(1+\delta) \approx 1 - \delta + \delta^2 + \ldots$. Using $\overline{\delta} = \frac{\delta}{1+\delta}$ all chromatic effects are contained in the linear dependence in $\overline{\delta}$.

3.2.3.1. dipoles

In the case of bending magnets, horizontal here, the vector potential A_s is the solution of a differential equation given by $B_0 = (\nabla \times \vec{A})_y$ where the rotational operator is expressed in curvilinear coordinates. The solution[31] is of the form

$$A_s = \frac{B_0\ \rho}{2}\ (1 + \frac{x}{\rho})^2 \tag{3.6}$$

There are two terms of importance in this potential. The first one, $B_0 x$, represents the main bending field and cancels the term x/ρ in (3.5) so that, as was expected since we are in curvilinear coordinates, the main bending field disappears form the Hamiltonian of dipole magnets. The second term of interest is proportional to x^2/ρ^2 and is the expression of a weak-focusing effect in the horizontal plane.

Dipole magnets at the FFTB have typically a bending radius $\rho = 725m$ and the typical excursion from the central trajectory is a few hundreds of microns giving $x/\rho \approx 10^{-7}$. The weak-focusing effect is therefore dropped altogether with higher-order effects in x/ρ. The only remaining term in the potential is the dispersion $\overline{\delta} x/\rho$ and the Hamiltonian we assume for dipole magnets has the final form:

$$H = \frac{1}{2}(x'^2 + y'^2) - \frac{\overline{\delta} x}{\rho} \tag{3.7}$$

3.2.3.2. multipoles

For multipoles, $1/\rho = 0$ and the magnetic vector potential is a solution of an equation of Laplace in two dimensions. This equation is easily obtained by writing the condition $\nabla \times \vec{B} = 0$ together with $\vec{B} = \nabla \times \vec{A}$. The solution is of the general form $\mathrm{Re} \sum_n \frac{c_n}{n!} (x+iy)^n$, with c_n complex, containing all the normal as well as skew multipole terms. The order of the solution and the constant for a given magnet are determined by its geometry (number of poles, aperture) and the value of the field at the pole tip. By arguments of symmetry one can show that the solution of order n corresponds to a magnet with $2n$ poles and the orientation of the poles determines whether the element is "normal" or "skewed". One is a rotation of the other by an angle $\pi/2n$ around the longitudinal axis.

A "normal" element is by definition one that has the horizontal midplane symmetry: A particle with a trajectory starting in the horizontal plane remains in the horizontal plane when passing through this element. The consequence on the symmetry of the transverse components of the field is

$$\begin{aligned} B_x(x,-y,s) &= -B_x(x,y,s) \\ B_y(x,-y,s) &= \ B_y(x,y,s) \end{aligned} \tag{3.8}$$

The strength of the multipole is given by the boundary condition at $\sqrt{x^2+y^2} = a$ the radius of the aperture of the magnet where the field is equal to the pole tip magnetic field B_0. The solutions at order n for the normal and skew multipole elements respectively are written as the real and imaginary part of the general solution above:

$$\begin{aligned} -\frac{e}{p_0}\, A_s &= \frac{K_n}{n!}\ \mathrm{Re}\ (x+iy)^n \\ -\frac{e}{p_0}\, A_s &= \frac{K'_n}{n!}\ \mathrm{Im}\ (x+iy)^n \end{aligned} \tag{3.9}$$

The absolute values of the strengths are defined, with the magnetic rigidity $(B\rho) = \frac{p_0}{e}$, as

$$|K_n| = |K'_n| = (n-1)!\ \frac{B_0}{a^{n-1}(B\rho)} \tag{3.10}$$

For example the following Hamiltonians determine the dynamics of a particle in respectively a drift space (no field), a quadrupole, a skew quadrupole and a sextupole:

$$\begin{aligned} \text{drift space:} \quad & H = \frac{1}{2}(x'^2+y'^2) \\ \text{quadrupole:} \quad & H = \frac{1}{2}(x'^2+y'^2) + \frac{1}{2}\ K_2\ (1-\overline{\delta})\ (x^2-y^2) \\ \text{skew quadrupole:} \quad & H = \frac{1}{2}(x'^2+y'^2) + K'_2\ (1-\overline{\delta})\ xy \\ \text{sextupole:} \quad & H = \frac{1}{2}(x'^2+y'^2) + \frac{1}{3!}\ K_3\ (1-\overline{\delta})\ (x^3-3xy^2) \end{aligned} \tag{3.11}$$

3.2.3.3. summary

The following table lists the potential part of all normal and skew multipoles at order up to five. I define the potential part of a Hamiltonian as the part deriving from a potential, in our case $-\frac{e}{p_0} A_s (1-\overline{\delta})$, while the kinematic part exists even in the absence of a potential. The Hamiltonian of a drift space contains only a kinematic part.

element	normal	skew
dipole	$\overline{\delta}\, x/\rho$	$\overline{\delta}\, y/\rho$
quadrupole	$\frac{K_2}{2} (1-\overline{\delta}) (x^2-y^2)$	$K_2' (1-\overline{\delta})\, xy$
sextupole	$\frac{K_3}{3!} (1-\overline{\delta}) (x^3-3xy^2)$	$\frac{K_3'}{3!} (1-\overline{\delta}) (3x^2y-y^3)$
octupole	$\frac{K_4}{4!} (1-\overline{\delta}) (x^4-6x^2y^2+y^4)$	$\frac{K_4'}{4!} (1-\overline{\delta}) (4x^3y-4xy^3)$
decapole	$\frac{K_5}{5!} (1-\overline{\delta}) (x^5-10x^3y^2+5xy^4)$	$\frac{K_5'}{5!} (1-\overline{\delta}) (5x^4y-10x^2y^3+y^5)$

Table 3.1. The potential parts, normal and skew, of the Hamiltonians for te first few orders. Note that for dipoles and since we are in curvilinear coordinates, only the dispersive part appears here and no order one effects are present.

The Hamiltonians defined contain all the dynamics of the system, considering of course the approximations made in the preceding section, and one can now treat a multipole element in the same way I have treated the two simple examples in the previous chapter. Note that the uniform motion example is to be compared to that of a drift here and the example of the harmonic oscillator is analogous to the case of the quadrupole.

Notice here that no Hamiltonians of order one appear in the above table since the main bending field disappears by virtue of the curvilinear coordinates. Hamiltonians of order one will however appear when considering dipole correctors, which are not a part of the design lattice, or errors or misplaced elements.

3.3. Principles

3.3.1. Thin elements

The Lie transformation associated with the Hamiltonian as defined above is written, for a small slice of length ds, $\exp(-ds{:}H{:})$. H is in general composed of a linear part

H_l of order two in the generalized coordinates and $\overline{\delta}$, and a non-linear part H_{nl} of order three and higher. It is possible, in the thin-lens approximation $ds \rightarrow 0$, to rewrite the Lie transformation associated with the slice, as the product

$$\exp(-ds{:}H{:}) = \exp(-ds{:}H_l{:})\ \exp(-ds{:}H_{nl}{:}). \tag{3.12}$$

The linear part H_l contains the kinematic part of the Hamiltonian as well as the potential part of order two if present. This is equivalent to neglecting all the terms in $ds^n, n \geq 1$ in the CBH expansion since H_l and H_{nl} do not commute.

3.3.2. Linear Transformations

A Lie transformation of the form $M = \exp(-l{:}H_l{:})$ where H_l is of order two is a linear transformation that can be represented by a linear map. Following section (2.7) this map can be represented in a matrix form $[M]$. Although maps are used for the transformation of functions, the matrix form of a linear map is obviously equal to the familiar linear R matrix representing the linear optics in the Transport formalism.

$$[M] = R \tag{3.13}$$

The tools and methods developed for linear optics in any matrix manipulation codes such as Transport[8] can then be used to treat the linear optics in this Lie algebra framework.

3.3.3. Outline of the Methods

I have now shown how one can separate the linear optics from the non-linear terms in the Hamiltonians developed above. The linear optics is simply treated using the well-known Transport matrix theory. The rest of the analysis will consist in taking a series of thin-lens transformations and first assemble them into a thick element. Similarly taking a series of thick elements, the beamline itself can be assembled.

3.4. Thick Elements

3.4.1. Method

Having defined the thin-lens expression of the Lie transformations, I can now concatenate the thin slices, taking the product of the transformations, to form a thick element. I choose to represent this thick element as the combination of two linear maps $M_{l/2}$ and a single nonlinear transformation at the center:

$$\prod_{i=1}^{n} M_{ds_i}\, e^{-ds_i:H(s_i):} = M_{l/2}\, e^{-l:H_t:}\, M_{l/2} \tag{3.14}$$

The linear transformation M_{ds_i} is the same for all the slices while each slice at location s_i has a nonlinear Hamiltonians $H((x(s_i), y(s_i))$. By successive application of the similarity transformation, following the rules defined in the previous chapter, I transform all the nonlinear kicks of individual slices to the center of the element:

$$M_{l/2}\, e^{-l:H_t:}\, M_{l/2} = (\underbrace{MM\ldots M}_{n/2}) \prod_{i=1}^{n} e^{-ds_i:H'_{nl}(i):} (\underbrace{MM\ldots M}_{n/2}) \tag{3.15}$$

The linear $M_{l/2}$ is obviously equal to the product of the linear transformation of half of the total number of slices, corresponding to the linear map across half the length of the thick element. And following the rule for transforming the nonlinear terms, the $H'_{nl}(i)$ are expressed at the center of the element by simply transforming the coordinates in the $H(x(s_i), y(s_i))$, *i.e.* writing $x(s_i)$ and $y(s_i)$ as a function of the coordinates at the center.

The last step is to obtain a single non-linear Hamiltonian H_t using the CBH theorem:

$$lH_t = \sum_{i}^{n} H'_{nl}(i)ds_i + \frac{1}{2}\sum_{i=1}^{n}\sum_{j=i}^{n}[H'_{nl}(i), H'_{nl}(j)]ds_i ds_j + \ldots \tag{3.16}$$

3.4.2. First order in CBH

The first term in the above expansion is simply the kick of the elementary slices summed over all the slices or the main effect of the multipole, now expressed at the center of the element. In the limit $ds \rightarrow 0$ the summation becomes an integral over the length of the magnet:

$$\sum_{i}^{n} H'_{nl}(i)ds_i = \sum_{i}^{n} H_{nl}(x(s_i), y(s_i))ds_i \rightarrow \int_{-L/2}^{L/2} H_{nl}(x(s), y(s))ds \tag{3.17}$$

where $H(s)$ is a function of the elementary coordinate functions $x(s)$ and $y(s)$. The evolution of the elementary coordinate functions along the magnet is supposed known from the linear matrix theory.

3.4.2.1. multipoles

For multipoles of order three and higher, *i.e.* without a quadrupole part, the linear transport is that of a drift space; $x(s) = x_c + sx'_c$; $y(s) = y_c + sy'_c$.

Taking the sextupole as an example the integral yields

$$H = \frac{K_3}{3!}L(x_c^3 - 3x_c y_c^2) \; + \; \frac{K_3}{24}L^3(x_c x_c'^2 - 2x'_c y_c y'_c - x_c y_c'^2). \tag{3.18}$$

The first term is the main sextupole effect for the magnet. The second term is a higher-order effect in the length of the magnet and is typically smaller than the first one by a factor $(L/\beta)^2$. At the FFTB this factor is at least equal to 10^{-6}. The second term can be neglected in our case.

3.4.2.2. quadrupoles

For quadrupoles, and all elements with a quadrupole component of strength K, the linear transport is given, with $\phi(s) = \sqrt{|K|}s$ and for $K > 0$, by

$$\begin{aligned} x(s) &= \cos\phi(s)\; x_c + \frac{1}{\sqrt{|K|}}\sin\phi(s)\; x'_c \\ y(s) &= \cosh\phi(s)\; y_c + \frac{1}{\sqrt{|K|}}\sinh\phi(s)\; y'_c \end{aligned} \tag{3.19}$$

The role of x and y are exchanged for $K < 0$. For a pure quadrupole the integral yields :

$$H = \frac{1}{2}\, K\, L\, \bar{\delta} \quad [\, x_c^2\, \frac{1}{2}\, (1 + \frac{\sin\phi}{\phi}) \;+\; x_c'^{\,2}\, \frac{1}{2|K|}\, (1 - \frac{\sin\phi}{\phi}) \\ - \; y_c^2\, \frac{1}{2}(1 + \frac{\sinh\phi}{\phi}) \;-\; y_c'^{\,2}\, \frac{1}{2|K|}\, (1 - \frac{\sinh\phi}{\phi})\,] \tag{3.20}$$

which can be rewritten

$$H = \frac{1}{2}\, K\, L\, \bar{\delta} \quad [\, a_x\, x_c^2 \;+\; \frac{1}{|K|}\, b_x\, x_c'^{\,2} - \; a_y\, y_c^2 \;-\; \frac{1}{|K|}\, b_y\, y_c'^{\,2}] \tag{3.21}$$

For $K < 0$, one needs only exchange a_x with a_y as well as b_x with b_y.

The a_x, b_x, a_y, b_y are corrections to the simple minded Hamiltonian for the quadrupole. For most quadrupoles at the FFTB the phase ϕ is of the order of 0.3 radians and the following approximations are reasonably good: $a_x \approx 1, a_y \approx 1$ and $b_x \approx \frac{\phi^2}{12}, b_y \approx \frac{\phi^2}{12}$. The final quadrupoles are much stronger and have a phase of the order of one radian. The following table lists the FFTB magnets by type and shows the values of the phase and correction factors. Note that the final quadrupoles (QC2, QX1, QC1) are sufficiently strong that there is a correction of about 10% to the thin-lens approximation chromaticity calculation. Since the final quadrupoles also produce most of the chromaticity of the line, one must take these corrections into account.

3.4.3. second-order in CBH

The second term in the expansion of the CBH theorem represents the interaction of the main multipole term with itself; the effect of the kick produced by a given slice on the kicks produced by the subsequent slices. It can also be replaced by integrals over the length of the magnet:

$$\frac{1}{2}\sum_{i=1}^{n}\sum_{j=i}^{n}[H'_{nl}(i), H'_{nl}(j)]ds_i ds_j \\ = \frac{1}{2}\sum_{i=1}^{n}\sum_{j=i}^{n} ds_i ds_j\, [H'_{nl}(x(s_i), y(s_i)), H'_{nl}(x(s_j), y(s_j))] \\ \rightarrow \frac{1}{2}\int_{-L/2}^{L/2} ds \int_{s}^{L/2} ds'\, [H(x(s), y(s)), H(x(s'), y(s'))] \tag{3.22}$$

Note that the Poisson bracket can be developed and expressed in terms of the elementary

quad. type	ϕ (rad.)	a_x	b_x	a_y	b_y
Q5	0.2058	1.0035	-0.0035	0.9965	0.0035
Q6	0.1816	0.9973	0.0027	1.0028	-0.0028
QA0	0.1050	0.9991	0.0009	1.0009	-0.0009
QA1	0.2826	0.9934	0.0066	1.0067	-0.0067
QA2	0.2111	1.0037	-0.0037	0.9963	0.0037
QN1	0.3181	0.9916	0.0084	1.0085	-0.0085
QN2	0.3216	1.0087	-0.0087	0.9914	0.0086
QN3	0.2338	0.9955	0.0045	1.0046	-0.0046
QM1	0.3216	0.9914	0.0086	1.0087	-0.0087
QM2	0.3181	1.0085	-0.0085	0.9916	0.0084
QM3	0.2338	1.0046	-0.0046	0.9955	0.0045
QT1	0.3137	0.9918	0.0082	1.0082	-0.0082
QT2	0.2871	1.0069	-0.0069	0.9932	0.0068
QT3	0.3292	0.9910	0.0090	1.0091	-0.0091
QT4	0.2231	1.0042	-0.0042	0.9959	0.0041
QC5	0.2643	1.0058	-0.0058	0.9942	0.0058
QC4	0.1727	1.0025	-0.0025	0.9975	0.0025
QC3	0.1279	1.0014	-0.0014	0.9986	0.0014
QC2	0.9509	0.9280	0.0720	1.0788	-0.0788
QX1	0.2820	1.0067	-0.0067	0.9934	0.0066
QC1	1.1535	1.1185	-0.1185	0.8963	0.1037

Table 3.2. Correction factors to the first order Hamiltonians for the FFTB quadrupoles. The factors are defined in the text and are dimensionless.

$[x(s), x(s')]$ and $[y(s), y(s')]$. In the case of multipoles of order three and higher for which the linear transport is that of a drift, they are

$$[x(s), x(s')] = [y(s), y(s')] = s' - s. \tag{3.23}$$

The integral is then easily calculated and gives the long element effect in terms of the

coordinates at the center of the magnet.

Note that since this long-element Hamiltonian involves the calculation of a Poisson bracket, its order is $(2n-2)$ if n is the original multipole order. The long sextupole term $H_{ls} = \frac{K^2L^3}{48}(x_c^2 + y_c^2)^2$ is of order four (octupole like) and its calculation is given in detail in Appendix B.

In the case of the quadrupole and with $\Delta\phi = \sqrt{|K|}(s'-s)$, $K > 0$, the elementary Poisson brackets are written,

$$\begin{aligned} [x(s), x'(s)] &= \frac{1}{\sqrt{|K|}} \sin\Delta\phi \\ \text{and} \qquad [y(s), y'(s)] &= \frac{1}{\sqrt{|K|}} \sinh\Delta\phi. \end{aligned} \tag{3.24}$$

The result of the double integral gives the so called second-order chromaticity, taking $H(s) = \frac{K_2}{2}\overline{\delta}(x(s)^2 - y(s)^2)$ and $\phi = \sqrt{|K|}\ L$:

$$\begin{aligned} &\frac{1}{2}\int_{-L/2}^{L/2} ds \int_{s}^{L/2} ds' \Big[\frac{K_2}{2}\,\overline{\delta}\,(x(s)^2 - y(s)^2)\ ,\ \frac{K_2}{2}\,\overline{\delta}\,(x(s')^2 - y(s')^2)\Big] \\ &= \frac{K_2^2}{2}\,\overline{\delta}^2 \int_{-L/2}^{L/2} ds \int_{s}^{L/2} \Big\{\ x(s)\ x(s')\ [x(s), x(s')] + y(s)\ y(s')\ [y(s), y(s')]\ \Big\} \\ &= \frac{K_2 L}{2}\,\overline{\delta}^2 \Big\{ \quad x_c^2\,\frac{1}{8}\,(1 - 2\cos\phi + 2\frac{\sin\phi}{\phi} - \frac{\sin 2\phi}{2\phi}) \\ &\qquad + x_c'^2\,\frac{1}{8}\,(1 + 2\cos\phi - 2\frac{\sin\phi}{\phi} - \frac{\sin 2\phi}{2\phi}) \\ &\qquad + y_c^2\,\frac{1}{8}\,(-1 + 2\cosh\phi - 2\frac{\sinh\phi}{\phi} - \frac{\sinh 2\phi}{2\phi}) \\ &\qquad + y_c'^2\,\frac{1}{8}\,(1 + 2\cos\phi - 2\frac{\sinh\phi}{\phi} - \frac{\sinh 2\phi}{2\phi}) \quad \Big\} \end{aligned} \tag{3.25}$$

and assuming $K > 0$. This can be rewritten

$$\frac{K_2 L}{2}\,\overline{\delta}^2\ \{\ x_c^2\ c_x + x_c'^2\ d_x + y_c^2\ c_y + y_c'^2\ d_y\ \} \tag{3.26}$$

The coefficients c_x,d_x,c_y and d_y are those of the second-order chromaticity terms in quadrupoles. For $K < 0$, one needs only exchange c_x with c_y as well as d_x with d_y. The coefficients

are approximated for small ϕ by $c_x \sim \phi^2/6$, $d_x \sim -\phi^4/5!$, $c_y \sim \phi^2/6$ and $d_y \sim -\phi^4/5!$. The effect is very small for most quadrupoles at the FFTB.

Note that the CBH expansion (3.16) contains terms that involve more Poisson brackets which are therefore of even higher order. They are usually negligible but are accessible through a simple extension of the formalism.

3.5. Beam Line Analysis

3.5.1. First approach

The same methods using the similarity transformation, as a change of coordinates, and the CBH theorem can be used to treat a beamline. Starting from the concatenation of all the thick elements in the form of the product of alternatively linear and higher-order transformations, the similarity transformation is applied successively to change the coordinates of all nonlinear terms and express them at a single common location, usually the end of the line (IP). The total Hamiltonian H_t for the complete beamline is given by

$$\begin{aligned} e^{:H_t:} &= (M_1\ e^{:H_1:}\ M_1)\ \ldots\ (M_{n-1}\ e^{:H_{n-1}:}\ M_{n-1})\ (M_n\ e^{:H_n:}\ M_n) \\ &= (M_1\ e^{:H_1:}\ M_1)\ \ldots\ (M_{n-1}\ e^{:H_{n-1}:}\ M_{n-1}M_nM_n)e^{:H'_n:} \\ &= (M_1\ e^{:H_1:}\ M_1)\ \ldots\ M_{n-1}M_{n-1}M_nM_n\ e^{:H'_{n-1}:}e^{:H'_n:} \\ &= \tilde{M} \prod_{i=1}^{n} e^{:H'_i:} \end{aligned} \tag{3.27}$$

with $\tilde{M} = M_1M_1 \ldots M_nM_n = \prod_{i=1}^{n} M_i^2$ is the linear transformation for the entire line. It is known from the linear design and is related, as seen above, to the usual linear R matrices of the Transport formalism. The Hamiltonian H'_i is the Hamiltonian of element i transformed through $M_i \prod_{j=i+1}^{n} M_j^2$, hence H'_i is now expressed in terms of IP coordinates.

The second part contains the product of all the nonlinear transformations now collated in one single location, the IP. The nonlinear optics of the entire line is expressed in terms of one set of local coordinate functions. Successive applications of the CBH theorem to this product of Lie transformations yields a single final Hamiltonian containing the information on the nonlinear behavior of the whole line. The calculations are straightforward but tedious after a couple of elements. The FFTB has over thirty different elements to take into account.

This systematic method is one that can be automated easily and yields the total nonlinear Hamiltonian of the line giving a picture of the aberration content of the optics. While it is difficult with traditional matrix-based optics methods to get terms at third[11]order and quasi impossible to get higher-order[14]terms, the method I described can give results at practically any order although I will show later that it is not necessary to go beyond fifth order in the case of the FFTB. The maximum order is limited only by how far one carries the CBH expansion, provided the long elements effects have been taken into account correctly.

These methods may then seem like the panacea for getting knowledge on the nonlinear optics of accelerators. However since we are trying to carefully cancel harmful aberrations, one is also interested in studying these cancellations in detail as well as looking at how optical elements interact with each other. It might be possible to design better optics using this information. To this end I need to tell exactly which aberration is coming from which element or which combination of elements. Some fifth order aberrations that exist at the FFTB would certainly be detected with this method but the mechanism of their appearance, in short the interaction of the central quadrupole in the CCY, with the sextupoles around it, would be difficult to guess and possible correction nearly impossible to invent with this method alone. Oide[28]has identified these aberrations using a method based on kicks on individual trajectories. I show in the next section how to easily calculate them using Lie algebra techniques.

3.5.2. Looking for insight

There is a more powerful way to use these Lie algebra techniques, a methodology that gives a lot more insight in the optics than the one I have described in the previous paragraph. Note that the two methods are certainly not exclusive but are more complementary: the first one might detect a significant aberration in the total nonlinear Hamiltonian, the second method will help in the careful, insightful study of it.

Let me recall here that the optics of final focus systems is based on the cancellation by sextupoles of the chromaticity introduced by mostly the final quadrupoles. There are five large chromatic sources: four sextupoles and the final quadrupoles. The sextupoles are also sources of strong geometric aberrations.

In the method outlined above these strong Hamiltonians are mixed with weaker ones, like the chromaticity of other quadrupoles or the long-sextupole aberration. The approach

here is to select only the nonlinearities I am interested in and consider the rest of the optics as linear. I therefore treat only a chosen subset of the problem, allowing to treat one effect at a time.

After that the analysis could follow exactly the approach presented in the previous section: individual non-linear Hamiltonians are transformed (similarity transformations) to a common reference point (*e.g.* the IP) where they are combined using the CBH theorem. Since we are looking at only a few terms, this can be done analytically and the interplay of these terms is easily seen. There are other ways to do this refined analysis and as an example I use, in the next two sections, the particular symmetry of the CCS at the FFTB.

The Chromatic Correction Section indeed forms a self consistent section inside the final focus. Its purpose being to ideally introduce a single term, the chromaticity needed to cancel that of the final quadrupoles. The idea here is to treat the CCS as a beam line by itself, reducing it to the now familiar form of a linear transformation ($-I$) and a global Hamiltonian containing all of its nonlinear terms. The entire line can then be built from those reduced sections and other individual elements.

3.5.3. Geometrics cancellation in the CCS

The Chromatic Correction Sections are at first order $-I$ sections. That is they are transparent for the linear optics. I consider now the CCS as a small beam line starting at the first sextupole and ending at the second sextupole. The separation of the linear transformation and the higher-order Hamiltonians is made using the second sextupole as the reference location where all Hamiltonians will be transformed.

I choose to treat only the case of sextupolar aberrations in this section. All other elements within the CCS are considered linear, including the quadrupoles whose chromaticity is here neglected. The Hamiltonian of a sextupole is, in the presence of horizontal dispersion η and expressed in local coordinates:

$$\begin{aligned} H_s &= \frac{k_s}{3!}\left((x+\eta\bar{\delta})^3 - 3(x+\eta\bar{\delta})y^2\right) \\ &= \frac{k_s}{3!}\left(x^3 - 3xy^2\right) + \frac{k_s}{2}\,\eta\bar{\delta}\,\left(x^2-y^2\right) + \frac{k_s}{2}\,\eta^2\bar{\delta}^2\,x\; + \frac{k_s}{3!}\eta^3\bar{\delta}^3 \end{aligned} \tag{3.28}$$

The second line in (3.28) shows the main geometric ($H_g = \frac{k_s}{3!}\,\left(x^3 - 3xy^2\right)$) and the main chromatic ($H_c = \frac{k_s}{2}\,\eta\bar{\delta}\,\left(x^2-y^2\right)$) aberrations introduced by the sextupole. I further limit this

study to these two terms. The two remaining terms in (3.28) are the second-order dispersion and a purely chromatic term with no effect.

I can now represent the CCS, from sextupole center to sextupole center by the following sequence of transformations. Note that in local coordinates the aberrations of a sextupole commute and I can reorder them. The goal of this transformation being of course to separate the linear optics $(-I)$ from the nonlinear terms:

$$\begin{aligned} e^{:H_{ccs}:} &= e^{:H_c:}\ e^{:H_g:}\ (-I)\ e^{:H_g:}\ e^{:H_c:} \\ &= (-I)\ e^{:H_c:}\ (e^{:-H_g:}\ e^{:H_g:})\ e^{:H_c:} \\ &= (-I)\ e^{:2H_c:} \end{aligned} \tag{3.29}$$

Obviously the $(-I)$ transforms H_c into H_c since it is an even term in x and y and the dispersion is the same at both sextupoles, while H_g goes into $-H_g$ since it is an odd term in x and y. The geometric aberrations simply vanish at the second sextupole and one is left with the sum of the chromaticities introduced by the sextupoles, since they obviously commute. This is a well known result, the basis of chromaticity correction for final focus systems.

This result has an important consequence for the analysis of the rest of the line. The geometric aberrations having vanished locally there is no need to take them into account for the building of the Hamiltonian of the whole line. There cannot be any direct effect of the interaction between the sextupole geometric aberrations and the chromaticity of the final quadrupoles for example.

3.5.4. Fifth order aberrations

Other terms arise from the CCS if one considers a more extended model of it. Oide[28] has shown that some fifth order aberrations originate in the "chromatic breakdown" of the $-I$: Due to the chromaticity of the quadrupoles inside the CCS, the $-I$ is only exact for on-momentum particles. The linear optics is slightly different for off-energy particles. Therefore the chromatic and geometric aberrations they experience is different from what I have shown in the previous section: The net chromatic kick is not exactly twice that of a single sextupole and the geometric aberrations are not strictly cancelled, resulting in fifth order aberrations.

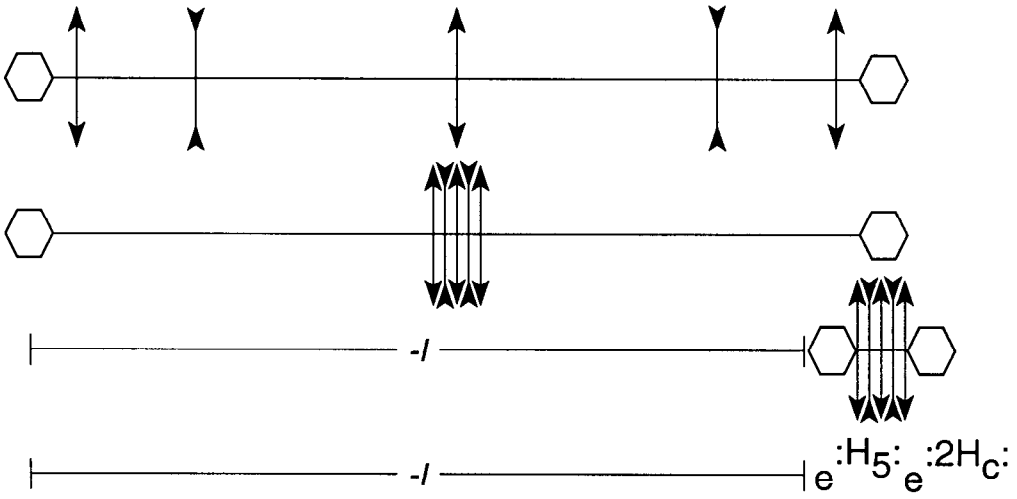

Figure 3.1. The model and the method used for the study of the CCS. After linear transport, shown in steps here, of all the elements into one location, the linear part of the line, $-I$, is virtually extracted. One is left with the non-linear kicks. The sextupole geometric kicks cancel and one is finally left with the chromaticity correction term, $2H_c$, and a fifth order residual and inherent aberration.

The model I choose to treat here is that of the full CCS at the FFTB: Two sextupoles separated by a $-I$ transformation made of five quadrupoles.

The first step is to combine the Hamiltonians representing the chromaticity for all five quadrupoles into a single Hamiltonian (*cf.* second line in above figure). The reference location I choose is the quadrupole at the center of the CCS. It is located exactly $\pi/2$ from either sextupole. The transformation is linear and is equivalent to a change of coordinates in the individual Hamiltonians. Using the CBH theorem one builds the single Hamiltonian H_q representing the total chromaticity of all the quadrupoles of the CCS. Expressed at the center quadrupole, it is of the general form

$$H_q = \overline{\delta}(ax^2 + bx'^2 + cy^2 + dy'^2) \tag{3.30}$$

where a, b, c and d are coefficients functions of the linear lattice in the CCS. Note that the end quadrupoles, closest to the sextupoles, contribute mostly to the b and d coefficients while the center quadrupoles contribute essentially to a and c.

Note that no term proportional to xx' or yy' appear in this formula. Since the section is symmetric the Hamiltonian is the same irrespective of the direction we use for the calculation.

This is equivalent to applying a time reversal for which x' is changed to $-x'$ and y' to $-y'$. No term of odd order in x' or y' can therefore appear.

The second step of this argument is very similar to the treatment of the geometrics of the CCS in the previous section: After linear transformation of the three "elements" to the center of the second sextupole of the pair (H'_q is the transformed of H_q), the situation is represented by the following product (*cf.* third line in above figure):

$$e^{:H_{ccs}:} = (-I)\; e^{:H_c:}\; (e^{:-H_g:}\; e^{:H'_q:}\; e^{:H_g:})\; e^{:H_c:} \tag{3.31}$$

The first similarity transformation gives

$$e^{:H_{ccs}:} = (-I)\; e^{:H_c:}\; e^{:H''_q:}\; e^{:H_c:} \tag{3.32}$$

where

$$\begin{aligned} H''_q &= e^{-:H_g:}\; H'_q \\ &= H'_q(e^{-:H_g:}x, \ldots, e^{-:H_g:}y') \\ &= H'_q(x, x' - \frac{\partial H_g}{\partial x}, y, y' - \frac{\partial H_g}{\partial y}). \end{aligned} \tag{3.33}$$

After insertion of an identity, a second similarity transformation yields

$$e^{:H_{ccs}:} = (-I)\; e^{:H'''_q:}\; e^{2:H_c:} \tag{3.34}$$

where now

$$\begin{aligned} H'''_q &= e^{:H_c:}\; H''_q \\ &= H'_q(x, x' - \frac{\partial H_g}{\partial x} + \frac{\partial H_c}{\partial x}, y, y' - \frac{\partial H_g}{\partial y} + \frac{\partial H_c}{\partial x}). \end{aligned} \tag{3.35}$$

Equation (3.34) shows that I have separated the main effect of the CCS, the chromaticity correction with the Hamiltonian $2H_c$, from the effect of the $-I$ breakdown represented by H'''_q. The study of this Hamiltonian shows that it indeed contains fifth order aberrations. Using (3.30) and the definition of H_g and H_c one can rewrite (3.35) as

$$H'''_q = \overline{\delta}\;(\; bx^2 \;+\; a\;(x' - \frac{k_s}{2}(x^2 - y^2) + k_s\eta\overline{\delta}x)^2 \;+\; dy^2 \;+\; c\;(y' + k_s xy + k_s\eta\overline{\delta}y)^2) \tag{3.36}$$

The expansion of H'''_q shows that the interaction of the quadrupole chromaticity with the geometric aberrations from the sextupoles generates three fifth order aberrations: $\overline{\delta}x^4$, $\overline{\delta}y^4$

and $\overline{\delta}x^2y^2$. The interaction of the quadrupole and sextupole chromaticities generates $\overline{\delta}^3x^2$ and $\overline{\delta}^3y^2$. There are also two cross terms: $\overline{\delta}^2x^3$ and $\overline{\delta}^2xy^2$.

These fifth order aberrations are proportional to the a and c coefficients of (3.30), themselves originating mainly from the center quadrupole. I have also neglected all the terms in x' or y' since the angles are typically orders of magnitude smaller than the trajectory amplitudes at the FFTB sextupoles.

3.5.5. Other uses of this formalism

Having reduced the CCS under the form of a linear $-I$, a fifth order Hamiltonian and the main chromaticity term, it is possible to insert it back into the FFTB beamline. Let me take the following model for the whole line, assuming only one CCS:

$$e^{:H:} = e^{:H_h:}\, e^{:H_5:}\, e^{:2H_c:}\, e^{:H_t:}. \tag{3.37}$$

All Hamiltonians are expressed at the IP. The front-end of the line is modeled by the non-linear Hamiltonian H_h comprising the chromaticity of all elements from the beginning of the line up to the CCS. The part from the CCS to the IP is in H_t and contains the very strong chromaticity of the final quadrupoles. Note that H_h is very small compared to H_t.

The following transformation assumes that the chromaticity cancellation is perfect ($e^{:H_h:}e^{:2H_c:}e^{:H_t:}$ = Unity) and shows that the only remaining part in the total Hamiltonian of the line are some higher (fifth) order effects:

$$\begin{aligned} e^{:H:} &= e^{:H_h:}\, e^{:H_5:}\, e^{:2H_c:}\, e^{:H_t:} \\ &= e^{:H_5':}\, e^{:H_h:}\, e^{:2H_c:}\, e^{:H_t:} \\ &= e^{:H_5':} \end{aligned} \tag{3.38}$$

Note that H_5' has been transformed through H_h, however since the front end of the line contains very little chromaticity*, the higher-order effects it could trigger combined with the fifth order effects are expected to be negligible. In other words $H_5' \sim H_5$. I will show in the next chapter which are the conditions necessary for high order terms to become significant.

$\star$ I assume here only one CCS in the line

There are, in conclusion, residual uncorrected fifth order aberrations at the FFTB. The cause of these terms is in the CCS and has been shown to be the interaction of the quadrupoles chromaticity with both the geometric and chromatic aberrations of the sextupoles. Another significant term already mentioned is the fourth order long-sextupole aberration. This has been established without any numerical calculation, simply by analysis of the structure of the beam line and its components.

A systematic analysis such as that presented earlier in this chapter would give a global aberration picture of the line and would quantify the importance of these aberrations. All the power of the Lie algebra methods I present is here, allowing both the detailed and analytic expression of specific effects and their global sizing through the detailed calculations element by element.

3.6. Errors and offsets

The previous sections showed how to treat a perfect line. I want to show here how one can take into account different displacements and errors in beam-line elements.

The connection between the similarity transformation and the displacement of an element is obvious:

$$e^{:-d_x x':} e^{:H(x,x',y,y'):} e^{:d_x x':} = \exp(e^{-:d_x x':} H) \tag{3.39}$$

and

$$\begin{aligned} e^{-:d_x x':} H &= H(e^{-:d_x x':} x, x') \\ &= H(x + d_x, x') \end{aligned} \tag{3.40}$$

The Hamiltonian is simply rewritten $H(x+d_x, x', y, y')$. Recall that x stands for the function representing the trajectory and d_x is a constant.

The introduction of offsets in the Hamiltonian gives rise to new terms. The corresponding aberrations are of order lower than that of the main term, they are called feed-down terms. For example the Hamiltonian of a horizontally displaced sextupole shows two new terms. A second-order term proportional to $d_x(x^2 - y^2)$ representing a quadrupole effect and a first order term proportional to $d_x^2 x$ representing some horizontal steering. There is also a constant term that has no effect and is dropped here. In the presence of lattice dispersion the same displacement also generates additional dispersion ($d_x \eta x$ and $d_x \eta y$), feed-down from the main

chromaticity terms. This formalism actually shows clearly that dispersion is a by-product of the chromaticity of a displaced element.

Feed-down terms of order two and one are not a part of the design and cannot be included in the design linear optics of the line. They are therefore treated with the non-linear Hamiltonians. The part of the optics that remains after the design linear optics has been removed now comprises non-linear as well as feed-down terms and is called the "rest". The methods outlined in this chapter are not specific to non-linear optics and can accommodate these new terms.

It was possible to express the displacement formally as a similarity transformation because it affects directly one of the coordinate functions. Other errors like strength errors cannot be expressed in this way but can still be shown in the Hamiltonian by directly changing the constant: $K_n \rightarrow K_n + \Delta K_n$. There are now feed-down terms generated by this error: an additional term with the same expression of the main term, and superimposed onto it. Strength errors for quadrupoles are treated as an additional quadrupole and are not treated in the design linear lattice.

Rotation errors and multipole content of an element can be represented as additional Hamiltonians inserted at the same location as the element. In the case of rotation error (ϕ), the Hamiltonian of the affected element is also subject to a strength error by reduction of the nominal strength $K \rightarrow K \cos\phi$.

It is of course now possible to study the effect on the optics of a single error in the line. The calculation of tolerances for the FFTB has been done using these methods. They are the object of chapter 5 of this thesis.

Note finally that the displacement of a section or even the whole line can be studied by inserting the corresponding Hamiltonian in equation (3.39), leading to the calculation of tolerances for the section or, in the case of the whole line, to incoming beam tolerances.

3.7. Conclusion

This chapter has taken us from the general formulation of the electromagnetic Hamiltonian to the ability to analyze the optical effects in a beamline with great selectivity. The key points are the use of the similarity transformation and the CBH theorem. The similarity transformation allows us to change the coordinates of a given Hamiltonian which leads to

the possibility to separate the linear and nonlinear optics. It is also helpful in the handling of compensation mechanism such as that of the geometrics in the CCS. The combination of remaining Hamiltonians is handled by the CBH theorem.

The same method can be applied from within a single element to obtain the Hamiltonian that takes into account the length effects, considering a subset of the line to locally eliminate some aberrations from the calculation as in the treatment of the CCS, or at the level of the whole line to get the global picture of the aberration content of the line.

The similar treatment applied to the single element and the whole beamline shows how scalable these tools are. This is of great help in the understanding of the optics and will ultimately prove very helpful for the building of a computer code based on them.

The introduction of errors has been mentioned in the last section and I now turn in the next two chapters to an analysis of the aberration content and the tolerances for the FFTB using the now complete set of tools using Lie algebra.

4. Aberrations at the FFTB

4.1. Introduction

Using the tools and methods developed in chapter 2 and 3, I analyze here the aberration content of the FFTB optics. The order of an aberration is to be understood in this chapter as the order of the corresponding monomial in the Hamiltonian. Therefore a third order aberration corresponds to a second order optical effect as defined in the *Transport* formalism, represented there by an entry in the T matrix.

After a few remarks on the classification and the number of aberrations we have to consider, I show how one can apply a few simple arguments to find whether the effect of a given aberration can be important or on the contrary is negligible. This will allow us to effectively analyze only the important aberrations. Then I turn to the systematic analysis of all the important aberration terms at up to fifth order for the FFTB.

Remember that by nature Lie algebra acts on functions, not on coordinates like mapping or matrix tools. All references to "coordinates" in the frame of Lie algebra should therefore be understood as "coordinate functions". Let me also recall that I am using here three different sets of coordinate functions. The usual set $\{x, x', y, y'\}$ refers to the local coordinate functions in a given beamline element. The usual coordinates at the IP are noted $\{x^*, x'^*, y^*, y'^*\}$. Finally the set of reduced coordinate functions, or "bar coordinates", is defined by the linear transformation:

$$\overline{y} = \frac{y^*}{\sqrt{\beta_y^*}} \qquad , \qquad \overline{p}_y = y'^* \sqrt{\beta_y^*} \tag{4.1}$$

and the corresponding formulas for the other plane. The Hamiltonian is unchanged by this scaling. Note that although I denote the conjugates of the position functions as $\overline{p}_x$ and $\overline{p}_y$ they are not momenta. The position and angle functions defined by (4.1) are both in units of square root meters ($[L]^{1/2}$).

The fifth general coordinate is the momentum deviation of the particle $\overline{\delta} = \frac{p-p_0}{p}$. Since I do not consider acceleration or radiation effects in this study, $\overline{\delta}$ is a constant. Its conjugate, the time of flight, is not critical at the FFTB so the set of coordinate functions we use for the rest of this chapter is $\{\overline{x}, \overline{p}_x, \overline{y}, \overline{p}_y, \overline{\delta}\}$.

4.2. Classification

Chapter 3 showed how to "remove" the first optical order from the problem of analyzing the optics with Lie algebra based techniques. This manipulation implies that all Hamiltonians describing individual elements are now expressed at the IP as polynomials in the set of $\{\overline{x}, \overline{p}_x, \overline{y}, \overline{p}_y, \overline{\delta}\}$.

The aberrations arising from the CBH combination of individual non-linear Hamiltonians, including the element length effects, exist in the line by design and I classify them as "inherent aberrations". They can be corrected, often by the insertion of specific correction lenses in the line. One purpose of final focus systems is to eliminate all such design aberrations that can affect the spot sizes at the IP. The largest is the chromaticity introduced by the quadrupoles. This goal can be summarized by $\frac{\partial H}{\partial \overline{p}_y} = 0$ and $\frac{\partial H}{\partial \overline{p}_x} = 0$ if H is the total non-linear Hamiltonian of the system.

In practice a beamline cannot be built exactly to design and we have to consider what the consequences of errors are on the aberrations, as well as on the linear optics. Errors (displacement, strength error, rotation) can be expressed as additional Hamiltonians in the line, some of them at first and second order as seen in chapter 3. The consequence is that we now find, when combining the Hamiltonians, some terms at first and second order as well as new terms at higher order. I call these aberrations that arise because of errors in the line "induced aberrations". The study of the induced aberrations is really a problem of tolerances and is the subject of the next chapter. I will however mention some of them in the present chapter.

4.3. Number of aberrations

4.3.1. Symplecticity

Before looking at the precise number of aberrations we have to investigate, it is interesting to make a comparison with the number of entries in the matrices representing the optics in the *Transport* formalism. The matrices must obey the symplectic condition which specifies some relations between matrix elements. For a $2n \times 2n$ linear matrix (R) the symplecticity condition is written

$$R^T J R = J. \tag{4.2}$$

where the matrix J

$$J = \begin{pmatrix} 0 & I \\ -I & 0 \end{pmatrix} \tag{4.3}$$

is built using the two $n \times n$ matrices: (I) identity or unit matrix and (0) the null matrix.

It can be shown that for 2×2 matrices the symplectic condition is written: $\mathrm{Det}R = 1$.

At higher orders the relation between matrix elements can also be seen starting from the Hamiltonian representation of the optics: As stated by Hamilton's equations, any non-zero derivative of H with respect to one of the $\overline{x}, \overline{p}_x, \overline{y}, \overline{p}_y$ represents a change in the conjugate variable, and therefore an aberration. The same Hamiltonian can then represent several optical aberrations and they are related to each other. For example consider the third order geometric aberration $H = C\ \overline{x}\ \overline{p}_x \overline{p}_y$. There are three non-zero derivatives and three matrix elements generated by this Hamiltonian, together with two relations: $T_{114} = T_{224} = T_{312}$. The three matrix elements constrained by two relations are of course equivalent to one coefficient (C) in the Hamiltonian.

The higher the order, the more relations one has to take into account, and it follows that a "catalog of aberrations" using Lie algebra methods requires less terms to keep track of, as compared to the *Transport* notation and methods, and there is no need to carefully establish the dependencies between the different optical aberrations in the matrices.[34]

4.3.2. Numbers

In order to evaluate the number of aberrations at a given order, one can naively start with the idea that all the possible monomials associated with geometric aberrations at order n are in the polynomial* $G_n = (\overline{x} + \overline{p}_x + \overline{y} + \overline{p}_y)^n$. The chromatic terms at order n are added to this collection by taking the product of the energy deviation $\overline{\delta}$ with all the aberrations (chromatic and geometric) at order $n-1$. At order n the list of all possible aberrations is then given, in the form of a polynomial by the recursive equation showing the separation between geometric and chromatic terms:

$$\begin{aligned} & H_n = (\overline{x} + \overline{p}_x + \overline{y} + \overline{p}_y)^n \ + \ \overline{\delta}\ H_{n-1} \\ \text{with} \quad & H_0 = 1 \end{aligned} \tag{4.4}$$

* the coefficients of this polynomial do not hold any special meaning here; they are just coming from the expansion and can be ignored.

The number of all the monomials in the expansion of n_v variables at all orders up to n_o is $N_m = \frac{(n_o+n_v)!}{n_o!\ n_v!}$. At order up to five and for five variables we get a total of 252 mathematically possible terms. This seems like an impressive number if we want to calculate those terms by hand but there are some arguments to reduce this number to a more manageable level.

4.3.3. Significant terms

The first argument depends on the optical structure of final focus systems with the characteristic phase advance pattern; most elements are located $(\pi/2 + n\pi)$ away from the IP.

Expressed in local coordinates the aberrations we are looking at, coming from the potential part of the Hamiltonian, are expressed as polynomials in the $\{x, y, \overline{\delta}\}$ coordinates.

Upon linear transformation to the IP, the coordinates are transformed according to $x \rightarrow a\overline{x} + b\overline{p}_x$ and $y \rightarrow a\overline{y} + b\overline{p}_y$. The phase pattern however ensures that $a/b = \text{cotg}\ \Delta\phi \ll 1$ and it is therefore sufficient to consider the leading term in $\overline{p}_x$. In other words an aberration x^n in local coordinates is transformed into the ${\overline{p}_x}^n$ at the IP and we can neglect the other terms $({\overline{p}_x}^{n-1}\ \overline{x}, \ldots)$. The only significant chromatic terms for example are ${\overline{p}_x}^2\overline{\delta}$ and ${\overline{p}_y}^2\overline{\delta}$ which happen to be corrected at the IP. The $\overline{x}\ \overline{p}_x\ \overline{\delta}$ and $\overline{y}\ \overline{p}_x\ \overline{\delta}$ are negligible.

This argument greatly reduces the potential number of aberration one has to investigate. In fact we can define the G'_n polynomials analogous to the G_n defined above but expressed in the set of $\{\overline{p}_x, \overline{p}_y, \overline{\delta}\}$. This now gives a total number of 56 aberrations to be studied at order up to five.

There is finally the case of the two elements at the center of the two CCS which are "in phase" with the IP, more exactly $n\pi$ away from the IP. Aberrations from these quadrupoles are expressed at the IP as functions of the $\overline{x}$ and $\overline{y}$ coordinate functions $(H(\overline{x}, \overline{y}))$. Since they are of order zero in the $\overline{p}_x$ and $\overline{p}_y$ functions their Poisson bracket with these functions are identically zero $([H(\overline{x}, \overline{y}), \overline{x}] = [H(\overline{x}, \overline{y}), \overline{y}] = 0)$ and there is no effect from these terms on the spot size at the IP. One might argue that the next leading term, in this case $\overline{x}\ \overline{p}_x\ \overline{\delta}$ and $\overline{y}\ \overline{p}_y\ \overline{\delta}$, do affect the spot size. However their coefficients are smaller than that of the main terms by a factor $a/b \gg 1$ and they are negligible.

The only remaining concern for these two elements is their possible interaction with other aberrations coming from elements at the other phase, sextupoles for example, as this

can lead to higher order effects.

The second argument to reduce the number of term is the further removal of terms that do not have an effect on the beam size at the IP. We are already working with the G'_n polynomials so the only remaining such terms are the purely chromatic $\overline{\delta}^n$. The conjugate of the energy deviation is the time of flight coordinate but since the bunch length is not a critical issue at the FFTB we will simply drop these chromatic terms (6 terms at order up to 5).

Finally there are a few terms at lower order that we have to consider despite the first argument given above. The first order $H = \overline{x}$ and $H = \overline{y}$ for example represent the angular steering of the beam at the IP. They are not too critical for the FFTB where this effect is largely dominated by the dispersion correction scheme. Also two geometric terms $\overline{x}\overline{p}_x$ and $\overline{y}\overline{p}_y$ must be included. These terms are difficult to produce within the FFTB for the reasons exposed above but they could be present in the form of correlations in the incoming beam. They represent a β-function mismatch at the IP. The leading terms ${\overline{p}_x}^2$ and ${\overline{p}_y}^2$ represent a motion of the waist or α-function mismatch at the IP. The Beta-Matching section at the entrance of the line will correct for these "aberrations".

Finally the count of the aberrations to be studied comes to 54 terms compared to the 252 we previously envisioned. And this number is only the number of possible terms, the number of actual aberrations involved is certainly lower.

4.4. Summary

Before turning to the systematic study of the FFTB aberrations the following table shows a summary of the situation. At first and second order we have only induced aberrations. At higher orders the distinction can be made between the geometrics and the chromatics. Recall that the chromatics can be built from the aberrations at one order lower times the momentum deviation $\overline{\delta}$. The geometric aberrations introduced at order n correspond to the $2n$-multipole principal term and all its variations (*cf.* the polynomial G_n above).

I have mentioned in broad terms the main aberration or the main source for each entry above. For example *quadrupole* under the term G_2 means not only the normal quadrupole aberrations (strength error, *etc.*) but also the skew quadrupole terms. The geometric term G_5 comes from decapolar fields and should not be present at the FFTB as will be shown

order 1	2	3	4	5
steering	*quadrupole*	*sextupole*	*long sextupole*	*?*
G'_1	G'_2	G'_3	G'_4	G'_5
	dispersion	*chromaticity*	*second order chrom.*	*chromatic breakdown*
	$G'_1\ \overline{\delta}$	$G'_2\ \overline{\delta}$	$G'_3\ \overline{\delta}$	$G'_4\ \overline{\delta}$
		$G'_1\ \overline{\delta}^2$	$G'_2\ \overline{\delta}^2$	$G'_3\ \overline{\delta}^2$
			$G'_1\ \overline{\delta}^3$	$G'_2\ \overline{\delta}^3$
				$G'_1\ \overline{\delta}^4$

Table 4.1. The classification of aberrations at the FFTB up to fifth order in the Hamiltonians. The G_n are polynomial at order n representing the geometric aberrations only. The source or the main effect for these aberrations is also mentioned at each order for both the geometrics and the chromatics. The geometric fifth-order terms figure in this table since they are mathematically possible at this point; The analysis will show that none of these terms can appear.

later in this chapter. In the case of chromatic terms I quote only the dominant aberration at each order. The following discussion now details these aberration term by term.

4.5. First and Second Order

The linear, first and second order, design lattice of the line has been removed already so that the aberrations listed in this section are all induced, appearing only because of errors and misalignments.

At first order we have to consider not only the $\overline{p}_x$ and $\overline{p}_y$ terms which represent the steering of the beam at the IP, but also the $\overline{x}$ and $\overline{y}$ terms representing the angular steering. The angle of the beam at the IP is not very important at the FFTB since we have a one-beam experiment. In a real collider like the SLC where both beams share part of the machine this is an important parameter. At the NLC with separate exit channels for the spent beams, this parameter is not so important in the point of view of the optics. It is however a cause of luminosity degradation and potential source for high backgrounds as experienced at the SLC and therefore should not be neglected.

At the FFTB we have correctors close to the final quadrupoles in order to steer the beam at the IP, or control the $\overline{p}_x$ and $\overline{p}_y$ terms. The angular steering terms will be dominated by the dispersion control mechanism.

The number of geometric effects to consider at second order is also increased with respect to the rules laid out in the previous sections: On top of the three terms representing the waist motion and the principal coupling term (first three lines in table 4.2), I have added two terms representing the change of β-function at the IP. Finally two chromatic terms are present and can be built from the first order geometrics times the energy deviation. They represent the dispersion terms.

monomial	status	origin
$\overline{p}_x{}^2$	quadrupole	quad. strength
$\overline{p}_y{}^2$	quadrupole	or sext. Horiz. offset
$\overline{p}_x\overline{p}_y$	coupling	quad. rotation or sext. V offset
$\overline{x}\ \overline{p}_y$	negligible	
$\overline{y}\ \overline{p}_x$	negligible	
$\overline{p}_x\overline{\delta}$	dispersion	quad. offset
$\overline{p}_y\overline{\delta}$	dispersion	or dipole strength

Table 4.2. Catalog of the second order aberrations at the FFTB. The terms shown as negligible should not appear at the FFTB IP. They are beta-matching terms and should be treated in the appropriate section at the head of the beamline.

Let me now detail the origin and cure for these aberrations.

The leading geometric terms ($\overline{p}_x{}^2$, $\overline{p}_y{}^2$ and $\overline{p}_x\overline{p}_y$) are caused by strength errors in quadrupoles, rotation of quadrupoles or offsets in sextupoles. The first two are β-matching terms, the last one is a coupling term.

The $\overline{p}_x{}^2$ term for example represents a motion of the waist away from the nominal focal point; its effect is to introduce here correlations between $\overline{x}$ and $\overline{p}_x$ or to tilt the phase ellipse. In terms of twiss parameters it is a change of the α-function. The $\overline{x}\ \overline{p}_x$ term on the other hand changes the widths of the distributions without affecting the orientation of the ellipse. This is interpreted as a change of the β-function in the corresponding plane.

The β-matching section (BM) and a skew quadrupole in the final transformer correct for these effects at the FFTB. The two terms $\overline{xp}_x$ and $\overline{yp}_y$ are small per the argument of

the preceding sections, although they could arise from a mismatched beam at the entrance of the line. They can be corrected in the BM section.

The main coupling term $\overline{p}_x\overline{p}_y$ is corrected by placing a skew quadrupole in the dispersion-free region of the FT where both β-functions are high. The next two terms for coupling ($\overline{x}\,\overline{p}_y$ and $\overline{p}_x\overline{y}$) correspond to a rotation of the beam in physical $x-y$ space but are small as we have shown.

They too can appear however in the incoming beam although, as mentioned in chapter 1, it is expected that they will be small. Note that even in the BM section there is no location where we could place skew quadrupole to control this rotation of the beam in phase space efficiently.

The second order chromatic effects can be obtained by multiplying all the first order terms by $\overline{\delta}$. Only two significant terms appear here: the dispersion in both planes. This induced effect appears from offsets in quadrupoles, or other multipoles or if dipoles depart from their nominal setting. Generally dispersion arises whenever the beam is offset in a chromatic element. It is easy to see this by calculation of the similarity transformation $e^{-:d_x x':}e^{:H_\xi:}e^{:d_x x':}$ where H_ξ is the chromaticity Hamiltonian. Of course, as shown in chapter 2, this is equivalent to intuitively replacing the function x by the function $x+d_x$ in H_ξ.

Following this remark, dispersion correction can be applied by intentionally creating an orbit offset in a region with high chromaticity quadrupoles. At the FFTB we use this technique in the final triplet, creating a bump with maximum offset at the final quadrupoles and zero position offset, but some angular offset, at the IP. Large amounts of incoming or internally generated dispersion can be corrected using this technique; the equivalent of seven sigmas at the IP for the FFTB.

These second order terms are all induced effects and we can see that after careful analysis we have to really worry about five of them: two for the motion of the waists, one coupling term and dispersion in both planes.

Before embarking for the third and higher orders, let me outline here the general approach one might use for this kind of systematic studies. The mechanism can be divided in three steps.

- The background lattice

Consider first a lattice containing only simple bending magnets and quadrupoles. I first suppose that the chromaticity of any given quadrupole is not too strong. The study of the aberrations introduced here is simple as we can limit ourselves to the first order of the expansion of the CBH theorem when combining elements together. In other words there is no need to consider the interactions between elements, the sum of the different Hamiltonians is sufficient to represent the beamline. At this point most of the aberrations present are induced; They are mostly a first and second order problem as will be outlined in chapter 5.

Table 4.3 lists the aberrations that can possibly be present in the line according to this model, separated in inherent and induced terms.

monomial	status	origin
$\overline{p}_x$	induced	dipole setting, quad offset
$\overline{p}_y$	induced	dipole rotation, quad offset
${\overline{p}_x}^2$	induced	quad setting error
${\overline{p}_y}^2$	induced	(idem)
$\overline{p}_x\overline{p}_y$	induced	quad rotation
$\overline{p}_x\overline{\delta}$	induced	quad offset, dipole setting
$\overline{p}_y\overline{\delta}$	induced	quad offset, dipole rotation
${\overline{p}_x}^2\overline{\delta}$	inherent	quadrupoles
${\overline{p}_y}^2\overline{\delta}$	inherent	quadrupoles

Table 4.3. The aberrations arising from the presence of the background lattice. The only higher order term is the chromaticity of the quadrupoles.

- Chromaticity correction

If we now assume that we have to worry about the very strong final quadrupoles, let us add to this picture two pairs of sextupoles in a dispersive region. They have to be placed and set so that their geometric effects cancel and the total chromaticity of the line is zero in both planes. This can be achieved by looking at the simple sum of the Hamiltonians, in other words there are still no interactions between elements in this picture. This is the work realized by most matrix based optics code that perform a "matching" of the T matrix to cancel a few terms.

Since the high chromaticity terms are laid out in view of this cancellation, they are all located at the same phase with respect to the IP. In other words, their Poisson brackets vanish and they cannot generate higher order terms.

- Interactions

Since the background lattice and the large terms themselves cannot generate higher order effects, it has to be their interactions that trigger those unwanted aberrations.

Let me first mention a general rule that is obvious when considering the Poisson bracket. The interaction of two Hamiltonians of order n and m respectively gives, through the Poisson bracket, a Hamiltonian of order $n + m - 2$.

This simple rule shows for example that the cross terms between the sextupole geometrics and a quadrupole chromaticity are of order $(3 + 3 - 2 = 4)$ or octupole-like. Similarly, in order for a given Hamiltonian to trigger lower order terms, one has to take its Poisson bracket with a term of order one to effectively "degrade" the resulting order.

Since it is the interaction of those large terms with the background lattice that generates the unwanted higher order aberrations, the number and importance of such higher order terms is limited by the number and importance of the large terms present in the first place.

In particular once we have shown the presence of a new term coming from this Poisson bracket interaction, we could in principle take again the Poisson bracket of this new term with other elements and generate even higher order terms. But since this new term has for coefficient the product of the coefficients of its generators and one of them is not large, the resulting aberration is not expected to have a very significant effect. However this moderate effect could, if coupled to a very strong third term generate another moderate effect but at even higher order.

But obviously there has to be an end to this argument since there are only a limited number of very strong elements in this lattice, mostly the four sextupoles and the final quadrupoles.

With these essential ideas laid out, let me turn back to the systematic study of the FFTB lattice.

4.7. Third order

The only significant sources of third order geometric aberrations at the FFTB are sextupoles. For this reason they are placed in pairs separated by a $-I$ module as shown in chapter 1 and 3. There are no third order geometric aberrations remaining at the IP. They cannot inherently appear from interactions between elements since we have removed the linear optics, second order, already. They can appear if induced by a detuned quadrupole inside the $-I$ modules. The tolerances are estimated in the next chapter.

Third order chromatic aberrations are built from the aberrations at second order times $\overline{\delta}$. The main terms are of course the chromaticities in both planes, $\overline{p}_x{}^2\overline{\delta}$ and $\overline{p}_y{}^2\overline{\delta}$, arising in quadrupoles as well as sextupoles located in a dispersive region. Chromaticity correction at the FFTB ensures that these terms vanish.

A careful study of the aberration picture at the FFTB shows that the above statement about the chromaticity terms vanishing is not true for the horizontal plane. There is some residual horizontal chromaticity at the IP. This is needed to achieve the maximum bandwidth and is found using a computer-based optimization. Since the chromaticity alone would reduce the bandwidth, this shows that there must be one or more other terms which are not exactly cancelled and whose effect counteracts to some extent that of the chromaticity term.

A likely candidate is the so-called second-order dispersion $\overline{p}_x\overline{\delta}^2$ which appears from the chromaticity of a quadrupole placed in a dispersive region. The main chromaticity term is, in local coordinates, $x^2\overline{\delta}$ where x is really the transverse displacement of the particle which is composed of a geometric as well as a dispersive part. Changing x into $x+\eta\overline{\delta}$ in this chromatic term reveals the second-order dispersion. This term is small but not negligible. Since there is no vertical dispersion in the line, there cannot be a vertical second-order dispersion term. The following shows the value of the dispersion function across the energy bandwidth at the FFTB, clearly revealing the second as well as third order dispersion.

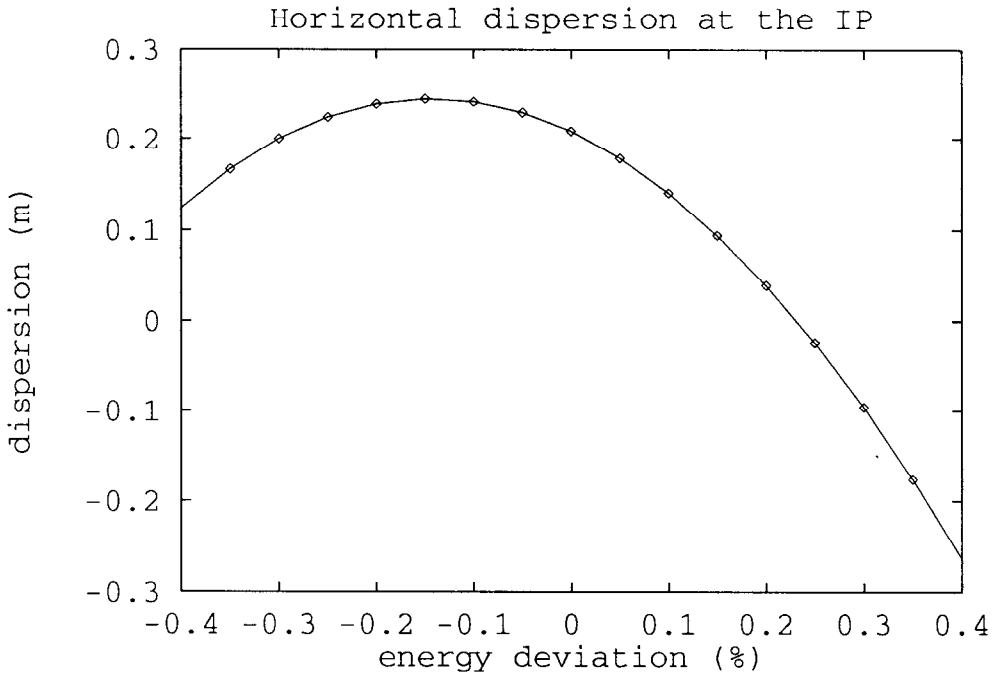

Figure 4.1. Horizontal dispersion at the FFTB IP across the energy bandwidth of the line. The slope at the origin indicates a second-order dispersion term while the curvature shows a third-order dispersion effect.

Note that there is some linear dispersion present at the IP according to this graph. The beamline used to obtain this data was an early version (FFTB68) and was not exactly matched. The contribution of this dispersion pattern to the IP spot size is only 0.01 μ^2 or an increase of the horizontal spot size of about 0.5%. The vertical spot size is not affected.

This second order dispersion is indeed the only inherent third order aberration in the FFTB design. All other aberrations are cancelled or simply do not appear. Note finally that this aberration is inherent to the design of the FFTB and cannot be eliminated. In other designs by K. Brown and R. Helm, this effect is cancelled by adding to the symmetry of the system. The formation of 2π modules for the CCS in the Brown-Helm design allows for the suppression of the BX section, so that the CCS are the only sections with non-zero horizontal dispersion. Inside the CCS all the quadrupoles are paired with a $-I$ transform in between and the same dispersion function at both quadrupoles. Each pair of quadrupoles locally cancel the second order dispersion and the net effect disappears. This is essentially the case at the FFTB inside the CCS. Outside the CCS however every quadrupole in a dispersive region contributes to the second-order dispersion.

The suppression of this term using the symmetry of Brown-Helm allows for a simpler optics design where one does not have to rely on a cancellation of two different effects to achieve the desired momentum bandwidth. The number of elements is higher and the overall length is increased however, one reason why this design was not chosen for the FFTB in the first place. It seems that final focus systems for the next generation of linear colliders would benefit from a more symmetric design, allowing the total cancellation of all inherent third order aberrations.

4.8. Fourth order

There are no octupole or higher order multipole at the FFTB so geometric fourth order effects have to arise from interactions. The only possibility is the interaction of two sextupolar geometric effects. More exactly it is the effect of the length of the sextupoles that appears here. This effect has already been discussed in chapter 1 and is described in detail in appendix B. Since it is exactly of octupolar form it could be easily corrected by the insertion of an octupole in the final tranformer for example. The effect is small enough however that we have decided not to implement the correction.

The skew octupole terms on the other hand cannot appear at the FFTB, except as induced by multipole errors in quadrupoles or other magnets.

In principle a fourth order geometric effect could also arise from the interaction of two different sextupoles but since they are placed in pairs at the FFTB, such an interaction is impossible. Another possibility would be the feed-down of a decapolar field in conjunction with a first order steering effect, effectively steering the beam off-axis in the decapole. But there are no such magnets at the FFTB.

Fourth order chromatic aberrations are a little more complicated. There are several potential sources:

- Quadrupole-Quadrupole interaction

The chromaticities of two quadrupoles located at different phases can trigger a term of the form $[\overline{p}_x{}^2\overline{\delta}, \overline{x}^2\overline{\delta}] = -4\ \overline{p}_x\ \overline{x}\ \overline{\delta}^2$ but due to the presence of the $\overline{x}$ this effect is expected to be small. This new term is a variation of the second-order chromaticity term $\overline{p}_x{}^2\overline{\delta}^2$. The same term in the other plane appears also.

- Quadrupole-Sextupole interaction

The same effect can appear from the interaction of a quadrupole with the chromaticity of the sextupoles, with the same comment on the strength.

Actually this result is obvious when one considers the treatment of the CCS using similarity transformation presented in chapter 3. Equation (3.36) shows five fourth order terms arising in the CCS: $\overline{x}\ \overline{p}_x\ \overline{\delta}^2$ and $\overline{yp}_y\overline{\delta}^2$ have already been identified. Also appearing are the interactions with the sextupole geometric aberrations: $\overline{x}\ \overline{p}_x{}^2\ \overline{\delta}$, $\overline{x}\ \overline{p}_y{}^2\ \overline{\delta}$ and $\overline{y}\ \overline{p}_x\ \overline{p}_y\ \overline{\delta}$.

But following arguments presented earlier in this chapter, the effects of these fourth order aberrations will be small owing to the fact that they all contain a $\overline{x}$ or $\overline{y}$ component.

4.9. Fifth order

As I recalled in the preceding paragraph, the whole CCS has already been treated in chapter 3 and equation (3.36) showed already the apparition of the fifth order aberrations. They are all important in the sense that none of them contains a $\overline{x}$ or $\overline{y}$ factor.

The other way to see those aberrations appear is to consider the fourth order aberrations of the preceding section and write their Poisson brackets with the strong chromatic aberrations of the final quadrupoles.

The two treatments are of course equivalent and correspond to two different ways to take the chromaticity into account. From the source point of view with the final quadrupoles or from the correction point of view with the analysis of the CCS.

Of course we have no decapoles at the FFTB and therefore no geometric fifth order aberrations are present.

4.10. Higher order

In order to get even higher order effects, we need to identify another strong source of aberrations. However the fifth order we have just described already takes into account all the large aberrations at the FFTB: the sextupoles and the final quadrupoles with the central quadrupoles of the CCS. There is just no possible combination that would give a sizable aberration of order higher than five in this line. Of course it is in theory possible to get very high order terms given a sufficient number of aberrations at third and higher order and these terms certainly exist in the case of the FFTB if one takes into account the exact

phase advance of all the elements. However the precise phase advance adjustment required for the chromaticity correction and to avoid the geometric aberrations form the sextupoles is enough to guarantee that these terms at order higher than five are minuscule, by ensuring that the large terms are in the right location, at the "right phase".

4.11. Conclusion

This chapter has exposed the approach made at the FFTB in order to evaluate the aberration content of the line. Some important results have been given, both for the FFTB and in view of a NLC:

At third order, the imperfect symmetry of the FFTB leaves the second order horizontal dispersion term uncorrected. I have mentioned that a solution to this problem is to adopt a higher symmetry lattice using 2π modules for the CCS and suppress the non-symmetric parts of the line: the dispersive parts of the Beta-Matching and the Final Transformer as well as the Beta Exchange section.

This would allow the correction of all inherent third order terms. At fourth order the long-sextupole aberration seems impossible to avoid. The correction of this aberration could be done with an additional octupole corrector. Other fourth order aberrations could be suppressed if we could change the linear lattice in order to avoid having a quadrupole placed at the wrong phase with respect to other elements. This would also suppress the fifth order terms. It is interesting to see that to some extent the high-order aberration content of the line is so much dominated by the linear lattice. The same is true for tolerances which we will consider in the next chapter.

5. Stability Tolerances.

5.1. Tolerance Budget.

We have chosen a criterion for the allowed increase in spot size from the FFTB aberrations. Since we expect about five aberrations in each plane and the experience with measuring small spots at the interaction point of the SLC shows that it is possible to measure a relative change of 10% in the size of the beam, the maximum allowed increase per aberration is set at 2%. We believe, following recent SLC experience, that with the ability to detect a 10% change in the spot size it is possible to tune out an aberration down to the 2% level.

This 2% IP spot size increase criterion, with σ_0 the nominal spot size and $\Delta\sigma$ the contribution of some aberration, can be expressed as

$$(\sigma_0^2 + (\Delta\sigma)^2)^{1/2} \leq 1.02\ \sigma_0 \tag{5.1}$$

which translates into

$$\Delta\sigma \leq \frac{1}{5}\ \sigma_0 \tag{5.2}$$

It is convenient to apply a linear transformation to the preceding formula back to the location where the aberration appears, *i.e.* where the kick occurs, which leads to an equivalent condition to the 2% criterion:

$$(\Delta x')_{rms} \leq \frac{1}{5}\sigma_{x'} \tag{5.3}$$

Now the coordinates are local and we compare an RMS value of the kick to the local divergence of the beam.

In terms of Hamiltonians, a kick is the action of a Hamiltonian on the coordinates of the particle through the Lie transformation: $e^{:H:}x' = x' + [H, x'] + ... = x' + (\Delta x') + ...$

Therefore if the Hamiltonian form of an aberration is known, one can derive the condition ensuring that this aberration does not enlarge the spot size by more than 2% of the linear value.

At the FFTB the total beam size growth above design is then expected to be 8% in the horizontal plane (4 contributing terms) and 14% in the vertical plane (7 contributing terms). In the following discussion we will quote tolerances according to this 2% criterion for individual elements. However as different elements can contribute to the same aberration and if one assumes that their departures from design are not correlated, one must combine their tolerances in quadrature to find the tolerance for this group, t_g, which give a 2% increase in spot size:

$$\frac{1}{t_g^2} = \sum_{i \in g} \frac{1}{t_i^2} \tag{5.4}$$

where t_i is the 2% tolerance for each individual element. We also refer to t_g as the RMS tolerance for the group.

We usually separate the elements into two or more sets from most sensitive to least sensitive, and can allocate a fraction of the 2% budget to each group, the largest fraction to the most sensitive group. Within each group, g, we can then calculate an RMS tolerance for the group, t_g according to

$$\frac{1}{t_g^2} = \left(\sum_{i \in g} \frac{1}{t_i^2}\right) \frac{1}{f_g} \tag{5.5}$$

where f_g is the fraction of the 2% allocated to this group.

5.2. **Steering.**

Our tolerances on steering permit beam centroid motion at the interaction point to be one standard deviation of the horizontal and vertical distributions *i.e.* we allow the spot to move by $\Delta x^* \approx \sigma_x^*$ and $\Delta y^* \approx \sigma_y^*$.

This criterion is different from the one quoted above and would clearly not be sufficient for a collider where the beams could miss each other by too much. However at the FFTB we have only one beam and the Orsay Beam Size Monitor[37] is insensitive to the position of the beam at the IP. Other methods such as the Laser-Compton monitor proposed by T. Shintake (KEK) or the liquid wires developed by F. Villa (SLAC) are sensitive to the spot position at the IP and a movement of no more than a fifth of the spot size should be allowed. The scaling of tolerances for steering aberrations is linear.

The expansion of the quadrupole Hamiltonian, in the presence of a displacement d_x, $H_q = \frac{1}{2}\, k_q\, ((x + d_x)^2 - y^2)$, gives the Hamiltonian of the "steering aberration": $H_{st} = k_q d_x x$ and the corresponding kick $[H_{st}, x'] = k_q d_x$ giving the condition $k_q d_x \leq \sigma_{y'}$ or

$$d_x \leq \frac{1}{k_q}\sqrt{\frac{\epsilon_x}{\beta_{x_q}}} \tag{5.6}$$

and similarly

$$d_y \leq \frac{1}{k_q}\sqrt{\frac{\epsilon_y}{\beta_{y_q}}} \tag{5.7}$$

The individual tolerances are presented on figure 5.1 for the horizontal plane and figure 5.2 for the vertical plane. Ignoring for now the final lenses (QC2, QX1, QC1 and FQ on the graphs) the tolerances range from 1 to 10 microns in the horizontal plane and from 0.5 to 5 microns in the vertical. Note that the two quadrupoles located at the midpoints of the two CCS have loose tolerances due to their phase relations ($n\pi$) with the IP. Taking the RMS value as defined above for these tolerances the RMS tolerances for all quadrupoles except the final triplet are 0.75 microns and 0.2 microns for the horizontal and vertical planes respectively.

The case of the final quadrupole triplet can be treated separately as these lenses are strongly tied together[3] and the dominant motion will be one of all quadrupoles moving in the same direction and by the same amount.

A very simple model of this final triplet is that of a non-realistic single optical lens focusing a parallel beam in both planes. The tolerances on the motion of the lens is then equal to the criterion we choose, in other words a given movement of the final lens moves the beam by the same amount at the focus ($(d_x)_{fq} \approx \sigma_x^*$ and $(d_y)_{fq} \approx \sigma_y^*$). This simple model gives estimates for the tolerances on the final quadrupoles motions of the order of 1 micron and 60 nanometers for the FFTB.

A more detailed calculation uses the fact that steering is a linear effect and one can simply sum, or actually integrate, the effects of all three lenses when displaced by the same amount:

$$\Delta x^* = \int ds\; k_q(s)\; d_x\; \sqrt{\beta_x(s)\beta_x^*}\; \sin\Delta\phi^{s\rightarrow *} = \int ds\; k_q(s)\; d_x\; R_{12}^{s\rightarrow *} \tag{5.8}$$

and a similar expression for the other plane. The tolerances for the final quadrupoles taken

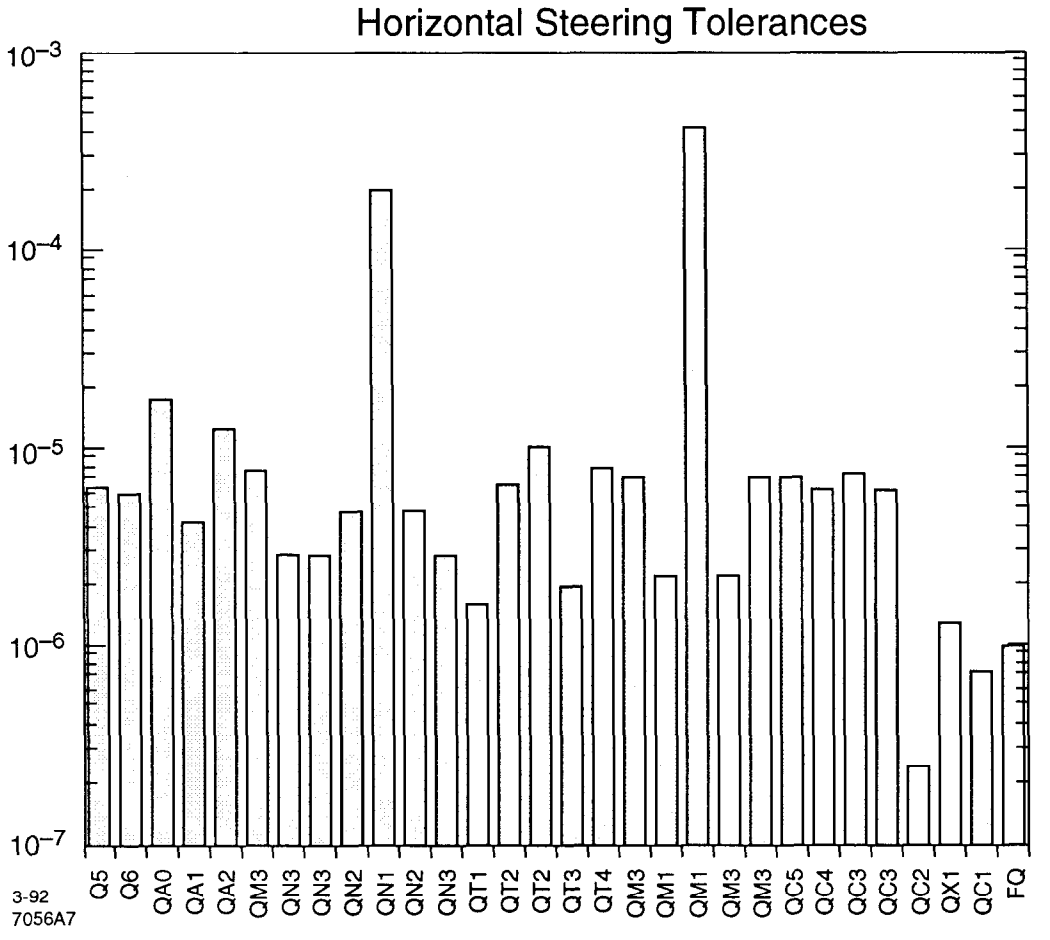

Figure 5.1. Horizontal steering tolerances at the FFTB, in meters. These values for individual elements stability tolerances correspond to a steering of one sigma of the beam distribution at the IP. The value quoted for the final quadrupoles taken as a single lens (FQ) correspond to the simple minded optical model mentioned in the text, approximating the final lenses to a parallel-to-point focusing system.

as a single unit are extremely close to those obtained through the simple model above or $d_x \leq 1\mu$ and $d_y \leq 60nm$.

The steering tolerances are indeed very tight but it should be emphasized that at least one of the foreseen method of determining the spot size at the FFTB, the Orsay BSM, is insensitive to the beam position. The Compton-Laser spot size monitor will be attached directly to the final quadrupole support table so motion of the final lenses should not affect it either. Excluding the final doublet we expect that the spot position at the IP will be dominated by the beam jitter from the linac. We have the ability at the FFTB to control this position jitter at the level of one fifth of the spot size by means of a feedback system after the end of the linac. Slower drifts of the spot position at the IP can be controlled by

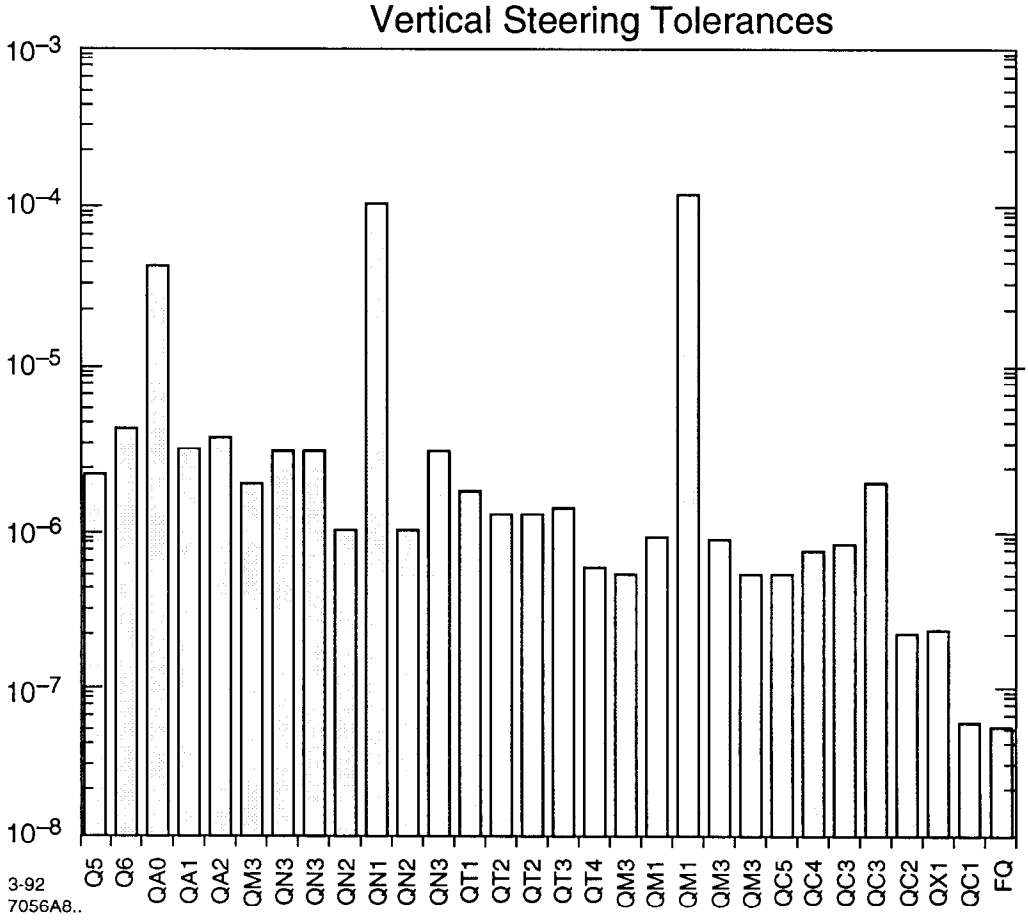

Figure 5.2. Vertical steering tolerances at the FFTB, in meters. These values for individual stability tolerances correspond to a steering of one sigma of the beam distribution at the IP. The value quoted for the final quadrupoles taken as a single lens (FQ) correspond to the simple minded optical model mentioned in the text.

feedback using a pair of air-core correctors close to the final quadrupoles.

5.3. **Dispersion.**

Dispersion arises from an offset of the beam in quadrupoles and is a consequence of the chromaticity of the quadrupole. The Hamiltonian of a quadrupole including chromatic effects is $H_q = \frac{1}{2}\frac{k_q}{1+\delta}(x^2+y^2) = \frac{1}{2}k_q(\ldots - x^2\overline{\delta} + y^2\overline{\delta} + \ldots)$ with the second form showing only the chromaticity terms. In the presence of a displacement d_x, the Hamiltonian becomes $H_q = \frac{1}{2}k_q(\ldots - x^2\overline{\delta} - 2d_x x\overline{\delta} + \ldots)$, which shows the dispersive term $H_d = k_q d_x x\overline{\delta}$.

The 2% criterion is then written $k_q d_x (x\overline{\delta})_{rms} \leq \frac{1}{5}\sigma_{x'}$ or, since there are no more corre-

lations between the geometric part of the position of the particles and their energies,

$$d_x \leq \frac{1}{5\ k_q\ \overline{\delta}_{rms}} \sqrt{\frac{\epsilon_x}{\beta_{xq}}} \tag{5.9}$$

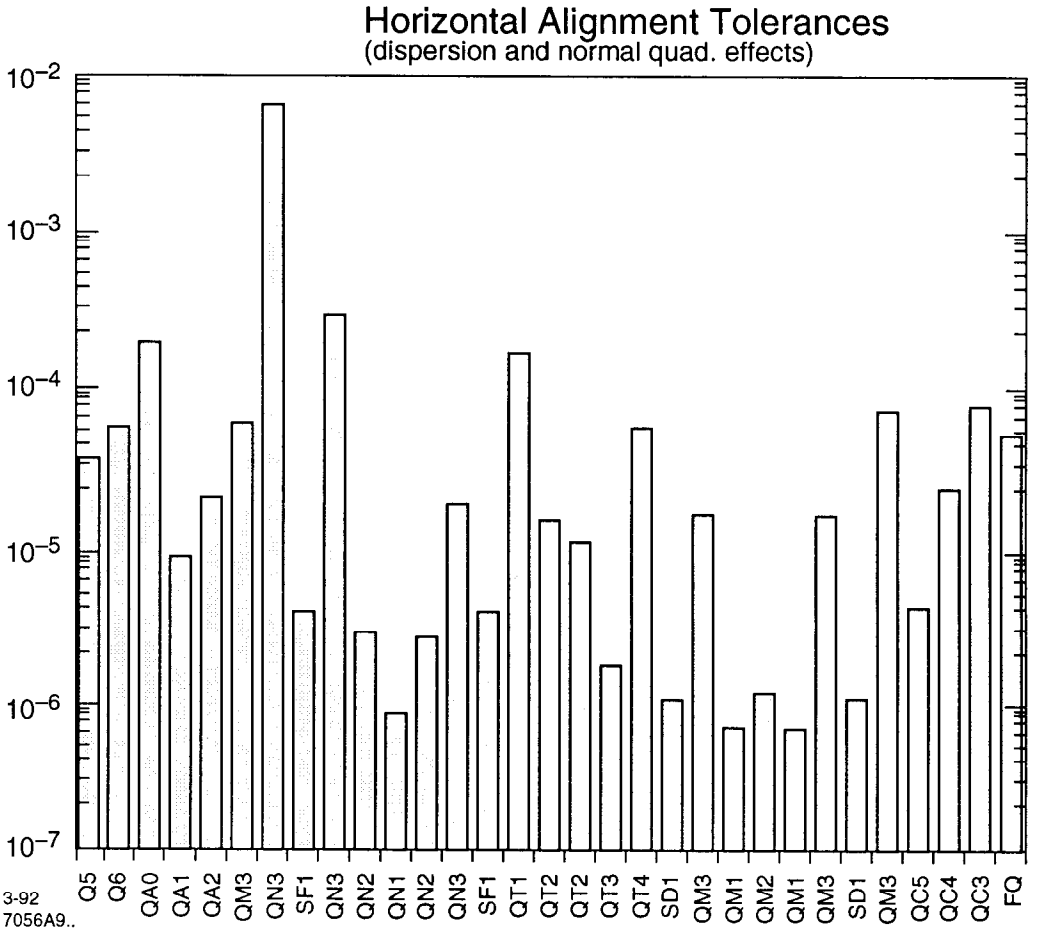

Figure 5.3. Horizontal alignment tolerances at the FFTB, in meters. These values include the effect of dispersion both created directly and as a consequence of the orbit oscillation launched by a displaced quadrupole. Also included is the normal quadrupole effect induced by a horizontal offset in sextupoles. This second effect dominates the tolerances for sextupoles and the elements within both CCS.

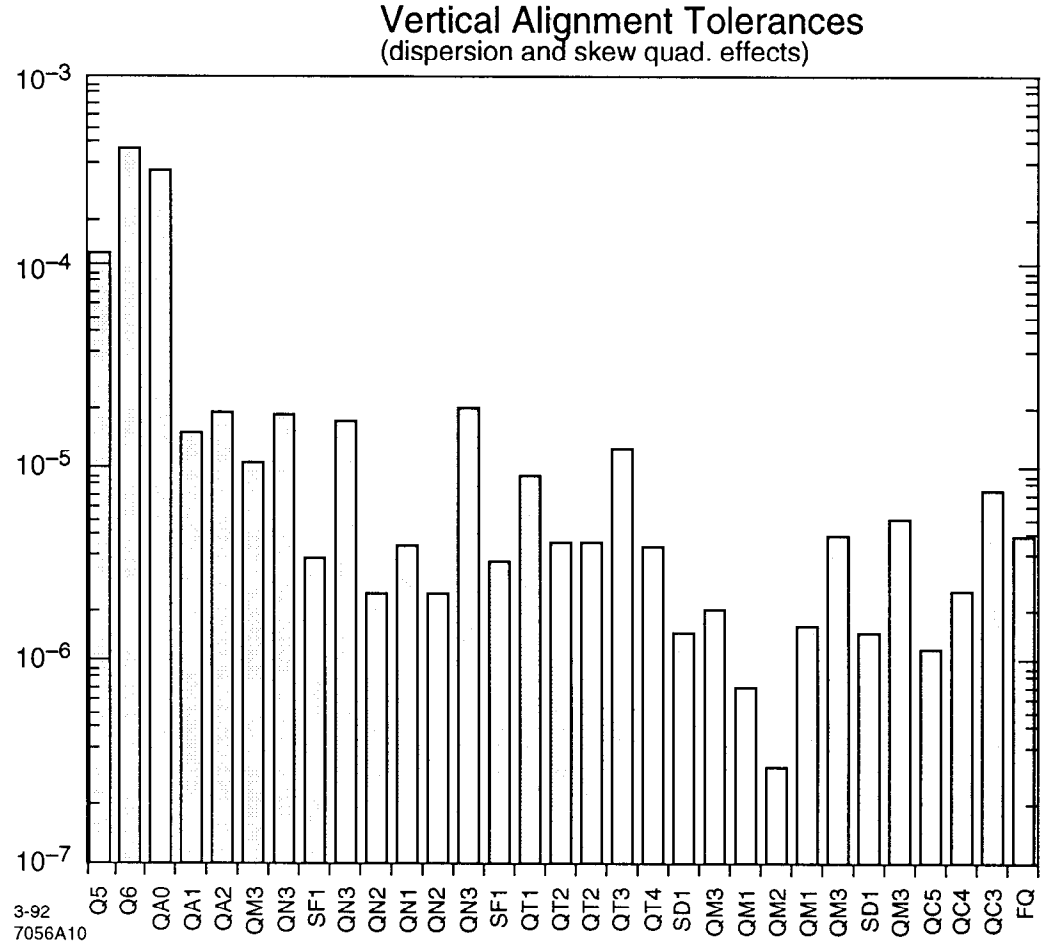

Figure 5.4. Vertical alignment tolerances at the FFTB, in meters. These values include the effect of dispersion both created directly and as a consequence of the orbit oscillation launched by a displaced quadrupole. Also included is the skew quadrupole effect induced by a vertical offset in sextupoles. This second effect dominates the tolerances for sextupoles and the elements within both CCS.

5.3.1. Final quadrupoles

Under the same model of a single lens focusing parallel to point, we have $k_q \sim \frac{1}{f}$ the inverse focal length of the system and the above expression can be approximated by

$$d_x \leq \frac{1}{5\,\overline{\delta}_{rms}}\sigma_x^* \tag{5.10}$$

Note that even the formula (5.9) above is only an approximation of the correct expression because the Hamiltonian we considered in the first place is a kick approximation and does not take into account the thick lens effects which are particularly important for the final

quadrupoles. Taking this into account one gets

$$d_x \leq \frac{1}{5\ \delta_{rms}} \frac{\sigma_x}{\xi_x} \tag{5.11}$$

where σ_x is taken at the center of the final quadrupole and $\xi_x = \int k_q \beta_x(s) ds$ is the horizontal chromaticity of the final quadrupole.

5.3.2. Other quadrupoles

The offset at the final quadrupole can be created by a direct movement of the final quadrupole or by a displacement of another quadrupole upstream steering the beam off-axis in the final lens. To study this second effect we introduce the notion of lattice multipliers defined as the amplification factor between the offset of a given quadrupole and the centroid offset in the final quadrupole. Note that the two displacements have opposite signs in the hamiltonian, hence the minus sign in the following formula.

$$(d_x)_{fq} = -(k_q R^{12}_{q \rightarrow fq})\ (d_x)_q \tag{5.12}$$

Lattice multipliers depend only on the lattice structure, not on the focal point parameters or the beam properties. The greater this multiplier the tighter the dispersion tolerances on the element.

For most quadrupoles at the FFTB this second part is dominant over the direct dispersion generated by the displaced quadrupole itself. In fact the lattice multipliers are so large in the FT that we use this property to globally cancel dispersion at the IP: Intentionally creating a controlled orbit offset in the final lenses gives us the ability to generate up to seven sigmas of dispersive contribution to the beam at the IP. Of course this bump is not closed across the IP and the beam is at an angle there. The closure is easily done in the dump line. This is not a problem for the FFTB where we have only one beam. It would cause a loss of luminosity for a real collider. The SLC is very sensitive to this effect for masking reasons since the outgoing beam must travel on the same path as the opposite incoming beam. Future linear colliders will have separate exit paths for the outgoing beam and therefore the situtaion is very similar to that of the FFTB.

5.3.3. Sextupoles

Sextupoles are also chromatic elements in the presence of a main dispersion term and their displacement, either directly or by orbit offset, is therefore source of dispersion. The Hamiltonian of a sextupole in a dispersive region is $H_s = \frac{k_s}{3!}(\ldots + 3\eta_x\bar{\delta}x^2 - 3\eta_x\bar{\delta}y^2 + \ldots)$ and translates into $H_s = \frac{k_s}{3!}(\ldots + 6\eta_x\bar{\delta}d_x x - 6\eta_x\bar{\delta}d_y y + \ldots)$ in the presence of displacements d_x and d_y.

This effect through orbit offsets is to be added to the previous ones when determining the alignment tolerance of a given quadrupole.

The figures 5.3 and 5.4 present the results of these tolerances calculations. For quadrupoles outside the CCS, these numbers are those for dispersion only. One notices that the front quadrupoles have very loose tolerances. This is obvious since the chromaticity from these front quadrupoles to the IP is corrected, therefore an orbit oscillation will produce dispersion in each chromatic element but these different contributions also cancel each other at the IP. On the other hand, as already mentioned, the tolerances for a few elements in the FT are very tight since the chromaticity from there to the IP is only that of the final quadrupoles and is not cancelled.

For quadrupoles inside the CCS, these graphs present also another effect which is analyzed later. Horizontal and vertical beam offsets in sextupoles also produce quadrupole and skew quadrupole components. These effects in fact dominate the tolerances for those elements situated within a sextupole pair and the associated tolerances are derived in section 5.5.2 and 5.7.2 .

5.4. **Normal Quadrupole.**

A change in quadrupole strength will result, for most quadrupoles at the FFTB, in a movement of the waist away from the focal point and cause an increase of the spot size at the focal point. The Hamiltonian representing this aberration is $H = \frac{1}{2}\,\Delta k\,(x^2 - y^2)$ giving a kick $\Delta x' = \Delta k\; x$. The 2% increase criterion for the horizontal plane is

$$\begin{aligned} \Delta k\;(x)_{rms} &\leq \frac{1}{5}\sigma_{x'} \\ \Delta k &\leq \frac{1}{5}\frac{\sigma_{x'}}{\sigma_x} \\ \Delta k &\leq \frac{1}{5\beta_x} \end{aligned} \tag{5.13}$$

and finally the strength tolerance is, considering both planes:

$$\frac{\Delta k}{k} \leq \frac{1}{5\ k\ \mathrm{Max}(\beta_x, \beta_y)} \tag{5.14}$$

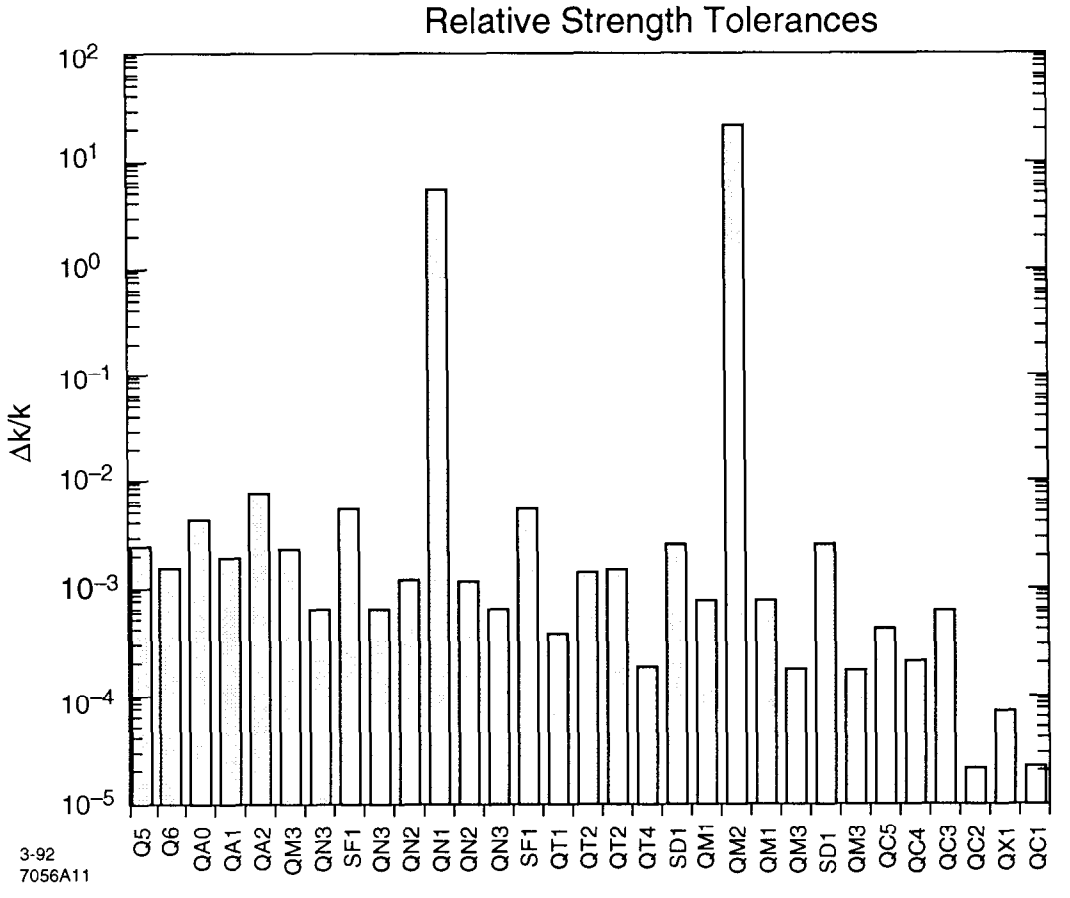

Figure 5.5. Strength stability tolerances at the FFTB. Note that the expression of these tolerances for sextupoles is not derived in the text and corresponds to individual sextupole tolerances. Placing each pair of sextupole on a single power supply would increase the tolerances accordingly.

Individual tolerances are shown on figure 5.5. The final quadrupoles have the tightest tolerances as expected; the strength of QC2 and QC1 must be controlled at the level of $\Delta k/k = 2.\ 10^{-5}$, requiring special power supplies. Other quadrupoles in the line typically have tolerances of the order of a few 10^{-4} up to a few 10^{-3}. The tightest tolerances for quadrupoles other than the final lenses are achieved for those elements around the sextupoles in the CCY with $\Delta k/k \sim 1.7\ 10^{-4}$. The RMS tolerance for all quadrupoles except the final triplet is $\Delta k/k = 7.3\ 10^{-5}$ which is a tight value for usual magnet power supplies.

However these tolerances may be relaxed in the specific case of the Orsay BSM. This device is not sensitive to the longitudinal position of the waist within the length of a slit of typically 400 microns, and the depth of focus at the FFTB is of the order of $\beta_y^* = 100\mu m$, allowing the waist to move around the nominal position without affecting the measurement of the minimum spot size. A 2% increase in spot size corresponds to a waist movement of 20 microns for the nominal $\beta_y^* = 100\mu$. In the case of other spot size monitors such as the liquid wires, we will have to meet these tight tolerances.

The FFTB power supplies have been specified according to these values. The goal for their stability is 0.001% or 10^{-5} of the full power for both long and short term stability. Some magnets do not solicit the full power from the power supplies so this value will not be as good for the real current delivered. It is expected however that the tolerances presented here will be met.

Finally some higher order effects are also triggered by strength errors of quadrupoles within the CCS. The tolerances[56] for these effects are at the level of $\frac{\Delta k}{k} \leq 10^{-3}$ and therefore should not be a problem.

5.5. **Horizontal Sextupole Alignment.**

5.5.1. Sextupoles

The same quadrupole effect (waist motion) appears when the beam is horizontally offset in a sextupole. The Hamiltonian of a sextupole in the presence of a horizontal displacement is

$$\begin{aligned} H_s &= \frac{k_s}{3!}((x+d_x)^3 - 3(x+d_x)y^2) \\ &= \frac{k_s}{3!}(\ldots + 3d_x x^2 - 3d_x y^2 + \ldots) \end{aligned} \tag{5.15}$$

which shows a quadrupole aberration of the form

$$H_a = \frac{k_s d_x}{2}(x^2 - y^2) \tag{5.16}$$

The condition for the 2% criterion is then

$$d_x \leq \frac{1}{5\ k_s\ \mathrm{Max}(\beta_x, \beta_y)} \tag{5.17}$$

The tolerance for horizontal sextupole alignment in the CCX is 3.5μ while it is only 0.9μ

for the CCY where the vertical β-function is very large (*cf.* figure 5.3).

5.5.2. Orbit offset

Similar to the dispersion case, a sextupole offset can be the consequence of an actual sextupole displacement or a quadrupole upstream steering the beam off-axis in the sextupole. The notion of multipliers applies also here with the reference being now at the sextupole.

$$(d_x)_s \;=\; k_q \, R^{12}_{q\to s} \, (d_x)_q \tag{5.18}$$

The tolerance on quadrupole alignment regarding this effect is obtained by summing over the subsequent sextupoles:

$$(d_x)_q \leq \sum_{s>q} \frac{(d_x)_s}{k_q \, R^{12}_{q\to s}} \tag{5.19}$$

Two sextupoles of the same pair have the same d_x tolerance and are separated by a $-I$ transformation, therefore if the beam is off-axis in the first sextupole the effect will be cancelled by the equal and opposite displacement in the second sextupole of the pair. This means that quadrupole alignment within a sextupole pair is of special importance and the orbit jitter or a quadrupole displacement before entering the chromatic correction section is not crucial for this aberration*.

This effect is reflected in figure 5.3. The horizontal alignment tolerances of quadrupoles within the CCS are dominated by this effect. Notice that the central quadrupole in the chromatic correction section is especially ill-placed with regard to this effect since its position maximizes the multiplier to the second sextupole. This leads to very tight tolerances for these central quadrupoles: 0.7μ for QN1 in the CCX and 1.0μ for QM2 in the CCY

$\star$ It is of importance for other aberrations like dispersion.

5.5.3. Bending magnets

Finally another source of orbit offset at the sextupoles are the fluctuations of the field, through power supply jitter, in bending magnets. Because of the length of these magnets and the fact that optical functions vary a lot across them, we define the multipliers as an average across the magnet; The $\overline{R_{12}}$ is the average value of the R_{12} between the value at the entrance and the value at the exit of the bend. Several bending magnets connected in series to one power supply are treated as one large bend. The displacement induced at the sextupole,

$$(d_x)_s \;=\; \Delta\theta\; \overline{R^{12}_{b\rightarrow s}}, \tag{5.20}$$

yields the tolerance on power supply stability since $\theta \propto B$:

$$\frac{\Delta B}{B} \leq \frac{1}{5\; k_s\; \overline{R_{12}}\; \theta\; \mathrm{Max}(\beta_x, \beta_y)_s} \tag{5.21}$$

Notice that since, by design of the CCS, we have $\overline{R_{12}}\;\theta \;= 2\eta_x$ at the sextupole, the preceding formula can be rewritten, with $\xi_x = 2\; k_s\; \eta_x\; \beta_x$ and $\xi_y = 2\; k_s\; \eta_x\; \beta_y$ the horizontal and vertical chromaticities introduced by the sextupole pair:

$$\frac{\Delta B}{B} \leq \frac{1}{5\;\mathrm{Max}\;(\xi_x\;,\;\xi_y)} \tag{5.22}$$

Here also only the bends between the sextupoles of a pair are significant for this effect. Field jitter of bending magnets outside these sections contribute to other aberrations such as dispersion. The stability on the power supplies for the bends has to be better than $3.3\;10^{-5}$ for the CCX and only $1.0\;10^{-5}$ for the CCY. This last value corresponds to the goal set for the power supply stability at full power. It is also the tightest requirement for power supplies at the FFTB, even tighter than the tolerances set for the stability of the final lenses.

Note finally that this calculation accounts only for the geometric effect of the sextupoles. The change in bending angle also creates additional dispersion at the sextupole and therefore an additional chromatic kick. The change in dispersion from a bending field error is actually equal to the beam offset at the sextupole $\overline{R_{12}}\; d\theta$. This chromatic effect is however smaller than the geometric effect by a factor $\bar{\delta}$, so that the tolerance is looser by a factor $1/\bar{\delta}_{rms}$ or about 400.

5.6. **Skew Quadrupole.**

The roll, rotation around the longitudinal axis, of a quadrupole by an angle θ introduces a skew-quadrupole component of strength $k_{sq} = k_q \sin 2\theta$ which couples the horizontal and vertical planes. In the limit of small angles the Hamiltonian of the skew-quadrupole aberration is

$$H_{sq} = \frac{1}{2}\, k_q\, \sin 2\theta\, (2\, xy) \approx 2\, k_q\, \theta\, xy \tag{5.23}$$

giving one kick in each plane. However in the flat beam regime, which is the case for most final focus systems, *i.e.* with $\epsilon_x \gg \epsilon_y$, the effect of coupling $x \rightarrow y$ is dominant so we can consider the vertical kick only. The tolerance criterion is

$$2\, k_q\, \theta\, \sigma_x \leq \frac{1}{5}\, \sigma_{y'} \tag{5.24}$$

$$\theta \leq \frac{1}{10\, k_q\, \sqrt{\beta_x \beta_y}} \sqrt{\frac{\epsilon_y}{\epsilon_x}} \tag{5.25}$$

Except for the final quadrupoles, all lenses in the line have tolerances better than 100 μrad when taken individually. The RMS value however is only 40 μrad. Note that the two high values for QN1 and QN2 are not significant since the above formula was obtained in the approximation of small angles. However these two magnets are located at a multiple of π in phase away from the IP and therefore their rotations does not affect the final spot size.

The final doublet has much tighter roll tolerances with a lowest for QC2 where the product $\beta_x \beta_y$ is very high. Note that for a general final doublet, it has been shown by John Irwin that the rotation tolerances of both lenses are the same. In our case, with the split final lens (QX1-QC1), this property is verified if we consider this split final lens to be one unique element. This tolerance is of the order of 10 μrad. However for practical purposes the last three lenses can be considered to be one single rigid body, tied together by the stabilization table designed by KEK. Using this model, the rotation tolerance for the QC2-QX1-QC1 group is 33 μrad.

A skew quadrupole has been placed in the final transformer where the product $\beta_x \beta_y$ is maximum. This element can correct only one phase of the coupling, the $\overline{p}_x \overline{p}_y$ term. I have

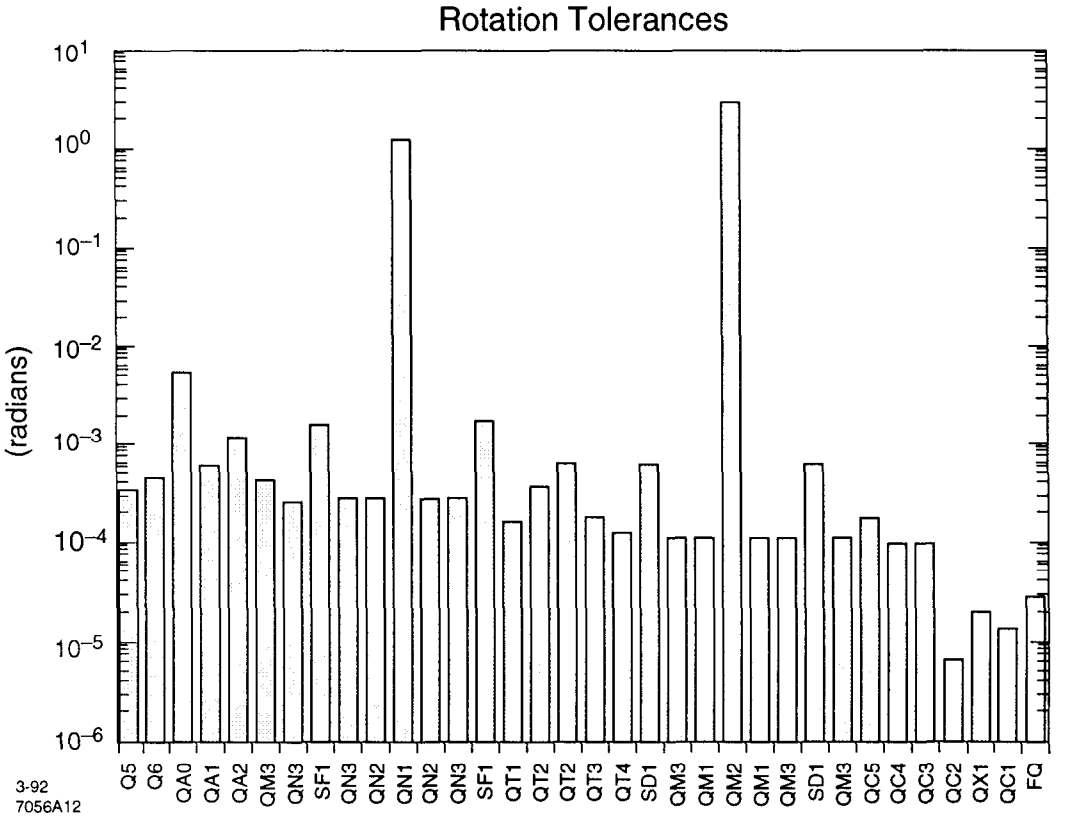

Figure 5.6. Quadrupole rotation (roll) tolerances. Note that the formula used here assumes a small angle approximation so the two peaks obtained for QN1 and QN2 are meaningless. These two magnets being $(n\pi)$ away in phase from the IP do not influence the size of the beam through this effect, which is the real meaning of these large values. For the sextupoles, the tolerances are estimated for the geometric skew-sextupole effect.

argued already* that, due to the phase advance pattern at the FFTB, this term is the only one that can arise significantly in this line. Incoming coupling from the linac is corrected in the Beta Matching section using two skew quadrupoles.

Also on figure 5.6 are the tolerances for sextupole rotation. The effect considered here is that of the geometric skew sextupole. The tolerances are higher than those for the quadrupoles, at the level of one to two milliradians.

$\star$ *cf.* chapter 4.

5.7. Vertical Sextupole Alignment.

5.7.1. Sextupoles

The same coupling effect arises when the beam is vertically offset in a sextupole. Similar to the normal quadrupole case this can be caused by a sextupole displacement, vertical steering from a quadrupole offset or dipole rotation inside the CCS. The Hamiltonian of a sextupole in the presence of a vertical displacement is

$$\begin{aligned} H_s &= \frac{k_s}{3!}(x^3 - 3x(y+d_y)^2) \\ &= \frac{k_s}{3!}(\ldots - 6d_y xy + \ldots) \end{aligned} \tag{5.26}$$

showing a skew-quadrupole aberration of the form

$$H_s = \frac{k_s d_y}{2} xy \tag{5.27}$$

Using only the vertical kick again, the condition for the 2% criterion is then

$$d_y \leq \frac{1}{5\ k_s \sqrt{\beta_x \beta_y}} \sqrt{\frac{\epsilon_y}{\epsilon_x}} \tag{5.28}$$

As shown on figure 5.4, the tolerances are 3.5 μm and 1.4μm for respectively CCX and CCY.

The following table summarizes the sextupole alignment tolerances for both the horizontal and vertical displacements.

	Horizontal	Vertical
CCX	3.5 μm	3.5 μm
CCY	0.9 μm	1.4 μm

Table 5.1 Sextupole alignment tolerances at the FFTB.

5.7.2. Orbit offset

The same effect we have seen for dispersion and normal quadrupole tolerances appears here: a quadrupole offset upstream of the sextupoles can generate an orbit offset in the sextupoles leading to a skew-quadrupole effect. Similarly to the case of horizontal sextupole offset, this can only happen for quadrupoles located in the CCX or the CCY, within a sextupole pair. The effects from the two sextupoles cancel each other for a quadrupole offset in the BM or BX sections.

The multipliers for quadrupole vertical alignment tolerances are

$$(d_y)_s \;=\; k_q \; R^{34}_{q\to s} \; (d_y)_q \tag{5.29}$$

Here also the two quadrupoles at the midpoint of the CCS maximize these multipliers and this leads to tolerances of 4 μm for CCX and only 0.3 μm for the CCY. The latter is the tightest alignment tolerance at the FFTB. This quadrupole is physically located inside the Beam Switch Yard where the temperature is expected to be stable. Special care must however be given to the alignment of this critical lens. Some diagnostic and correction tools to control this skew quadrupole effect are also being designed.

5.7.3. Bending magnets

The rotation of bending magnets within the CCX and CCY also leads to an orbit offset in the sextupoles. The multipliers for bending magnet rotation, defined as the ratio of the orbit offset at the sextupoles to the dipole rotation angle $\Delta\phi$ leads to the following tolerances,

$$\Delta\phi \leq \frac{1}{5\; k_s\; \overline{R_{34}}\; \sqrt{\beta_x \beta_y}\; \theta} \sqrt{\frac{\epsilon_y}{\epsilon_x}} \tag{5.30}$$

where $\overline{R_{34}}$ is the average value of the R_{34} across the bends taken separately.

The rotation tolerances are $\Delta\phi \leq 37\ \mu rad$ for the CCX but only $\Delta\phi \leq 14\ \mu rad$ for the CCY. This is the tightest rotation tolerance at the FFTB.

5.8. **Sextupole and Skew Sextupole.**

The tolerances on the sextupole and skew sextupole content of quadrupoles are usually expressed as a ratio of the allowed sextupole or skew sextupole field component to the nominal quadrupole field taken at some reference point (usually 70% of the aperture of the magnet) $(B_{ns}/B_q)_{a=a_r}$. One can also express this in terms of some equivalent sextupole strength k_{ns} given by

$$\left(\frac{B_{ns}}{B_q}\right)_{a=a_r} = \frac{k_{ns} a_r}{2k_q} \tag{5.31}$$

The general sextupole Hamiltonian, neglecting chromatic effects as well as the effect of dispersion, $H_{ns} = \frac{k_s}{3!}(x^3 - 3xy^2)$, can give rise to three different kicks, two in the horizontal plane and one in the vertical plane. We first derive the 2% criterion condition for each kick.

- x kick from the x^3 term $\Delta x' = \frac{k_{ns}}{2}x^2$

$$\frac{k_{ns}}{2}(\sqrt{2}\sigma_x^2) \leq \frac{1}{5}\sigma_{x'} \tag{5.32}$$

$$k_{ns} \leq \frac{\sqrt{2}}{5\sigma_x \beta_x} = t_{x1} \tag{5.33}$$

- x kick from the xy^2 term $\Delta x' = \frac{-k_{ns}}{2}y^2$

$$\frac{k_{ns}}{2}(\sqrt{2}\sigma_y^2) \leq \frac{1}{5}\sigma_{x'} \tag{5.34}$$

$$k_{ns} \leq \frac{\sqrt{2}}{5\sigma_y \sqrt{\beta_x \beta_y}} \sqrt{\frac{\epsilon_x}{\epsilon_y}} = t_{x2} \tag{5.35}$$

- y kick from the xy^2 term $\Delta y' = -k_{ns}xy$

$$k_{ns}\ \sigma_x \sigma_y \leq \frac{1}{5}\sigma_{y'} \tag{5.36}$$

$$k_{ns} \leq \frac{1}{5\sigma_x\ \beta_y} = t_y \tag{5.37}$$

For the compounding of these conditions, one notices that the effect of the x and y kicks are orthogonal in the sense that they affect respectively the horizontal and vertical spot size; therefore we can take the minimum of the two conditions — one in each plane — as the final expression for sextupole field tolerances.

For the two conditions related to the x kick, one can consider that they are separate aberrations affecting the same parameter and that their effects are therefore to be added in quadrature. The tolerance t_x is then given by $1/t_x^2 = 1/t_{x1}^2 + 1/t_{x2}^2$ and we finally have

$$k_{ns} \leq \mathrm{Min}\left[\frac{\sqrt{2}}{5\sigma_x\beta_x\sqrt{1+\sigma_y^4/\sigma_x^4}} \; ; \; \frac{1}{5\sigma_x\beta_y} \right] \tag{5.38}$$

The same calculation can be made for the skew-sextupole component with the Hamiltonian $H_{ss} = \frac{k_s}{3!}(3x^2y - y^3)$, giving two vertical and one horizontal kicks, and yields

$$k_{ss} \leq \mathrm{Min}\left[\frac{\sqrt{2}}{5\sigma_y\beta_y\sqrt{1+\sigma_x^4/\sigma_y^4}} \; ; \; \frac{1}{5\sigma_y\beta_x} \right] \tag{5.39}$$

Although these numbers represent tight tolerances, the quadrupole magnets received at SLAC from INP (Novosibirsk) have all met or exceeded these tolerances, according to the magnetic measurements carried out at INP and SLAC.

The final quadrupoles represent an additional challenge with even tighter tolerances, especially for QC2. Recent results from KEK have shown that it is possible to meet and exceed these tolerances by using trim windings: In order to suppress the drift of the quadrupole center with magnet excitation, the use of trim windings has been suggested by Nakayama at KEK. The excitation of the trims being proportional to that of the main coils. A side effect of this method, observed on the prototype magnet, is the cancellation of the sextupole and skew sextupole terms in these final quadrupoles to a level better than the required tolerances.

Additionally we have proposed a global correction of these terms by use of two sextupole and two skew-sextupole correctors in the Final Transformer. These four small magnets would allow us to tune out the four terms appearing in the two Hamiltonians quoted above. If the trim windings of the final quadrupoles to be installed in the tunnel also suppress the sextupolar components of these lenses, these correctors might not be needed.

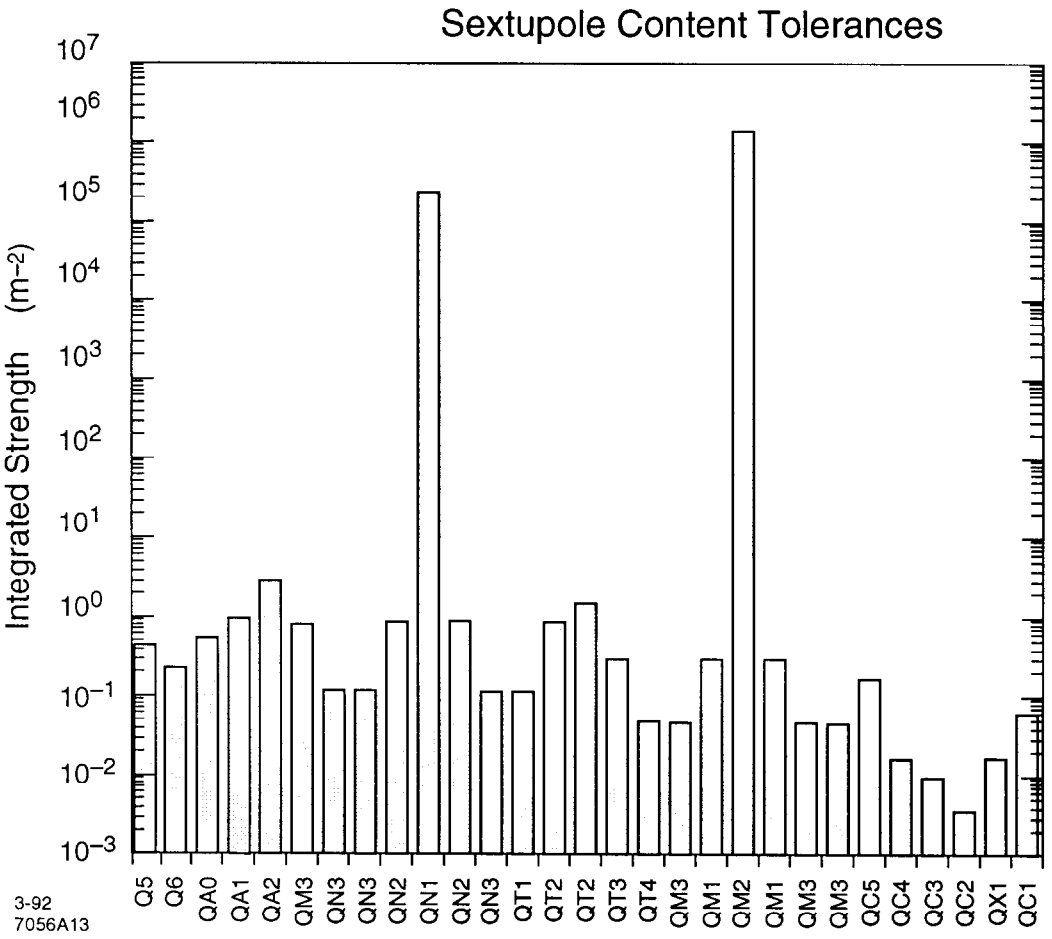

Figure 5.7. Sextupole and skew sextupole harmonic tolerances in quadrupoles. The worst of the two components is shown here. The tolerance is expressed in terms of equivalent integrated strength. The main sextupoles at the FFTB have an integrated strength of about 20 m^{-2}.

5.9. Conclusion

I have shown in this chapter how we obtained stability tolerances for the FFTB. The use of Lie algebra based methods is here limited to the expression of the kick in most cases. The study of sextupolar tolerances however is one where the combination of the different terms is greatly simplified by the use of the Hamiltonian formulation of the source of the effects. For all these calculations however it would be possible to derive the same results without Lie algebra formulation. However it is my experience that Lie algebra based methods, as presented in the previous chapters, provide here also a very convenient and clear framework for this type of studies.

For all practical purposes the stability tolerances are very tight at the FFTB. The SLC final focus has looser tolerances by typically an order of magnitude when compared to the

FFTB. Studies[23] have shown that tolerances for a final focus system for a next generation linear collider, typically a 500 GeV per beam machine, will be tighter by another order of magnitude.

Of particular importance in the results of this chapter is the notion of lattice multipliers. The optics of final focus systems typically alternate very high and very low β-functions. This leads naturally to high lattice multipliers. It is not always possible to limit the values of these β-functions but it should be possible, at least very desirable, to suppress the ill-placed elements such as the two central quadrupoles located at the symmetry points of both CCS. The position tolerances of these two elements are the tightest of all at the FFTB.

Another important result is the level of stability required for the bending magnets, especially in the CCY. They hold the tightest tolerances for strength and roll stability, aside from the final lenses of course.

Much is to be learnt from the tuning and operation of the FFTB and this is especially true for tolerances. Whether one can achieve the stability levels required here is one issue. The other question is, if the stability tolerances cannot be achieved, do we have a mechanism by which one can go around the limitations by using simple feedback systems and careful tuning strategies for example? We believe that it is possible to relax some initial tolerances at the FFTB by as much as an order of magnitude by using beam-based alignment techniques and bump-based quadrupole tuning schemes. Global correctors such as the dispersion suppression and the sextupole corrector magnets are other techniques that are being investigated at the FFTB.

Conclusion

The Final Focus Test Beam is now well underway and the first beam should be delivered by spring 1993. This will be the start of a very interesting period on the way to future linear colliders. We will test on a full scale machine the hardware we think is critical for the NLC. The beam position monitors, magnet movers, wire scanners and a number of stabilization and monitoring devices will be commissioned. The software side will also be scrutinized with the correction and tuning techniques that are now being developed at SLAC. These are especially important for their potential impact on the tolerances. The optics itself will be probed of course, and once the tuning and corrections are applied, the measurements techniques will be commissioned: the Orsay-Beam Size Monitor, but also the liquid wires and the Laser-Compton device. I think we can expect a great harvest of information with the FFTB and certainly learn even more than we did with the SLC final focus. Parallel to this design work on NLC final focus lattices is being pursued.

The FFTB is also unique in the sense that it is the first beamline for which Lie algebra based techniques were used from the design up to the derivation of correction and tuning procedures. They have certainly proven helpful in all the areas of the work. The mechanisms of cancellation and the generation of new higher order aberrations is now very well understood. The fact that the list of aberrations at the FFTB is closed at fifth order has been shown using these tools. Finally the tolerances have been analyzed with those same methods and already some ideas have emerged in order to reduce some of them. Part of the problem has been identified as coming from the first order design of the line. Work is underway in different laboratories to confirm this. Some ideas have also been proposed to design ways to cope with others, or find techniques for monitoring the stability of the line with a precision better than the tolerances. Quadrupole tuning at the FFTB is one of these techniques that uses bumps to precisely test the local lattice and detect a strength error in quadrupoles with a precision better than the tolerances. The potential consequences on the specification of tolerances for future machines could be very important; The relaxation of most tolerances by a factor two, and possibly as high as ten, is of great significance at the very tight levels we deal with.

It is my hope that the techniques exposed in this thesis will become a popular design and analysis tool for accelerator opticians. They have been around for some time but although they were known it is only recently that they have started to gain fame and momentum. I believe there are two necessary ingredients for this trend to continue: The methods need to be more widely publicized and explained and there is a need for a computer based tool. The first part is mostly a task of education and explanation. Although they are not very difficult in their mathematical basis as shown in this thesis, the learning curve for these new methods is fairly steep for newcomers and especially for people who have been using the matrix formalism for some time. It is a totally different way of seeing the basic same mechanisms although, as shown in this thesis, the two complement each other very well. Explanations and examples still need to be provided and this thesis is one attempt at this.

The other part required for the wide acceptance and use of these methods is the ability to use a computing tool that will free the user of the sometimes tedious calculations involved. Since the methods presented are so much oriented towards analytical results a code should be designed that preserves that option and allows analytical studies of a beamline as much as possible. There are a few codes that implement already some close variations of these methods. I mentioned already *Marylie* which implements Lie Algebra methods at up to third order currently. A fifth order version is being developed. A very interesting code is *Cosy-Infinity* written by M. Berz. Although it implements only Differential Algebra methods, it has been envisioned for some time to adapt it for our techniques. The originality of this code is that it provides the user with a meta-language that can be used to literally program the physics. That is the user is no longer constrained to using the physics "canned" by the programmer in a preset command; on the contrary, all the variables are accessible to the user who can define his own algorithms. Following a slightly different path and using the new, at least in our field, ideas of object oriented programming, the code *MXYZPTLK* written by L. Michelotti at Fermilab uses C++ as the programming language. The software is now reduced to a simple "class library" that the user can incorporate to his own C++ code. The class library takes care of all the implementation details and the user can concentrate on the physics.

None of these tools was found to be the ideal basis to implement the Lie Algebra methods as derived in this thesis. *Marylie* for it is a closed code that cannot be modified easily, *Cosy-Infinity* was found to be too much geared towards Differential Algebra methods and

MXYZPTLK was not tested but C++ is known to have a rather steep learning curve. The last direction of investigation to be mentioned, which I believe stands the best chance to provide us with the needed tool is *Mathematica*.[33] This code was designed to perform analytical as well as numerical calculations on computers and is much in use worldwide. This ability of analytical manipulation together with a strong object oriented programming environment, the possibility for the user to define his own programs on top of the package, and the much desirable feature of interactivity makes it the ideal candidate for these studies. At SLAC, the effort is led in this direction by J. Irwin and N. Walker. Some basic optics package is already developed and a Lie Algebra tool should soon come out. On top of being a good tool for accelerator physics analysis, this should also be the ideal support for newcomers to explore these techniques through tutorials.

There is one area that has been mentioned in the first chapter of this thesis and is not solved yet by the methods that have been described. Synchrotron radiation is an essential process in final focus systems since it is the source of the main limiting terms. The stochastic nature of the process makes it impossible to describe it through a Hamiltonian formulation. The only way at present to check for this effect is, except for analytical calculations as shown in appendix A, the use of tracking methods. Most tracking codes now implement different simulations of the synchrotron radiation process. But we are back here to the "blind" approach of designing a system and checking a posteriori its validity. This area is one where some effort and new ideas are needed.

After the excellent work of Dragt and the big step made under the impulse of John Irwin, I believe that these techniques based on Lie algebra will soon become a standard tool for the accelerator physicist. There is however still a lot of room for improvements and new ideas.

Appendix A

Chromatic effects due to synchrotron radiation at the FFTB

Introduction

I review here two effects induced by synchrotron radiation and their consequences on the final spot size at the Final Focus Test Beam. The first one is the chromaticity unbalance generated in a final focus system by the energy loss in bending magnets between the sextupoles and final quadrupoles. The second more general effect is the emittance growth from radiation fluctuations. The latter has already been studied[52]by Matthew Sands and I will use his results to derive a somewhat simpler and more practical formulation of this effect. An application to the case of the FFTB is given in both cases.

Chromaticity unbalance

In a final focus system the chromaticity introduced by the very strong final lenses is cancelled at the interaction point by placing sextupoles in a dispersive region giving a chromatic kick which can be made equal and opposite to that of the final lenses.

However one needs some bending magnets inside and after the chromatic correction section to manipulate the dispersion. In these bending magnets, the particles lose energy through synchrotron radiation; the energy of the particle in the sextupoles is slightly different from its energy when it reaches the final quadrupoles. As a result the chromatic kicks do not balance each other exactly and there is an increase in the spot size at the focal point.

Katsunobu Oide has already estimated this effect[5]but I give here a more extended derivation of it.

Basic formulation

The chromatic kick given by the final quadrupoles is given by $\Delta y' = k_q \bar{\delta} y$ and is balanced by the chromatic kick at the sextupole, under the hypothesis that there is only one sextupole correcting all the chromaticity, $\Delta y' = k_s \eta \bar{\delta} y$. If the particle loses energy* between the two we have $\bar{\delta} \rightarrow \bar{\delta} - \frac{du}{E_0}$ at the final quadrupole and the net chromatic kick is

$$\Delta y' = k_q \frac{du}{E_0} y \tag{1}$$

where E_0 is the energy of the beam and du is the energy lost through radiation. The change in position at the IP is written, with y_q the particle position at the final quadrupole:

$$\Delta y^* = k_q \sqrt{\beta_q \beta^*} \frac{du}{E_0} y_q \tag{2}$$

and the increase in spot size at the IP is generally written

$$\Delta \sigma_y^* = \sqrt{\langle \Delta y^{*2} \rangle - \langle \Delta y^* \rangle^2} \tag{3}$$

Because the two variables y_q and du are not correlated in first approximation as there is no design vertical dispersion, and since this effect does not change the centroid of the beam $\langle y_q \rangle$ which remains zero we have

$$\langle \Delta y^* \rangle \propto \langle du \rangle \langle y_q \rangle = 0 \tag{4}$$

and

$$\begin{aligned} \langle \Delta y^{*2} \rangle &= k_q^2 \beta_q \beta^* \frac{1}{E_0^2} \langle du^2 y_q^2 \rangle \\ &= k_q^2 \beta_q \beta^* \frac{1}{E_0^2} \langle du^2 \rangle \langle y_q^2 \rangle \\ &= k_q^2 \beta_q \beta^* \frac{1}{E_0^2} \langle du^2 \rangle \sigma_{y_q}^2 \\ &= k_q^2 \beta_q^2 \frac{1}{E_0^2} \sigma_y^{*2} \langle du^2 \rangle \end{aligned} \tag{5}$$

Finally if we replace $k_q \beta_q$ in the previous expression by $\xi_y = \int_{line} k_q \beta(s) ds$; *i.e.* if we assimilate the chromaticity of the final quadrupoles to that of the entire line† we have for the spot size increase at the focal point:

$\star$ Note that I define $\bar{\delta} = \frac{p - p_0}{p}$

$\dagger$ this is a valid assumption in final focus systems where most of the quadrupole chromaticity comes from the final quadrupoles

$$\frac{\Delta\sigma_y^{*2}}{\sigma_y^{*2}} = \frac{\xi_y^2}{E_0^2}\langle du^2\rangle \tag{6}$$

Energy loss considerations

There are two terms in the energy loss through synchrotron radiation. The first one is the so-called "classical or average energy loss" $\langle du\rangle$; the second one is a consequence of the quantum nature of synchrotron radiation and leads to an increase in the energy spread and quantum excitation of oscillations; it is stochastic in nature.

The average energy loss in our case has for a consequence that the energy of the beam at the entrance of the final quadrupoles is slightly lower than the design value, the quadrupole then focuses this beam a little upstream of the nominal IP, hence some "spot size increase" at the IP. This effect can be compensated for by retuning the quadrupoles for the new beam energy.

Also the sextupoles need retuning since the chromatic kick now given by the quadrupoles is smaller as the beam energy and the quadrupole strength are now lower than the design value. This effect will be automatically corrected for in the sextupole strength optimization procedure during the tuning of the final spot size.

We see here that the average energy loss can be compensated for and should therefore be removed from the present calculation. The stochastic component of synchrotron radiation cannot be corrected due to its very nature and this is the effect of interest to us.

One can then rewrite equation (6) as

$$\frac{\Delta\sigma_y^{*2}}{\sigma_y^{*2}} = \frac{\xi_y^2}{E_0^2}(\sigma_{du}^2 + \langle du\rangle^2) \tag{7}$$

and dropping the second term which is correctable,

$$\frac{\Delta\sigma_y^{*2}}{\sigma_y^{*2}} = \frac{\xi_y^2}{E_0^2}\sigma_{du}^2 \tag{8}$$

Note that σ_{du} represents here the fluctuations in the emission of energy with respect to the mean value $\langle du\rangle$ and is composed of two terms since the energy radiated can be

affected by two variables, the energy of the individual photons emitted and the number of photons emitted.[52] Each emission of a photon being independent of the others the first term is simply the quadratic sum over the average number of photons of the spread in the energy distribution of the photons. The second term is characterized by the spread in the number of emitted photon times the average photon energy. Since the number of emitted photon is distributed according to a Poisson distribution with mean N, the mean square of the distribution is also N

$$\begin{aligned}\sigma_{du}^2 &= (\frac{l_b}{c}N)\sigma_u^2 + \langle u\rangle^2\frac{l_b}{c}\sigma_n^2 \\ &= \frac{l_b}{c}N(\sigma_u^2 + \langle u\rangle^2) \\ &= \frac{l_b}{c}N\langle u^2\rangle\end{aligned} \tag{9}$$

and finally,

$$\sigma_{du}^2 = \frac{55}{24\sqrt{3}}\frac{\theta^3}{l_b^2}\gamma^5 r_e \lambda_e E_0^2 \tag{10}$$

Result

The final result for the increase of the spot size at the Interaction Point is then

$$\frac{\Delta\sigma_y^{*2}}{\sigma_y^{*2}} = \frac{55}{24\sqrt{3}}r_e\lambda_e\xi_y^2\gamma^5\frac{\theta^3}{l_b^2} \tag{11}$$

With a chromaticity $\xi_y \sim 17 \times 10^3$, a beam energy of 50 GeV giving $\gamma \sim 10^5$ and a bending magnet with length $l_b = 5.2\ m$ and bending angle $\theta = 7.4\ mrad$ one gets $\frac{\Delta\sigma_y^{*2}}{\sigma_y^{*2}} = 0.06$, corresponding to an increase in the spot size of $\frac{\Delta\sigma_y^*}{\sigma_y^*} = 1 - \sqrt{1+.06} \sim 3.\%$

THE WHOLE LINE

Note that the preceding calculations were made assuming one bending magnet between a single sextupole and the final quadrupoles. At the FFTB we have two pairs of sextupoles and six (groups of) bending magnets arranged in the following way:

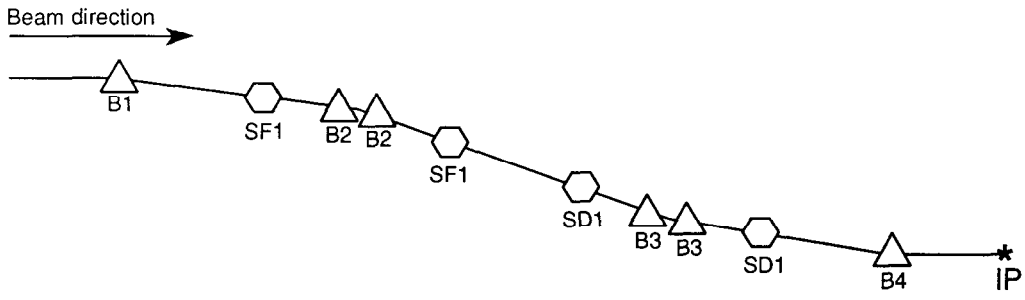

Figure 7.1. The disposition of bending magnets at the FFTB.

It is clear that magnet B_1 does not contribute to the process we describe since the total chromaticity of the line from B_1 to the interaction point is zero by design. Magnet B_4 contributes the most to this effect as it affects the full chromaticity of the final quadrupoles. Most of the vertical chromaticity is corrected in the CCY and even if we assume that 10% of it is corrected by the CCX, the effect on $\frac{\Delta\sigma^2}{\sigma^2}$ is down to the 1% level due to the square of the chromaticity appearing in the final formula. Assuming then that the whole chromaticity of the line is corrected in the CCY (we neglect the CCX altogether), each of B_3 sees only half of the total chromaticity, contributing only a factor one-fourth to the total result.

For the FFTB line we therefore have

$$\begin{aligned} \frac{\Delta\sigma_y^{*2}}{\sigma_y^{*2}} &= (1+\frac{1}{4}+\frac{1}{4})\,\frac{55}{24\sqrt{3}} r_e \lambda_e \xi_y^2 \gamma^5 \frac{\theta^3}{l_b^2} \\ &= \frac{55}{16\sqrt{3}} r_e \lambda_e \xi_y^2 \gamma^5 \frac{\theta^3}{l_b^2} \end{aligned} \tag{12}$$

Finally for the whole FFTB line we have

$$\frac{\Delta\sigma_y^{*2}}{\sigma_y^{*2}} = 0.09 \tag{13}$$

corresponding to

$$\frac{\Delta\sigma_y^{*}}{\sigma_y^{*}} \sim 4.5\% \tag{14}$$

This is the dominant remaining "design aberration" at the FFTB. By design aberration I mean an aberration which is inherent to the design and not induced by errors of any kind. The second dominant one is the thick sextupole effect which has been derived somewhere else.

EMITTANCE GROWTH

Introduction and conditions

In this section I rely on the results developed by Sands in reference [52] and I use them without further proof or explanation. However I will recall here the three conditions under which those results were obtained.

– *the transport system is linear.*

This is essential to the method since a linear system allows one to apply a solution superposition principle; namely the displacement of the trajectory as a consequence of the emission of a number of photons is just the sum of the individual displacements each emission would generate by itself. Non linear lenses complicate the process of adding the displacements at the end of the line. Although the FFTB is intrinsically non-linear (strong sextupoles are present in the lattice and the chromaticity of the final quadrupoles is very important) I will assume for the moment that this first condition is verified.

– *there is no coupling in the optics*

This condition simplifies the treatment of the problem by assuming that there exists everywhere in the line a midplane symmetry. Then the emittance growth takes place only in the horizontal plane, leaving the vertical emittance untouched (if we neglect the energy spread increase which affects both planes of course). This condition is verified in the case of the FFTB design in the absence of errors.

– *the radiation effects can be described by their characteristics on the central design trajectory.*

The main implication for the FFTB is that we neglect the radiation in quadrupoles and other lenses since the central trajectory, on-axis in those lenses assuming that we compensate this trajectory for the average energy loss along the line, sees no field hence experiences no radiation. The case of radiation in quadrupoles and the resulting limitation on the beam size at the focal point has been studied[54]for final focus systems by Katsunobu Oide. Also the weak focusing effect in bending magnets is ignored.

Results and "residual dispersion"

Sands calculates the contribution to the second moments of the beam distribution in respectively equations (10), (11) and (12) in SLAC/AP-47, where C_2 is a constant $C_2 = \frac{55}{24\sqrt{3}}\frac{r_e \hbar c}{(mc^2)^6} = 4.13 \times 10^{-11} m^2 (GeV)^{-5}$.

$$\begin{aligned}
\langle x^2 \rangle &= C_2 \int_0^L G^3 \, E^5 \, D^2 \, ds &&= \frac{C_2 E_0^5}{\rho^3} \int_0^{l_b} D^2(s) \, ds \\
\langle x'^2 \rangle &= C_2 \int_0^L G^3 \, E^5 \, D^{\dagger 2} \, ds &&= \frac{C_2 E_0^5}{\rho^3} \int_0^{l_b} D^{\dagger 2}(s) \, ds \\
\langle x x' \rangle &= C_2 \int_0^L G^3 \, E^5 \, D \, D^{\dagger} \, ds &&= \frac{C_2 E_0^5}{\rho^3} \int_0^{l_b} D(s) \, D^{\dagger}(s) \, ds
\end{aligned} \tag{15}$$

The main assumption used to get the final form in the above equations are that the energy $E(s)$ and therefore the local trajectory curvature $G(s) = 1/\rho(s)$ (in a uniform bending magnet) do not change significantly along the path of the electron. This is actually equivalent to the third condition of Sands approximating the characteristics of the radiation to that of an ideal particle on the central trajectory. The integrals have also been written assuming one bending magnet of length l_b followed by a region where $1/\rho$ is uniformly zero.

The functions $D(s)$ and $D^{\dagger}(s)$ are the "residual dispersion" functions, *i.e.* the dispersion function from point s in the bend to the end of the line, and its derivative. In *TRANSPORT* notation, they are the R_{16} and R_{26} terms calculated for the partial transport system from s to the end of the line. End of the line here refers to some arbitrary point where we want the emittance growth calculated. In the case of the FFTB this point is the final focal point (IP).

To calculate these second moments, Sands expresses the residual dispersion functions in terms of the betatron and off-energy functions ($\beta(s)$ and $\eta(s)$) as well as the phase advance along the line. I find it more convenient to use the following argument using only the knowledge of the optics in terms of linear matrices.

I can split the partial transport system (from point s to the IP) into two parts. The first one is from point s inside the bending magnet (the origin $s = 0$ is at the entrance) to the

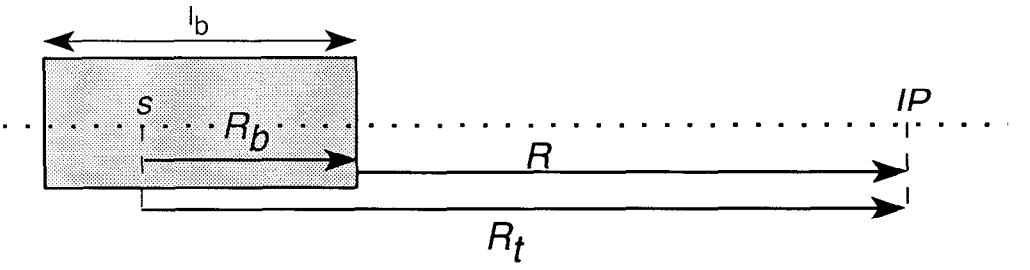

Figure 7.1. The transport system used for the calculation of emittance growth created by a single bend along with the notations used in the text.

end of the magnet and the second part is from the end of the bending magnet to the end of the line as represented on the figure below.

Let R_b and R be the respective first order transport matrices for these two parts and R_t be the first order matrix for the whole line from point s to the end so that we have $R_t = R.R_b$ and

$$\begin{aligned} D(s) &= (R_t)_{16} = R_{11}(R_b)_{16} + R_{12}(R_b)_{26} + R_{16} \\ D^{\dagger}(s) &= (R_t)_{26} = R_{21}(R_b)_{16} + R_{22}(R_b)_{26} + R_{26} \end{aligned} \tag{16}$$

Now we assume that we know the design of the line to first order and therefore the R_{ij} are known. We also know that, upon the assumption that the energy is not varying too much when the particle emits a photon and therefore ρ does not change along the magnet, the dispersion functions have the following expression inside the bending magnet of length l_b:

$$(R_b)_{16} = \frac{1}{2}\frac{(l_b - s)^2}{\rho} \qquad \text{and} \qquad (R_b)_{26} = \frac{(l_b - s)}{\rho} \tag{17}$$

It is then trivial to carry out the integrals in equation (15). We have obtained here the second moments of the distribution of particles induced by the the energy loss process in one single magnet, and observed at some point in the line. The formula depends only on the physical characteristics of the bend (length L and radius of curvature ρ on the central trajectory) the energy of the beam E_0 and the linear optics between the bend and the point

of observation (R matrix) :

$$\begin{aligned}
\langle x^2 \rangle &= \frac{C_2 E_0^5}{\rho^5} L \left[\frac{L^4 R_{11}^2}{20} + \frac{L^3 R_{11} R_{12}}{4} + \frac{L^2 R_{12}^2}{3} + \frac{L^2 R_{11} R_{16} \rho}{3} \right. \\
&\left. + L R_{12} R_{16} \rho + R_{16}^2 \rho^2 \right] \\
\langle x'^2 \rangle &= \frac{C_2 E_0^5}{\rho^5} L \left[\frac{L^4 R_{21}^2}{20} + \frac{L^3 R_{21} R_{22}}{4} + \frac{L^2 R_{22}^2}{3} + \frac{L^2 R_{21} R_{26} \rho}{3} \right. \\
&\left. + L R_{22} R_{26} \rho + R_{26}^2 \rho^2 \right] \\
\langle x x' \rangle &= \frac{C_2 E_0^5}{\rho^5} L \left[\frac{L^4 R_{11} R_{21}}{20} + \frac{L^3 R_{12} R_{21}}{8} + \frac{L^3 R_{11} R_{22}}{8} + \frac{L^2 R_{12} R_{22}}{3} \right. \\
&\left. + \frac{L^2 R_{21} R_{16} \rho}{6} + \frac{L^2 R_{11} R_{26} \rho}{6} + \frac{L R_{22} R_{16} \rho}{2} + \frac{L R_{12} R_{26} \rho}{2} + R_{16} R_{26} \rho^2 \right]
\end{aligned} \tag{18}$$

Emittance growth

The calculation of the emittance growth from these formulas is justified by Sands in the definition of the RMS emittance as the three quantities $\langle x^2 \rangle$,$\langle x'^2 \rangle$ and $\langle x x' \rangle$ combined according to

$$\epsilon_x{}^2 = \langle x^2 \rangle \langle x'^2 \rangle - \langle x x' \rangle \tag{19}$$

The folding of two RMS emittances ϵ_a and ϵ_b, under the assumption that the transport system is linear, is given by the addition in quadrature of the individual elements defining the emittance:

$$\begin{aligned}
\langle x^2 \rangle_f &= \langle x^2 \rangle_a + \langle x^2 \rangle_b \\
\langle x'^2 \rangle_f &= \langle x'^2 \rangle_a + \langle x'^2 \rangle_b \\
\langle x x' \rangle_f &= \langle x x' \rangle_a + \langle x x' \rangle_b
\end{aligned} \tag{20}$$

Finally we get for the total line the following formula defining the emittance increase, where the 0 subscript denotes the nominal emittance and the t subscripts the total emittance:

$$\begin{aligned}
\langle x^2\rangle_t &= \langle x^2\rangle_0 + \sum_n \langle x^2\rangle_n \\
\langle x'^2\rangle_t &= \langle x'^2\rangle_0 + \sum_n \langle x'^2\rangle_n \\
\langle xx'\rangle_t &= \langle xx'\rangle_0 + \sum_n \langle xx'\rangle_n
\end{aligned} \tag{21}$$

with the $\langle x^2\rangle_n$, $\langle x'^2\rangle_n$ and $\langle xx'\rangle_n$ defined in equation (18).

Note that with the introduction of the nominal beam (subscript zero) I have introduced not only the nominal emittance of the beam but also the design values of the optical functions at the IP. It is a remarkable fact that the contributions of the bending magnets does not depend on the beam but depends only on the design of the line, including the design energy. I introduce here the sigma matrix

$$\sigma = \begin{pmatrix} \langle x^2\rangle & \langle xx'\rangle \\ \langle xx'\rangle & \langle x'^2\rangle \end{pmatrix} = \epsilon \begin{pmatrix} \beta & -\alpha \\ -\alpha & \gamma \end{pmatrix}$$

with the condition that the determinant is equal to one giving $\gamma = (1+\alpha^2)/\beta$. It is simply another representation of the set of the three second-order moments of the beam distribution in one plane, the three variables being now the emittance ϵ and the optical functions β and α.

Application to the case of the FFTB

The FFTB line contains six main bending magnets arranged in four groups. The following table lists the individual contributions of each of these bends at the final focal point and the last line lists the resulting emittance including emittance growth. The version of the optics used for this calculation is FFTB90F and the nominal horizontal emittance is $3.0\ 10^{-10} m.rad$.

The most interesting result for the FFTB is the beam size increase at the IP. It is directly obtained from $\sigma_x = \sqrt{\langle x^2\rangle}$, assuming* $\langle x\rangle = 0$. For the FFTB I get $\frac{\Delta\sigma_x}{\sigma_x} = 2.6\%$.

From the definition of the RMS emittance (19) one can also obtain the emittance growth $\frac{\Delta\epsilon}{\epsilon} = 2.7\%$.

$\star$ The beam is supposed to be on axis since the average energy loss can be corrected for.

element	$\langle x^2 \rangle$	$\langle x'2 \rangle$	$\langle xx' \rangle$	emittance
B01	$1.7311\ 10^{-14}$	$2.8735\ 10^{-13}$	$-7.0502\ 10^{-14}$	$1.9452\ 10^{-15}$
B02	$2.0580\ 10^{-14}$	$1.3887\ 10^{-13}$	$5.1064\ 10^{-14}$	$1.5829\ 10^{-14}$
B02	$4.1179\ 10^{-15}$	$4.5616\ 10^{-13}$	$4.0916\ 10^{-14}$	$1.4293\ 10^{-14}$
B03	$7.9982\ 10^{-16}$	$5.3104\ 10^{-14}$	$6.3063\ 10^{-15}$	$1.6443\ 10^{-15}$
B03	$1.5954\ 10^{-15}$	$5.9703\ 10^{-14}$	$-9.3029\ 10^{-15}$	$2.9505\ 10^{-15}$
B04	$3.8719\ 10^{-15}$	$3.7801\ 10^{-14}$	$-1.1852\ 10^{-14}$	$2.4264\ 10^{-15}$
nominal	$9.0\ 10^{-13}$	$1.0\ 10^{-7}$	0.	$3.0\ 10^{-10}$
total	$9.4828\ 10^{-13}$	$1.0\ 10^{-7}$	$6.6293\ 10^{-15}$	$3.0794\ 10^{-10}$

Table 7.1. The contribution to the emittnace growth of the different FFTB bends. The folding of the different second order moments is described in the text.

Since we have $\sigma_x = \sqrt{\beta\epsilon}$, the emittance growth alone accounts for only about 1.3% of the spot size increase. The calculation of the emittance and optical functions using the sigma matrix definition above shows that there is also a change in the optical functions at the IP due to this effect. In the case of the FFTB the relative change $\frac{\Delta\beta}{\beta}$ is about equal to the emittance growth or 2.6 %.

The spot size increase at the IP is therefore due to an increase of the emittance as well as as increase of the β-function. The emittance increase cannot be compensated for. The change in the optical functions can be compensated by retuning the line, lowering the linear beta at the IP. The increased beta can be made equal to the β-function we designed the line for in the first place. The effect has not disappeared but it would not impact the goal of obtaining a given spot size at the IP.

Lowering the β-function at the IP entails that it should increase at the final quadrupoles. However the same effect that increases the β-function at the IP must reduce it at the final quadrupoles since there is only a linear transport system between the two and the phase difference is $\pi/2$. From (21) it is obvious that $\langle x^2 \rangle = \beta\epsilon$ cannot decrease but it is possible for ϵ and β to vary in opposite directions. The emittance can increase while the β-function decreases; the net effect still being that all second moments of the beam actually increase. One should look in more details at this effect. A direct calculation taking the final quadrupole as the end of the line would I believe confirm the above analysis.

Note that there is also a rotation of the beam in phase space shown by a non-zero $\langle xx' \rangle$. The beam ellipse is not upright at the nominal focal point. This however is a negligible effect at the FFTB.

Appendix B

Long sextupole aberration at the FFTB

Introduction

In a final focus system the chromaticity introduced by the very strong final lenses is cancelled at the interaction point by placing sextupoles in a dispersive region giving a chromatic kick which can be made equal and opposite to that of the final lenses.

Sextupoles are non-linear magnetic lenses giving rise to strong geometric aberrations at the focal point of a final focus system. In order to cancel some of these aberrations we place the sextupoles in pair separated by a $-I$ transformation. The third-order geometric aberrations then cancel out. However, because of the finite length of the sextupole itself, higher order geometric aberrations (fourth and higher) do appear.

Katsunobu Oide has already estimated this effect[5] for the FFTB but I give here a more detailed derivation of it. In addition I present another way of deriving the same result based on Lie algebra techniques.

First order transport and kicks

Inside a sextupole the first order transport is that of a drift space; the coordinates are changing according to the following equations:

$$x_s = x_0 \; + \; s \; x_0' \quad , \qquad y_s = y_0 \; + \; s \; y_0' \tag{1}$$

and the nonlinear kick for an elementary slice ds of the sextupole of strength $K = \frac{2\,B_0}{a^2(B\rho)}$ is of the form:

$$\Delta x' = \frac{1}{2} K \; (x^2 - y^2) \; ds \quad , \qquad \Delta y' = -K \; x \; y \; ds \tag{2}$$

We can now take into account this non-linear kick in order to find the true positions x_s and y_s along the sextupole. In effect it is this slight departure from the linear trajectory coupled to the non-linear kick given by the remaining part of the sextupole that gives rise to this fourth order effect. Assuming zero slope in the trajectory at the entrance we have

$$
\begin{aligned}
x(s) &= x_0 + \int_0^s (s - s')\ \Delta x'(s') \\
&= x_0 + \int_0^s (s - s')\ \frac{K}{2}\ (x_0^2 - y_0^2)\ ds' \\
&= x_0 + \frac{K}{4}\ s^2\ (x_0^2 - y_0^2) \\
\text{and similarly} \qquad y(s) &= y_0 - \frac{K}{2}\ s^2\ x_0 y_0
\end{aligned}
\tag{3}
$$

Replacing x and y in equation (2) by their expression in equation (3) and integrating over the length of the sextupole we get the total change in angle or equivalent kick. We evaluate here only the vertical kick as this is the critical plane for flat beam final focus systems.

$$
\begin{aligned}
\Delta y' &= \int_0^{l_s} -K\ x(s)\ y(s)\ ds \\
&= -K \int_0^{l_s} \left[\ x_0 + \frac{Ks^2}{4}(x_0^2 - y_0^2)\right] \left[\ y_0 - \frac{Ks^2}{2} x_0\ y_0\right] ds \\
&= -Kl_s\ x_0 y_0\ -\ \frac{K^2 l_s^3}{12}\ y_0\ (x_0^2\ +\ y_0^2)\ +\ \frac{K^3 l_s^5}{40}\ x_0 y_0\ (x_0^2\ -\ y_0^2)
\end{aligned}
\tag{4}
$$

The first term in the above equation is the normal sextupolar kick (second order) that we use to correct the chromaticity*. It is also the reason why we introduce the sextupoles in pairs so that their purely geometric parts cancel when considering the entire chromatic correction section.[55] Indeed all geometric terms of even order, such as the third term (order four) above, do cancel across the $-I$.

The second term is that of interest to us and represents the long-sextupole, octupole-like kick of order three.

Considering finally the global kick given by a pair of sextupoles separated by a $-I$ transformation we get the long-sextupole non-linear kick at the end of the second sextupole

$\star$ the sextupoles are placed in a dispersive region so just change x into $x + \eta\delta$ to see the chromatic term appear.

of the pair

$$\Delta y' = -\frac{K^2 l_s^3}{6} y_0 (x_0^2 + y_0^2) \tag{5}$$

or with $k_s = K l_s$ the integrated strength of the sextupole:

$$\Delta y' = -\frac{k_s^2 l_s}{6} y (x^2 + y^2) \tag{6}$$

Lie algebra derivation

I will now use Lie algebra based techniques to derive the same result. I hope that the reader will profit from this parallel derivation and will catch a glimpse of the ease and possibilities of this method for higher orders.

The hamiltonian of a slice ds of sextupole can be given by

$$Hds = \frac{K}{3!} ds (x^3 - 3xy^2) \tag{7}$$

The effect of a long sextupole is obtained by combining the hamiltonians of these elementary slices into one global hamiltonian for the whole magnet according to the Campbell-Baker-Hausdorff theorem which can be expressed in our case

$$H_{whole} = \sum_i H(s_i) ds_i + \frac{1}{2} \sum_i \sum_{j>i} [H(s_i) ds_i, H(s_j) ds_j] + \quad \ldots \tag{8}$$

The first term in the above formula is simply the total sextupole kick we use for chromaticity correction. The second term represents the interaction of the slices of sextupole two by two and is the term we are interested in. Note that there are more terms in this expansion and although they are not significant here they are also very easy to calculate, involving only more Poisson brackets.

Upon transforming the sums into integrals over the length of the magnet the long sextupole term is written

$$\begin{aligned} H_{ls} &= \frac{1}{2}\int_{-L/2}^{L/2} ds \int_{s}^{L/2} ds'[H(s), H(s')] \\ &= \frac{K^2}{72}\int_{-L/2}^{L/2} ds \int_{s}^{L/2} ds'[x(s)^3 - 3x(s)y(s)^2, x(s')^3 - 3x(s')y(s')^2] \end{aligned} \tag{9}$$

Using relations like

$$[x(s)^3, x(s')y(s')^2] = 3x(s)^2y(s')^2[x(s), x(s')] = 3x(s)^2y(s')^2(s'-s) \tag{10}$$

the Poisson bracket can be expressed in terms of the elementary $[x_i(s), x_j(s')]$ which are evaluated from the linear optics in the element: *e.g.* $[x(s), x(s')] = [x(s), x(s)+(s'-s)x'(s)] = s'-s$.

Integrating over the lengths one needs only keep the lowest order in L which is equivalent to approximating $x(s)$ by its value at the magnet center x_c before integrating. This is justified by the fact that terms of higher order in L involve also the angles of the trajectory at the center of the magnet, x'_c and y'_c which are typically two or more orders of magnitude smaller than the x_c and y_c due to very high beta functions at the sextupoles in final focus systems.

We finally have the following hamiltonian for the long sextupole effect:

$$H_{ls} = \frac{K^2L^3}{48}(x_c^2 + y_c^2)^2 \tag{11}$$

In order to find the effect of this hamiltonian on the trajectory, one needs only take its Poisson bracket with the corresponding coordinate function. For example the long sextupole vertical kick is given by

$$\Delta y' = [H_{ls}, y'] = \frac{\partial H_{ls}}{\partial y} = \frac{K^2l_s^3}{12}(y_c^3 + y_c x_c^2) \tag{12}$$

Taking into account a sextupole pair separated by a $-I$ transformation one finds the same kick we had in equation (6).

K. Oide making an estimate of this effect (*cf.* SLAC-Pub 4953) argues that since the contribution of the horizontal plane is small compared to that of the vertical plane at the second pair of sextupoles, we can retain only the term in y^3 in equation (6). Since the beam sizes are comparable in our case ($\sigma_y \sim 1.6\ \sigma_x$) this statement may not be obvious at first glance. I carry out here the detailed calculation.

The displacement at the interaction point corresponding to this kick is

$$\Delta y^* = \sqrt{\beta_{y_s}\beta_y^*}\ \frac{k_s^2}{6}\ l_s\ y(x^2+y^2) \tag{13}$$

and the spot size increase is given by

$$\Delta\sigma_y^{*2} = \langle \Delta y^{*2} \rangle - \langle \Delta y^* \rangle^2 \tag{14}$$

We assume in the following that there is no coupling in the optics so that the variables x and y are not correlated. The two terms of equation (14) then evaluate to the following, neglecting the change in centroid position induced by the sextupoles

$$\begin{aligned} \langle y(x^2+y^2) \rangle &= \langle y^3 \rangle + \langle y \rangle \langle x^2 \rangle = 0 \\ \text{and} \qquad \langle y^2(x^2+y^2)^2 \rangle &= \langle y^6 \rangle + 2\langle y^4 \rangle \langle x^2 \rangle + \langle y^2 \rangle \langle x^4 \rangle \end{aligned} \tag{15}$$

Using the formula $\langle z^{2n} \rangle = (2n-1)!!\ \langle z^2 \rangle^n$ for Gaussian distributions we get

$$\langle y^2(x^2+y^2)^2 \rangle = 15\sigma_y^6 + 6\sigma_y^4\sigma_x^2 + 3\sigma_y^2\sigma_x^4 \tag{16}$$

Finally for the spot size increase we have, with the quantities on the right hand side evaluated at the sextupoles

$$\Delta\sigma_y^{*2} = \beta_y\beta_y^*\frac{k_s^4 l_s^2}{36}(15\sigma_y^6 + 6\sigma_y^4\sigma_x^2 + 3\sigma_y^2\sigma_x^4) \tag{17}$$

or equivalently

$$\frac{\Delta\sigma_y^{*2}}{\sigma_y^{*2}} = \frac{5}{12}\ k_s^4\ l_s^2\ \beta_y^4\ \epsilon_y^2\ (1 + \frac{2}{5}\frac{\sigma_x^2}{\sigma_y^2} + \frac{1}{5}\frac{\sigma_x^4}{\sigma_y^4}) \tag{18}$$

If we neglect the contribution of the horizontal plane, the final result for the pair of sextupoles

is

$$\frac{\Delta\sigma_y^{*2}}{\sigma_y^{*2}} = \frac{5}{12}\, k_s^4\, l_s^2\, \beta_y^4\, \epsilon_y^2 \tag{19}$$

RESULTS FOR THE FFTB

In the case of the FFTB we anticipate that the largest contribution comes from the second pair of sextupoles where the beta functions are much larger than at the first pair. We consider here the two pairs of sextupoles as independent and giving rise to independent aberrations that need to be added in quadrature to find the overall effect.

CCY

Let us first examine the second pair of sextupoles, located in the second chromatic correction section or CCY*. The integrated strength of the sextupoles is $k_s = 21.30\ m^{-2}$ with a length $l_s = 0.25\ m$ and the vertical beta function is $\beta_y = 10135\ m$ with a vertical emittance of $\epsilon_y = 3.\ 10^{-11}\ m.rad$. Finally the ratio of the horizontal to vertical spot size is $\sigma_x/\sigma_y = 0.66$ and we have

$$\begin{aligned} \frac{\Delta\sigma_y^{*2}}{\sigma_y^{*2}} &= 0.051 \times (1 + .174 + .038) \\ &= 0.062 \end{aligned} \tag{20}$$

which gives rise to a $\Delta\sigma_y^*/\sigma_y^* = 1 - \sqrt{1 + .062} \approx 3\%$ increase in the final vertical spot size.

Neglecting the contribution of the horizontal plane we have $\Delta\sigma_y^*/\sigma_y^* \approx 2.5\%$. We see here that the approximation of neglecting the horizontal contribution is justified a posteriori.

CCX

The parameters for the first pair of sextupoles are $k_s = 21.57\ m^{-2}$, $l_s = 0.25\ m$, $\beta_y =$

$\star$ The values quoted here are those for the FFTB91D version of the FFTB optics

268 m and $\sigma_x/\sigma_y = 10.27$ giving

$$\begin{aligned} \frac{\Delta\sigma_y^{*2}}{\sigma_y^{*2}} &= 2.62\ 10^{-8}\ (1\ +\ 42\ +\ 2225) \\ &= 6.\ 10^{-5} \end{aligned} \tag{21}$$

which is negligible compared to the CCY. Here the horizontal contribution is far dominant over the vertical one as was expected.

Conclusion

We have estimated the effect of the length of the sextupoles on the final spot size at the FFTB. This aberration comes quasi exclusively from the second sextupole pair and taking into account only the vertical contribution is a good approximation. The effect is expected to increase the vertical spot size by about 3% of the linear size. It could be corrected by introducing an octupole in the line, presumably just before the final quadrupoles since it has to be in a dispersion free region in order to avoid introducing new chromatic aberrations. Although the effect is not very important at the 3% level, it is giving a higher contribution than the limit we establish to estimate the tolerances of the elements of the beam line to different errors.[42]

REFERENCES

1. *SLAC Linear Collider Design Handbook*, 1984

2. P. Bambade (SLAC), *Optical Tuning in the Arcs and Final Focus Sections of the Stanford Linear Collider.* SLAC-0340, Mar 1989. Ph.D. Thesis. Also LAL-89-02 in French.

3. *Final Focus Test Beam: Project Design Report.* SLAC-0376, Mar 1991.

4. *FFTB Optics Handbook.* In preparation.

5. Katsunobu Oide (SLAC), *Design of optics for the Final Focus Test Beam at SLAC.* SLAC-PUB-4953, May 1989.

6. E.D. Courant and H.S. Snyder, Ann. Phys. (N.Y.) **3**, 1 (1958).

7. David C. Carey (FNAL), *The optics of Charged Particle Beams*, Harwood Academic Publishers, (1986)

8. Karl L. Brown, Frank Rothacker, David C. Carey, F.C. Iselin (SLAC), *TRANSPORT: a computer program for designing charged particle beam transport systems.* SLAC-0091 Rev. 2, May 1977.

9. Hans Grote, F.Christoph Iselin (CERN), *The Mad Program (methodical Accelerator Design) Version 8.4: User's Reference Manual, CERN-SL-90-13-AP-REV.2, Aug 1991.*

10. R. Servranckx (Saskatchewan U. and SLAC), Karl L. Brown (SLAC), Lindsay Schachinger, David Douglas (SSCL), *Users Guide to the Program Dimad*, SLAC-0285, May 1986.

11. David C. Carey (Fermilab), *Third Order Transport with Mad Input.* FERMILAB-TM-1546, Sep 1988.

12. F. Schmidt, *SIXTRACK version 1*, CERN-SL-90-11, Oct. 1990.

13. A.J. Dragt, L.M. Healy, F. Neri, R.D. Ryne (Maryland U.), D.R. Douglas, E. Forest (LBL, Berkeley), *Marylie 3.0: A Program for Nonlinear Analysis of Accelerator and Beam Line Lattices.* IEEE Trans. Nucl. Sci. 32 (1985) 2311-2313.

14. M. Berz and H. Wollnik (Giessen U.), *The program Hamilton for the analytic solution of the equations of motion through fifth order*, Nucl. Instr. Meth. A258 (1987) 364-373.

15. M. Berz (Michigan State U.), *Users' guide to COSY-Infinity. The code can be obtained directly from its author.*

16. J. Irwin, S. Peggs (SSCL), *XMAP: A Differential Algebra Tool Generating Accelerator Maps.* SSC-N-604, Mar 1989.

17. T. Sen, Y. Yan (SSCL), J. Irwin (SLAC), *LIEMAP: A Program for Extracting a one Turn Single Exponent Lie Generator Map.* SSCL-443, May 1991.

18. A.J. Dragt (Maryland U.), *Lectures on Nonlinear Orbit Dynamics.* In Batavia 1981, Proceedings, Physics Of High Energy Particle Accelerators, AIP Conf. Proc. 87, 147-313, 1981.

19. A.J. Dragt, J.M. Finn (Maryland U.), *Lie Series and Invariant Functions or Analytic Symplectic Maps.* J. Mathematical Phys.17 (1976) 2215-2227, 1976

20. John Irwin (SLAC), *The Application of Lie Algebra Techniques to Beam Transport Design.* SLAC-PUB-5315, Aug 1990. Submitted to Nucl. Instrum. Methods A.

21. Karl L. Brown (SLAC), R. Servranckx (Saskatchewan U.), *A Magnifying Magnetic Optical Achromat.* Nucl. Instr. Meth. 203 (1982) 73.

22. Karl L. Brown (SLAC), *A Second Order Magnetic Optical Achromat.* SLAC-PUB-2257, Feb 1979. 32pp. Submitted to Nucl. Instr. Methods

23. John Irwin, Ghislain Roy (SLAC) *A comparison of two final focus systems for linear colliders based on tolerances.* Snowmass Summer Study, 1990

24. Tor Raubenheimer, private communication.

25. John Seeman, private communication.

26. Jim Spencer, private communication.

27. R. Brinkmann (DESY), *Optimization of a final focus system for large momentum bandwidth.* DESY-M-90-14, Nov 1990.

28. K. Oide, private communication.

29. Landau and Lifchitz, *Mécanique*, Editions MIR, (Moscou)

30. R.D. Ruth, *Nonlinear Dynamics Aspects of Particle Accelerators*, Lecture Notes in Physics, **247**, Springer, Berlin, 1986.

31. this solution was easily obtained, along with other results in this thesis, using the program *Mathematica,a system for doing mathematics with computers.* It is also developped in the next reference.

32. W.E. Gabella, *PhD. Thesis (1991)*,

33. Stephen Wolfram, *Mathematica, a system for doing mathematics by computer.*

34. H. Wollnik and M. Berz (Giessen U.), *Relations between elements of transfer matrices due to the condition of symplecticity*, Nucl. Instrum. Meth. A238 (1985) 127-140.

35. Karl L. Brown (SLAC), *A Conceptual Design of Final Focus Systems for Linear Colliders.* SLAC-PUB-4159, Jun 1987.

36. J. Buon, F. Couchot, J. Jeanjean, F. Le Diberder, V. Lepeltier, H. Nguyen Ngoc, J. Perez-y-Jorba, P. Puzo (Orsay, LAL), P. Chen (SLAC), *Proposal of a Beam Size Monitor for the Final Focus Test Beam.* SLAC-AAS-NOTE-52, Sep 1990.

37. J. Buon, F. Couchot, J. Jeanjean, F. Le Diberder, V. Lepeltier, H. Nguyen Ngoc, J. Perez-y-Jorba, P. Puzo (Orsay, LAL), P. Chen (SLAC), *Beam Size Monitor for the Final Focus Test Beam.* Nucl. Instrum. Meth. A306 (1991) 93-111.

38. J. Buon, F. Couchot, J. Jeanjean, F. Lediberder, V. Lepeltier, H. Nguyen Ngoc, P. Puzo (Orsay, LAL), P. Chen (SLAC), *Status Report on the Beam Size Monitor for FFTB.* Print-90-0418, Jul 1990.

39. John Irwin, D.L. Burke (SLAC), *Linear Collider IR and Final Focus Introduction.* SLAC-PUB-5652, Sep 1991. Presented at DPF Summer Study on High Energy Physics: Research Directions for the Decade, Snowmass, CO, Jun 25 - Jul 13, 1990.

40. D.L. Burke *et al.*, *Linear Colliders.* SLAC-PUB-5597, Jul 1991.

41. John Irwin (SLAC), *Towards the Next Linear Collider.* SLAC-PUB-5651, Sep 1991.

42. G. Roy, F. Bulos, D.L. Burke, Richard H. Helm, John Irwin, N. Yamamoto (SLAC), *Review of Tolerances at the Final Focus Test Beam*, SLAC-PUB-5485, May 1991.

43. John Irwin, Karl L. Brown, F. Bulos, D.L. Burke, Richard H. Helm, G. Roy, R.D. Ruth, N. Yamamoto (SLAC), Katsunobu Oide (KEK, Tsukuba), *The Optics of the Final Focus Test Beam.* SLAC-PUB-5539, May 1991.

44. Richard H. Helm (SLAC), *First and second order beam optics of a curved, inclined magnetic field boundary in the impulse approximation.* SLAC-0024, Nov 1963.

45. F. Bulos, D.L. Burke, Richard H. Helm, John Irwin, A. Odian, G. Roy, R.D. Ruth, N. Yamamoto (SLAC), *Beam Based Alignment and Tuning Procedures for e^+e^- Collider Final Focus Systems.* SLAC-PUB-5488, May 1991.

46. John Irwin (SLAC), *Construction of High Order Maps for Large Proton Accelerators.* SLAC-PUB-5486, May 1991.

47. Lia Merminga, John Irwin, Richard H. Helm, R.D. Ruth (SLAC), *Optimizing a Nonlinear Collimation System for Future Linear Colliders.* SLAC-PUB-5507, May 1991.

48. Lia Merminga, John Irwin, Richard H. Helm, R.D. Ruth (SLAC), *Collimation Systems in the Next Linear Collider.* SLAC-PUB-5436, Feb 1991.

49. Ghislain Roy (Orsay, LAL), *An Effect of the Fringing Field in Sector Bending Magnets: the coupling of the Transverse Planes in the Solutions of the Equation of Motion at Second Order.* LAL-88-53, Nov 1988.

50. Karl L. Brown (SLAC), *A First and Second Order Matrix Theory for the Design of Beam Transport Systems and Charged Particle Spectrometers.* SLAC-0075-rev-4, Jun 1982.

51. Karl L. Brown (SLAC), R. Servranckx (Saskatchewan U.), *First and Second Order Charged Particle Optics.* SLAC-PUB-3381, Jul 1984.

52. M. Sands (SLAC), *Emittance Growth from Radiation Fluctuations.* SLAC/AP-047, Dec 1985.

53. *A Final Focus System for Flat Beam Linear Colliders.* By Katsunobu Oide (SLAC), SLAC-PUB-4660, Jun 1988. Nucl.Instr.Meth. A276:427,1989.

54. K. Oide (SLAC), *Synchrotron Radiation Limit on the Focusing of Electron Beams.* Phys. Rev. Lett. 61 (1988) 1713-1715.

55. This idea of pairing sextupoles for chromatic correction is due to Karl Brown and Roger Servranckx and was first introduced for the second order achromat.

56. these tolerances were calculated by John Irwin using a *Mathematica* program to calculate the size and effects of bumps across the lattice.